Functional Analysis of Mutants in the Transmembrane Region-1 and Octarepeat Region of Prion Protein

Dissertation

Zur Erlangung des
akademischen Grades des
Doktors der Naturwissenschaften
(Dr. rer. nat.)

an der Universität Konstanz
Mathematisch-Naturwissenschaftliche Sektion
Fachbereich Biologie

Vorgelegt von

Muriel MALAISÉ

Tag der mündlichen Prüfung: 18. Dez. 2007
Referent: Prof. Dr. A. BÜRKLE
Referent: Prof. Dr. C. HAUCK

NB: Due to typographical error on pages 14, 82, 88, 104, 112 and 113 the position of the amino acid histidine has been indicated as "His99". This term should be replaced with "His96".

Summary

The cellular prion protein (PrP^c) is a glycosyl-phosphatidyl-inositol (GPI)-anchored 35 kDa glycoprotein located on the outer surface of the plasma membrane and plays an essential role in the pathogenesis of several inherited and transmissible neurodegenerative diseases such as Creutzfeldt-Jakob disease (CJD) and Gerstmann-Sträussler-Scheinker syndrome (GSSS). Despite being the subject of many recent studies, the physiological function of PrP^c remains largely unresolved. Several candidate functions have been discussed, including binding and internalisation of copper or other metals, superoxide dismutase-like activity, signal transduction and regulation of cellular antioxidant activities. The transmembrane (TM1) region of PrP^c (codons 110-135) should play a key role in PrP^c function because of its high conservation throughout evolution. Moreover it contains an array of hydrophobic amino acids, and peptides derived from this region are neurotoxic.

The aim of the present study was to try to elucidate a possible role of PrP^c in the regulation mitochondrial membrane potential ($\Delta\Psi$), in the regulation of the basal level of endogenous reactive oxygen species (ROS) and in antioxidative defence. For this purpose transiently transfected mouse neuroblastoma cells overexpressing PrP, either as wild-type (wt) protein or as a deletion mutant lacking codons 114-121 (henceforth called Δ8TM1-PrP), were analysed. In addition a deletion mutant in the octarepeat region (Δocta-PrP) was studied. The results showed that wt-PrP and Δ8TM1-PrP have no impact on $\Delta\Psi$. Likewise, overexpression of PrP (wt or mutant) had no impact on endogenous ROS levels. However, under conditions of oxidative stress induced by H_2O_2 treatment of the cells, ROS levels were lower in cells transfected with wt-PrP or Δ8TM1-PrP expression plasmids.

Increased phosphorylation of ERK2 (p42) and decreased phosphorylation of JNK1/JNK2/3 seemed to be linked to this protective effect of PrP^c.

Two other systems derived from transgenic Δ8TM1-PrP mouse brain (whole-brain or cerebellar granular neurones [CGN]) were also studied, but no biological impact of the transgene Δ8TM1-PrP was observable, most likely due to the low expression level.

In conclusion, the protective effect of PrP^c against oxidative stress implicates its octarepeat region but *not* its TM1 domain; it does not manifest as lowered *basal* ROS level; and it seems to involve the MAPK pathway, especially p42 and JNK1/JNK2/3.

Zusammenfassung

Das zelluläre Prion-Protein (PrP^c) ist ein Glycosyl-Phosphatidyl-Inositol-verankertes Protein von 35 kDa, welches an der Außenseite der Plasmamembran lokalisiert ist. Es spielt eine wichtige Rolle bei der Pathogenese verschiedener erblicher bzw. infektiös übertragbarer neurodegenerativer Erkrankungen, wie der Creutzfeldt-Jakob Krankheit (CJD) und des Gerstmann-Sträussler-Scheinker-Syndroms (GSSS). Obwohl PrP^c Gegenstand zahlreicher aktueller Forschungsarbeiten ist, bleibt seine physiologische Funktion unklar. Einige vermutete Funktionen sind bereits untersucht worden, so z.B. die Bindung und Aufnahme von Kupfer oder anderer Metalle, eine Superoxiddismutase-ähnliche Aktivität, Signalübertragung sowie die Regulation der zellulären Antioxidantienaktivität. Aufgrund ihrer hohen evolutionären Konservierung sollte die Transmembranregion (TM1) von PrP (Codons 110-135) eine Schlüsselrolle spielen. Zudem umfasst diese Region zahlreiche hydrophobe Aminosäuren, und von dieser Region abgeleitete Peptide sind neurotoxisch.

Das Ziel vorliegender Arbeit war, eine mögliche Rolle von PrP^c bei der Regulation des mitochondrialen Membranpotentials ($\Delta\Psi$), des Basalspiegels von endogenen reaktiven Sauerstoffspezies (ROS) und bei der antioxidativen Abwehr zu charakterisieren. Um die physiologische Rolle der TM1-Domäne des PrP^c näher zu untersuchen, wurde eine Deletionsmutante mit Verlust der Codons 114-121 (Δ8TM1-PrP) sowie zusätzlich eine Mutante mit Deletion der „Octarepeat"-Region [Δocta-PrP]) sowie als Kontrolle wildtypisches PrP verwendet. Diese PrP-Versionen wurden in transient transfizierten Maus-Neuroblastomzellen überexprimiert. Die Ergebnisse zeigten, dass wt-PrP und Δ8TM1-PrP haben keinen Einfluss auf $\Delta\Psi$ haben. Ebenso hatte die Überexpression von PrP (als wildtypische oder mutierte Version) keinen Einfluss auf den Spiegel von endogenen ROS. Es konnte hingegen klar gezeigt werden, dass unter Bedingungen von oxidativem Stress der intrazelluläre ROS-Spiegel in Zellen, die mit wt-PrP oder Δ8TM1-PrP transfiziert waren, signifikant abgesenkt war.

Dieser Schutzeffekt von PrP^c scheint mit einer verstärkten Phosphorylierung von ERK2 (p42) und ein verminderten Phosphorylierung von JNK1/JNK2/3 in Verbindung zu stehen.

Außerdem wurden zwei weitere experimentelle Systeme, nämlich Primärzellkulturen aus dem Gehirn von transgenen Δ8TM1-PrP-Mäusen (gemischte Kulturen aus dem Gesamthirn bzw. zerebelläre granuläre Neuronen) untersucht. Es konnte jedoch keine biologische Auswirkung des Transgens festgestellt werden, vermutlich wegen des sehr niedrigen Expressionsniveaus.

Aus den Ergebnissen der vorliegenden Arbeit wird gefolgert, (1) dass der Schutzeffekt des PrP^c gegen oxidativen Stress durch die „Octarepeat“-Region, nicht jedoch durch die TM1-Domäne vermittelt wird; (2) dass der besagte Schutzeffekt sich nicht in einem niedrigeren basalen ROS-Niveau manifestiert; und (3) dass der MAPK-Pfad, insbesondere p42 und JNK1/JNK2/3, beteiligt zu sein scheint.

Table of Contents:

1 Introduction

1.1 Transmissible Spongiform Encephalopathies

Transmissible Spongiform Encephalopathies (TSE), also called prion diseases, are a group of neurodegenerative diseases that affect various mammalian species including humans. TSE are lethal and no effective treatment is known. The group of TSE comprise the following diseases, with the respective host species indicated in brackets: Scrapie (sheep, goat), Chronic Wasting Diseases (CWD) (deer, elk), Bovine Spongiform Encephalopathy (BSE) (cattle), Transmissible Mink Encephalopathy (TME) (mink), Feline Spongiform Encephalopathy (FSE) (cat), and Spongiform Encephalopathy of zoo animals (zoologic bovines and primates). In humans the most common TSE is Creutzfeldt-Jakob Disease (CJD), which can be subdivided in four distinct clinical entities: sCJD (sporadic form), fCJD (familial), iCJD (iatrogenic) and vCJD (variant). Other human TSE are Gerstmann-Sträussler-Scheinker syndrome (GSS), Kuru (which is an endemic form of CJD) and Fatal Familial Insomnia (FFI) (review (Collins, et al., 2004), (Aguzzi, 2006)).

TSE are characterized by spongiform ("sponge-like") changes, neuronal death, astrogliosis and accumulation of disease-associated isoform of prion protein (PrP) termed PrP^{Sc}, PrP^{CJD}, PrP^{BSE}, PrP^{CWD} etc., or collectively PrP^{res}.

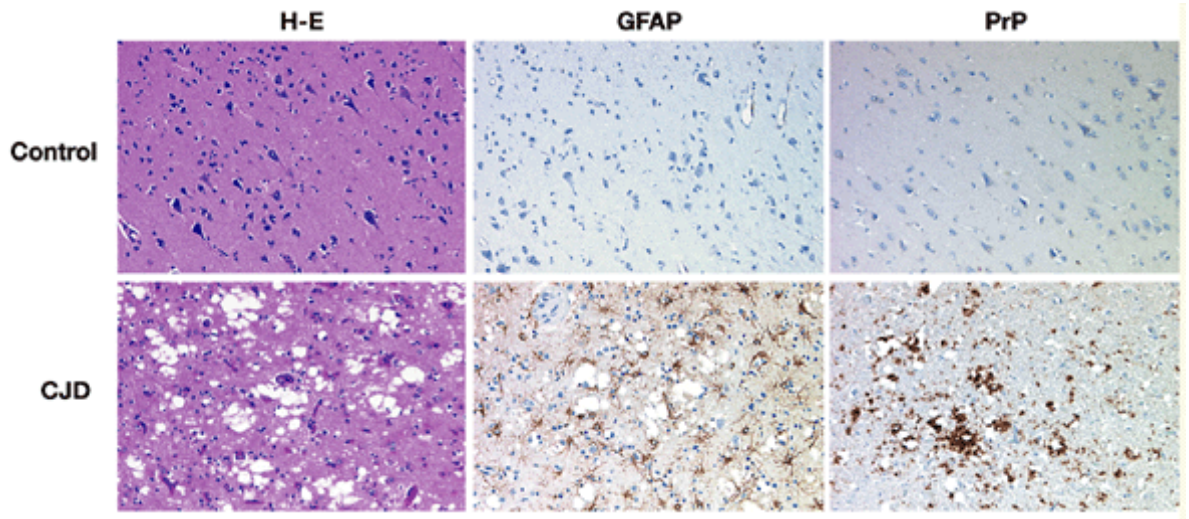

Fig1. **Thin sections of frontal cortex samples of a healthy person and of a CJD patient (Aguzzi, et al., 2001).** Note the characteristic spongiform appearance with vacuoles and PrP deposit in the case of CJD patient. H-E = haematoxylin-eosin staining, GFAP = staining with an antibody against glial fibrillary acidic protein, PrP = staining with an antibody against prion protein.

The first TSE was described in the mid-18th century, *i.e.* scrapie in sheep. The first reports on a human TSE were published in 1920 by Dr. Creutzfeldt and in 1921 by Dr. Jakob. The protein-only theory to describe the unconventional nature of the infectious agent that can cause TSE was first proposed in 1967 (Griffith, 1967) and the term "prion" was coined in 1982 (Prusiner, 1982). "Prion" stands for proteinaceous infectious particle. In 1987 the world heard for first time about BSE. This "mad cow disease" made prion diseases sadly "famous".

1.2 Prion protein (PrP)

1.2.1 Genetics of PrP

The prion protein PrP exists in at least two versions: PrP^{c} (c for cellular), which is the normal cellular form and PrP^{Sc} (Sc for Scrapie), which causes the disease. Both forms are isoforms of the same protein, encoded by the *Prnp* gene on chromosome 20 (human) or chromosome 2 for the mouse, which was identified in 1986 (Basler, et al., 1986), (Sparkes, et al., 1986).

This gene was highly conserved during evolution and especially during vertebrate evolution (Simonic, et al., 2000), (Rivera-Milla, et al., 2006). The PrP sequence is around 90% identical among mammalians (Wopfner, et al., 1999).

The overall sequence identity of the chicken PrP sequence to mammalian PrP is only around 30%, but nevertheless the secondary and tertiary structures are very similar. Despite significant differences in the N terminal repeat domain mammalian and chicken PrP share major biochemical and cellular properties such as copper binding (Shields and Franklin, 2007), (Gabriel, et al., 1992), (Harris, et al., 1991), (Harris, et al., 1993b), (Hornshaw, et al., 1995).

The turtle PrP sequence shares a homology of 40% with mammalian PrP and 58% with avian PrP. Turtle PrP shares with mammals and birds PrP same secondary and tertiary structures but possesses an intriguing additional feature, *i.e.*, aa213-224 exhibits an EF-hand Ca^{2+} binding motif (Simonic, et al., 2000).

Fishes possess two orthologous *PrP* loci (*PrP-1 PrP-2*). Despite the scarce sequence similarity they display an overall structural similarity to mammalian PrP (Rivera-Milla, et al., 2003), (Rivera-Milla, et al., 2006). *PrP-1* knock-down by morpholino antisense RNA injection in zebrafish (*Danio rerio)* leads to an early and lethal arrest at the onset of gastrulation and *PrP2* knockout to a disturbance of brain morphogenesis. Wt mammalian PrP or wt fish PrP could rescue these effects.

Different prion strains were also described in yeast and other fungi, such as [PSI] (Chernoff, et al., 1995), (Derkatch, et al., 1996), [URE3] (Wickner, 1994), [Het-s] (Coustou, et al., 1997), [PIN+] (Derkatch, et al., 2001). In contrast to mammalian PrP, yeast prions are cytosolic proteins (Wickner, 1997). These yeast prions can be helpful for understanding the formation of PrP^{Sc}. When the yeast prions are expressed in *E. coli* these proteins polymerized as fibrils and form amyloid-like plaques (Paushkin, et al., 1997).

1.2.2 Structure of PrP

PrP^{c} contains an octarepeat region (aa 51-91) and a highly hydrophobic region also called Trans-Membrane-like domain 1 (TM1) (aa110-135). PrP^{c} can be glycosylated on Asn180 and Asn196 and also carries a disulfide bridge between Cys178 and Cys213. PrP^{c} is a glycosyl-phosphatidyl-inositol (GPI)-linked glycoprotein, which is found enriched in detergent-resistant membrane fractions.

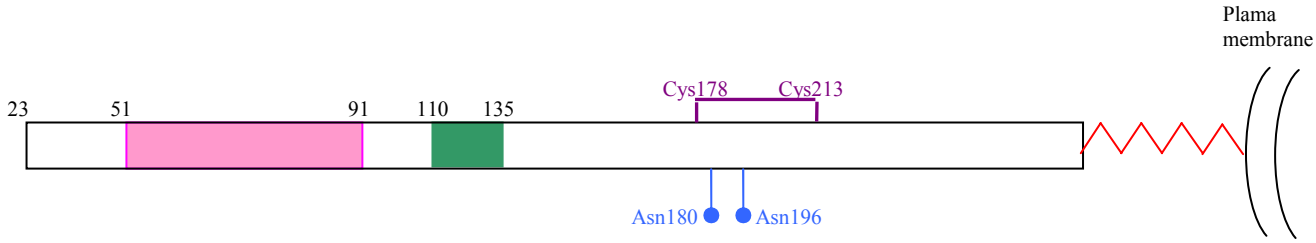

Fig2. **Prion protein primary structure.** The octarepeat region (pink) resides between amino acid (aa) 51 and aa91. The TM1 domain (green) resides between aa 110 and 135. The glycosylation sites (blue), the disulfide bridge (purple) and in the GPI anchor (red) are also indicated.

The molecular weight of PrP^{c} is 28kDa in its unglycosylated form, 32kDa as a monoglycosylated and 35kDa as diglycosylated protein (Collinge, 2001), (Pan, et al., 2002), (Pan, et al., 2005).

Over the last decade the NMR structures of PrP^{c} from a wide range of animal species, including humans (Zahn et al., 2000) have been determined by the Wüthrich group. PrP^{c} contains a long flexible amino terminal tail (aa 23-128) whereas the carboxyterminal part displays three α helices and two β sheets as highly conserved structural features (Fig. 3).

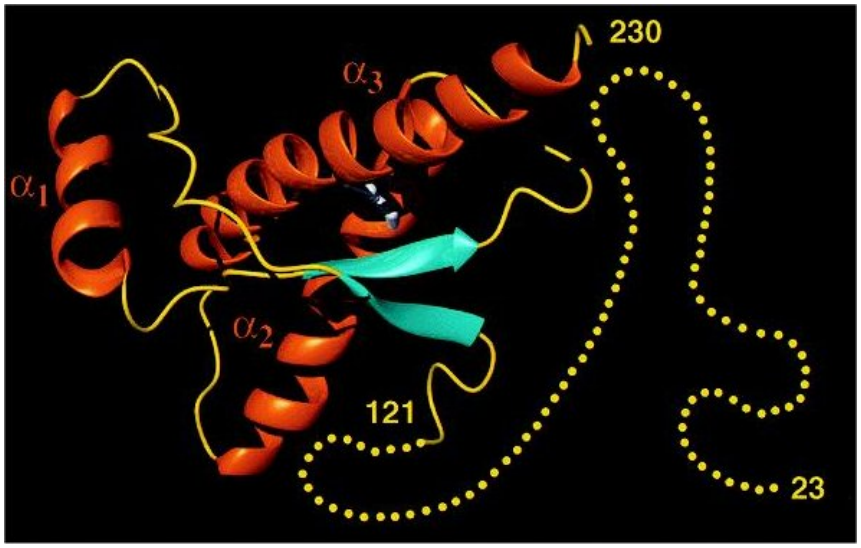

Fig3. **Human prion protein 3D structure (Zahn, et al., 2003).** The α helices are in red, the β sheets in blue and unstructured parts in yellow.

1.2.3 PrP^c life cycle and subcellular trafficking

PrP^c is translocated during its synthesis into the lumen of the endoplasmic reticulum (ER). PrP^c maturation takes place in the ER and includes the cleavage of the amino terminal leader sequence, the C terminal cleavage, addition of the GPI anchor, N-glycosylation and formation of a disulfide bridge. PrP^c then continues its travel along the secretory pathway through the Golgi apparatus and finally reaches the outer face of plasma membrane. PrP^c is mostly localised at cell surface in lipid rafts or caveolae (cholesterol-rich domains) due to its GPI-anchor. PrP^c can then be recycled by endocytosis or degraded after reaching lysosomes. In the ER misfolded PrP^c could be detected, which was subject to proteasomal degradation. Blockage of this clearance mechanism leads to aggregates, which are neurotoxic.

PrP^c can be proteolytically processed between aa 90 and 91 or between aa 110 and 111 (Harris, et al., 1993a), (Chen, et al., 1995), (Ettaiche, et al., 2000). The main endoproteolysis occurs between aa 110 and 111 (α-cleavage), leading to a 17kDa C-terminal fragment termed C1, which displays the same glycosylation pattern and plasma membrane localisation as PrP^c. The corresponding N-terminal N1 fragment is 9kDa in size. The C1 fragment is abundant both in normal brain and CJD brain. Another cleavage called β–cleavage can occur between aa 90 and 91 and can be observed in CJD brains, producing the 21-kDa C2 fragment plus a 7-kDa N2 fragment.

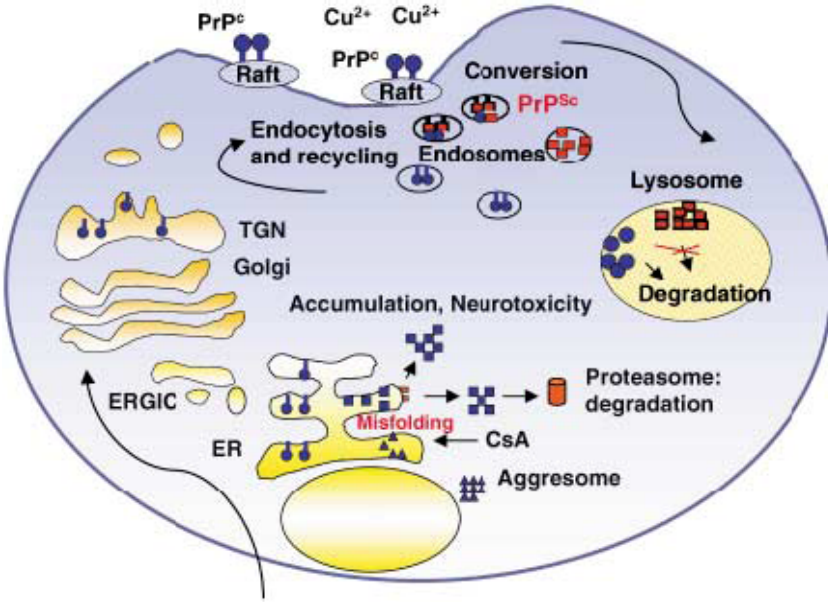

Fig4. **PrP subcellular trafficking (Nunziante, et al., 2003).** Blue circles represent PrP^{c}, which is transported along the secretory pathway (ER: endoplasmic reticulum, ERGIC: ER-Golgi intermediate compartment, Golgi apparatus and TGN: trans-Golgi network) in order to reach the cholesterol-rich domains at the plasma membrane. Conversion of PrP^{c} into PrP^{Sc} (red square) takes place at the cell surface or in endosomes. As PrP^{Sc} may not be totally degraded by lysosomes it accumulates and becomes neurotoxic. A misfolded PrP can be induced by cyclosporine A (CsA) treatment that also leads to protein aggregation.

The conversion of PrP^{c} into PrP^{Sc} takes place at the cell surface or in endosomes, but it is not efficiently degraded by lysosomes and thus accumulates, which leads to neurotoxicity. A similar accumulation can be obtained with PrP^{c} after cyclosporine A (CsA) treatment.

1.2.4 *In vivo* localisation of PrP

PrP^{c} is mostly found in the central nervous system (CNS) (neurons and astrocytes), but also in skeletal muscle, kidney, heart, lung, spleen, kidney, ovary, testis, in secondary lymphoid organs, in intestinal tract and blood lymphocytes (Aguzzi and Polymenidou, 2004), (Archibald, 2004), (Bendheim, et al., 1992), (Ford, et al., 2002, {Fournier, 1998 #1107)}, (Horiuchi, et al., 1995), (Manson, et al., 1992), (Mironov, et al., 2003), (Morel, et al., 2003), (Moser, et al., 1995).

Principal localisations of PrP^{c} in brain are in the hippocampus but also in cortex, caudate nucleus, corpus callosum, thalamus and cerebellum (Taraboulos, et al., 1992), (Moser, et al., 1995), (Laine, et al., 2001). PrP^{c} is more distinctly concentrated at the neuronal plasma membrane and at the synapses (Brown, 2001), (Sales, et al., 1998).

1.2.5 *Prnp* knockout mice

In 1992 Büeler and colleagues published the first *Prnp* knockout mouse model (also called Zürich I mice) (Büeler, et al., 1992). Surprisingly, those mice did not show any gross developmental defect, neurological or neupathological phenotype and thus did not give any clue as to the physiological function of PrP^c in the mouse.

Subsequently several different *Prnp* knockout mice were created such as Edbg, Ngsk, Npu, Rcm. In all cases minor changes in circadian rhythm and sleep pattern were observed (Büeler, et al., 1992), (Tobler, et al., 1996). Furthermore, electrophysiological and structural abnormalities in the hippocampus (Colling, et al., 1996), (Colling, et al., 1997), (Collinge, et al., 1994), (Manson, et al., 1995), (Whittington, et al., 1995), loss of cerebellar Purkinje cells (Sakaguchi, et al., 1996), (Li, et al., 2000b), (Nishida, et al., 1999) and alteration of intracellular calcium homeostasis (Herms, et al., 2000), (Fuhrmann, et al., 2006) were reported.

At the cellular level PrP^c deficient mice are more susceptible to oxidative stress damages (Brown, et al., 1997b), (Brown, et al., 1998a), (Brown, et al., 2002), (Klamt, et al., 2001), (White, et al., 1999), (Wong, et al., 2001) and less viable in culture as wild-type cells (Kuwahara, et al., 1999).

A conditional *Prnp* knockout mice system was constructed by using a Cre-LoxP system, which was activated 8-10 weeks after mice birth (Mallucci, et al., 2002). No spontaneous phenotype was observable.

Transgenic mice overexpressing wt PrP have also been created (Westaway, et al., 1994). These mice displayed degeneration of skeletal muscle, peripheral nerves and CNS as characteristic phenotypic changes.

The differences observed in different *Prnp* deficient mouse strains turned out to be due to an artefact, *i.e.* forced overexpression of the Doppel protein (Moore, et al., 1999). Doppel (Dpl) is a prion protein-like glycoprotein encoded by the *Prnd* gene located 26 kB downstream of *Prnp*. In adult wt mice Dpl is physiologically expressed in testis and heart. Dpl has 23% of identity to PrP^c in primary amino acid structure (Li, et al., 2000a), (Moore, et al., 1999), (Nicholson, et al., 2002). Dpl possesses neither an octarepeat region nor a palindromic sequence, which is important for PrP to adopt transmembrane topologies (Hegde, et al., 1998). In two *Prnp* knockout mice strains, which are predisposed to cerebellar ataxia Dpl is highly expressed in CNS but not in other $Prnp^{-/-}$ strains without ataxia. This suggested a role for Dpl in degeneration of Purkinje cells and ataxia (Moore, et al., 1999). Moreover this ataxia could be rescued by introduction of a singly copy of wt *Prnp*, which suggested some interaction between PrP and Dpl (Nishida, et al., 1999). Furthermore introduction

in *Prnp*$^{-/-}$ mice of an N-terminal truncated PrP, which resembles Dpl, induced ataxia and cerebellar granular cell degeneration (Shmerling, et al., 1998).

1.2.6 PrP functions

Several groups have reported a role of PrP in signal transduction, for example via interaction of PrP with the neuronal phosphoprotein synaptin Ib, the adaptor protein Grb2 and Pint1 (Spielhaupter and Schatzl, 2001), reggie-1 and reggie-2 (Stuermer, et al., 2004), the tyrosine kinase Fyn (Mouillet-Richard, et al., 2000) and an activation of the phosphatidylinositol 3 kinase (PI3K) dependent upon copper binding of PrP (Vassallo, et al., 2005).

The ability of PrP to bind copper on its octarepeat region and on two other histidines (His99 and His111) (Jones, et al., 2004), (Thompsett, et al., 2005) seems to play an important role for its function(s). PrP could act as a sensor for oxidative stress (Brown, et al., 1997b), (Klamt, et al., 2001), (Rachidi, et al., 2003), (White, et al., 1999) and should then lead to intracellular anti-stress response regulation. At the beginning of this study a putative SOD-like activity of PrP had been proposed (Brown and Besinger, 1998; Brown, et al., 2001; Brown, et al., 1999). Since then, this issue became quite controversial (Hutter, et al., 2003) and more recently it was suggested that PrP could interact with another protein possessing SOD activity (Sakudo, et al., 2005).

In summary, a long list of putative functions for PrP^{c} have been proposed such as immunoregulation (Krebs, et al., 2006), (de Almeida, et al., 2005), signal transduction (Krebs, et al., 2006), (Mouillet-Richard, et al., 2000), (Schneider, et al., 2003), (Spielhaupter and Schatzl, 2001), binding and sequestration of copper or other metals (Brown, et al., 1997a), (Burns, et al., 2003), (Chattopadhyay, et al., 2005), (Millhauser, 2004), synaptic transmission (Collinge, et al., 1994), induction of or protection against apoptosis (Gains, et al., 2006), (Kristiansen, et al., 2005), (Roucou, et al., 2005), SOD-like activity (Brown and Besinger, 1998), (Brown, et al., 1999), (Hutter, et al., 2003), or regulation of cellular antioxidant activities (Brown, et al., 2001), (Rachidi, et al., 2003).

1.3 The TM1 domain of PrP

The TM1 region of PrP is very interesting because it was highly conserved during evolution, which should implicate an essential role in the physiologic function of PrP. This region comprises aa 110 through 135 and comprises an array of hydrophobic amino acids. It is also a highly flexible and unstructured portion of PrP as revealed by NMR analysis of recombinant PrP (Zahn, et al., 2000).

Peptides derived from the region of aa 105-125 are neurotoxic (Brown, et al., 1998b), (Forloni, et al., 1993), (O'Donovan, et al., 2001). This region harbours a missense mutation in Familial GSS which leads to a stable transmembrane (ctm) conformation of PrP^{c}, *i.e.*, the C-terminal part of PrP is localized in the lumen of endoplasmic reticulum and the N-terminal part in the cytosol (Hegde, et al., 1998), (Hegde, et al., 1999), (Stewart and Harris, 2005).

Previously A. Bürkle's group showed that expression of a deletion mutant of 8 amino-acid in the TM1 domain (aa114-121) is sufficient to inhibit PrP^{Sc} accumulation in persistently scrapie-infected mouse neuroblastoma cells (Holscher, et al., 1998). Recently, transgenic mice carrying the same deletion mutant were also produced by the Bürkle group. These mice do not show any obvious spontaneous phenotype (Baumann, et al., 2007). Transgenic mice carrying PrPΔ114-121 on a *Prnp* $^{-/-}$ background were crossed with transgenic mice expressing PrPΔ94-134 or PrPΔ32-134. The latter types of transgenic mice suffer from the so-called "Shmerling syndrome", a spontaneous, non-infectious, lethal neurodegenerative condition characterised by ataxia, progressive cerebellar granule cell degeneration, and leukoencephalopathy. Wt-PrP^{c} can rescue this phenotype. It was shown that co-expression of PrPΔ114-121 enhanced the toxicity of PrPΔ94-134 whereas it diminished toxicity of PrPΔ32-134 (Baumann, et al., 2007).

1.4 Reactive oxygen species

Nowadays it is well established that a link between transition metal binding and neurodegenerative diseases including TSE exists (Milhavet and Lehmann, 2002). While in some cases this metal binding leads to protection against oxidation, it can enhance oxidative damage through disturbing free radical homeostasis (Simonian and Coyle, 1996), (Sayre, et al., 1999).

Oxidative stress has been defined as an imbalance between biochemical processes leading to the production of reactive oxygen species (ROS) and antioxidant defences.

The principal ROS are the hydroxyl radical (OH•), the superoxide anion (O_2^-•) and hydrogen peroxide H_2O_2. Ionization or chemicals can induce ROS artificially but ROS are also continually produced in the cell. Two major mechanisms of ROS production are the incomplete reduction of O_2 in the respiratory chain in mitochondria (mostly at complexes I and III) and during the "oxidative burst" mediated by NADPH oxidase.

Because ROS are continually produced the cell had also developed defences: cytosolic copper-zinc-superoxide dismutase (Cu-Zn SOD), mitochondrial manganese superoxide dismutase (Mn SOD), glutathione peroxidase, glutathione reductase, NAD(P) transhydrogenase, NADPH, vitamin E, vitamin C, thiol peroxidase and the mitochondrial respiratory chain itself (Kowaltowski and Vercesi, 1999).

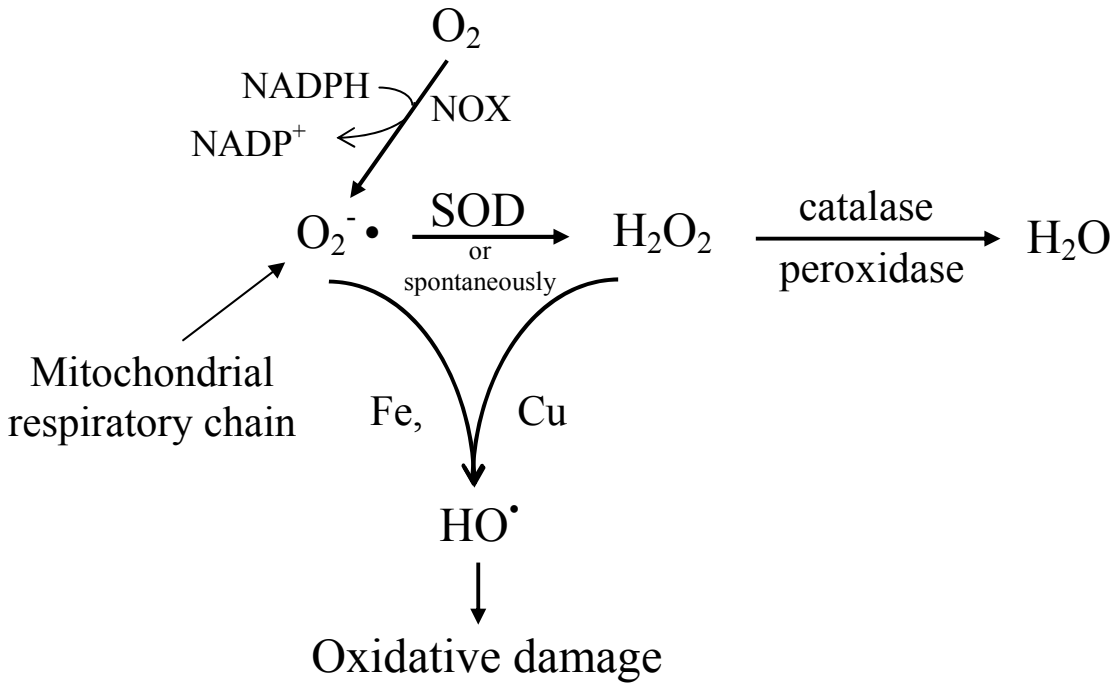

Fig5. **Production, action and detoxification of ROS.** The two major producers of ROS are the mitochondrial respiratory chain and NADPH oxidase. They both produce superoxide anion radicals which can be converted into hydrogen peroxide either spontaneously or by SOD. Hydrogen peroxide can be detoxified by catalase or peroxidase in water but it can also react with superoxide anion in presence of metal and form the hydroxyl radical. The hydroxyl radical is dangerous because it can directly damage lipids, proteins and DNA and thus trigger to apoptosis. SOD: superoxide dismutase, OH•: hydroxyl radical, O_2^-•: superoxide anion, H_2O_2: hydrogen peroxide, NOX: NADPH oxidase.

ROS have positive and negative roles. They play an important role in intracellular signalling (Droge, 2002) but excessive levels of ROS finally lead to cell death. For example H_2O_2 is an interesting second messenger for cell signalling: it can activate components of signalling cascades that are involved in cell survival, proliferation, differentiation and cell death (Boyd and Cadenas, 2002), (Thannickal and Fanburg, 2000). H_2O_2 is recognized as an important mediator of oxidative stress in neurons (White, et al., 1999)

1.5 Mitochondrial membrane potential

The mitochondrial membrane potential ($\Delta\Psi$) is the result of proton translocation from the mitochondrial matrix to the mitochondrial inter-membrane space through the action of the mitochondrial respiratory chain. The respiratory chain converts the high-energy potential of the reducing equivalents from NADH and $FADH_2$ into the mitochondrial proton gradient. $\Delta\Psi$ thereby reflects the mitochondrial activity of the cell. Mitochondrial activity can generate ROS by occasional escapes of electrons from the respiratory chain.

Hyperpolarisation of $\Delta\Psi$ leads to increased ROS production which as feed back induces a decrease of $\Delta\Psi$ and so an equilibrium is maintained, otherwise calcium, cytochrome c and other mitochondrial constituents are released and cause apoptosis (Nagy, et al., 2003).

The collapse of $\Delta\Psi$ induces colloid osmotic swelling of the mitochondrial matrix (Gunter and Pfeiffer, 1990), the redistribution of calcium, magnesium, glutathione and NADPH across the inner membrane, defective oxidations, the cessation of the ATP synthesis, and production of ROS (Bai, et al., 2001).

So it is very important to maintain $\Delta\Psi$ in physiological range or to correct any deviation very quickly. Some proteins are known to prevent the loss of $\Delta\Psi$, such as Bcl-2 and Bcl-X_L, by preserving mitochondrial integrity and calcium release. In case of calcium overload mitochondria open their transition pore, which disrupts $\Delta\Psi$. This induces the collapse of $\Delta\Psi$ and the release of cytochrome c which leads to caspase activation and finally to apoptosis (Smaili, et al., 2003), (Smaili, et al., 2000).

1.6 Aim of the work

In past 15 years our knowledge prion has increased dramatically, but nevertheless the function of PrP^c function remains elusive. Knockout mice cannot directly help because they do not show any overt phenotype. The biggest question in the field of prion research therefore still is: What is the physiologic role of cellular PrP?

In order to help elucidate this question two systems were used in the present study, *i.e.*, transiently transfected neuroblastoma cells and primary cells derived from mouse brain. The neuroblastoma cells were transfected either with wt-PrP or with a deletion mutant in the TM1 region of PrP. Mice were either non-transgenic or transgenic expressing a deletion mutant in the TM1 region, on various genetic background (*Prnp*$^{+/+}$, *Prnp*$^{+/-}$, *Prnp*$^{-/-}$).

The aims of this study were the following: Does PrP^c, and more precisely its TM1 domain, have an effect on the mitochondrial membrane potential ($\Delta\Psi$) or on the basal endogenous ROS level or on the ROS level after induction of oxidative stress? Does the PrPΔ114-121 mutant (henceforth termed Δ8TM1-PrP) protect against oxidative stress as much as wt-PrP does? In order to address these questions different probes were used. TMRE served to monitor changes in $\Delta\Psi$ and H_2DCFDA was used to quantify the endogenous ROS level. With incoming results new questions emerged: Which pathways are involved in the PrP^c-mediated modulation of the cellular reaction to oxidative stress? Does PrP^c possess an SOD-like activity of its own or lead to an increase in total cellular SOD activity? Moreover, because PrP can bind copper, does copper binding have any effect on the above parameters?

2 Materials and Methods

2.1 Materials

2.1.1 Chemicals and reagents

2.1.1.1 Chemicals, basal cell culture media and supplements

Name	*Manufacturer*
Acetic acid	VWR
Agarose	Biozym
Aqua Poly Mount	Polyscience
Ammonium persulfate (APS)	Serva
Biotinylated SDS PAGE standard broad range	Biorad
β–mercaptoethanol	Sigma
Bovine Serum Albumin (BSA)	Sigma
Bromophenol blue	Sigma
Buthionine sulfoximine (BSO)	Sigma
B27 without antioxidant (serum free supplement)	Gibco
Complete Protease inhibitor	Roche
Copper chloride hydrate ($CuCl_2$)	Sigma
Cytosine arabinoside	Sigma
Deoxynucleosides triphosphate set PCR grade	Roche
2', 7'dichlorohydrofluorescein diacetate (H_2DCFDA)	Molecular Probe
Dimethylsulfoxide (DMSO)	Sigma
Disodium hydrogen phosphate dihydrate (Na_2HPO_4 2 H_2O)	Roth
DNAse I	Roche
Dulbecco's Modified Eagle's Medium comprising 4500 mg/l glucose and L-Glutamine, without Pyruvate (DMEM)	Gibco / Life Technologies
Ethanol	Riedel de Haen

Ethylenediamine tetraacetic acid (EDTA)	Roth
F-12 Medium (Nutrient Mixture Ham)	Gibco
Fetal Calf Serum (FCS; heat inactivated)	Biochrom AG
Glucose	Sigma
L-Glutamine	Gibco
Glycine	Roth
Glycoprotein denaturing buffer	New England Biolabs
G7 reaction buffer	New England Biolabs
HEPES	Gibco
Hoechst	Molecular Probe
Hotmaster Taq buffer	Eppendorf
Hotmaster Taq DNA polymerase	Eppendorf
Hydrogen peroxide (H_2O_2)	Merck
Iscove´s Modified Dulbecco´s medium (IMDM)	Gibco
Isopropanol	Riedel de Haen
JetPEI	Qbiogene
Loading dye solution 6x (for DNA)	Fermentas
Magnesium sulfate heptahydrate ($MgSO_4$, 7 H_2O)	Merck
Mass ruler DNA ladder mix	MBI Fermentas
Methanol	Fluka
Milk powder (non-fat)	Rapilait
Neurobasal A medium	Gibco
NP40	Fluka
Paraformaldehyde (PFA)	Serva
Penicillin/Streptomycin	Gibco
Phenol red	Seromed
PNGase F	New England Biolabs
Poly-L-Lysine (PLL)	Sigma
Ponceau S	Roth
Potassium chloride (KCl)	Riedel de Haen
Potassium dihydrogenphosphate (KH_2PO_4)	Riedel de Haen
Prestained protein molecular weight marker	MBI Fermentas
PVDF-Membrane	Amersham

Rotiphorese Gel 30	Roth
SBTI (trypsin inhibitor)	Sigma
Sodium azide (NaN_3)	Merk
Sodium chloride (NaCl)	Riedel de Haen
Sodium deoxycholate	Fluka
Sodium dodecylsulfate (SDS)	Serva
Sodium hydrogencarbonate ($NaHCO_3$)	Life Technologies
Streptavidin HRP	Dynal Biotec
Sucrose	Merk
Sytox	Molecular Probe
Tetramethylethylenediamine (TEMED)	Serva
Tetramethylrhodamine ethyl ester perchlorate (TMRE)	Sigma
tert-butylhydroperoxide (tBOOH)	Fluka
Tris base	Sigma
Triton X-100	Sigma
Trypan Blue	Sigma
Trypsin	Sigma
0.25% Trypsin/EDTA solution	Sigma
Tween 20	Sigma

2.1.1.2 Buffers

Name	Composition
Agarose gel loading buffer 10x	0.5g/l Saccharose 2µl/ml EDTA (0.5 M) Bromophenol blue
Deoxynucleoside triphosphates set PCR grade (dNTP mix) 40mM	10mM dCTP 10mM dATP 10mM dGTP 10mM dTTP
FACS buffer	PBS 0.5% FCS 2mM NaN_3

Laemmli Buffer	250mM Tris base 1.92M Glycine 1% SDS
Organ Lysis buffer for WB	10mM EDTA 100mM NaCl 0.5% NP40 0.5% Sodium deoxycholate 10mM Tris HCl pH7.5
N_2A Lysis buffer for SOD assay	25mM Tris Phosphate pH7.8 10mM EDTA 50% Glycerol 5% Triton X-100
N_2A Lysis buffer for Western Blot	10mM Tris 100mM NaCl 10mM EDTA 0.5% Triton-X100 0.5% Na deoxycholate
PBS 1x (phosphate buffered saline)	3mM KH_2PO_4 10mM Na_2PO_4, $2H_2O$ 137mM NaCl
Ponceau S	0.2% Ponceau S 5% Acetic acid
Protein gel loading buffer 2x	62.5mM Tris pH6.7 10% SDS 8% β–mercaptoethanol 5% Glycerol Bromophenol blue
SDS-PAGE Gel 12%	12% Rotiphorese Gel 30 (acrylamide 30% solution) 0.4M Tris-HCl pH 8.9 0.1% SDS 0.05% APS 0.1% TEMED

Stacking-PAGE Gel	12% Rotiphorese Gel 30 (polyacryl 30% solution) 0.4M Tris-HCl pH 8.9 0.1% SDS 0.05% APS 0.1% TEMED
Semi-dry transfer buffer	25mM Tris 192mM Glycine 0.1% SDS 10% Methanol
Sytox/Hoechst	1mM Sytox 0.2g/l Hoechst
TEA 50x	2M Tris base 0.05M EDTA 1M acetic acid
Towbin buffer (wet-transfer buffer)	25mM Tris 192mM Glycine 0.1% SDS 20% Methanol
TNT	150mM NaCl 10mM Tris HCl pH 8 0.05% Tween 20

Buffers used for cerebellar granular neurons preparation:

Name	*Composition*
Solution 1	120.9mM NaCl 4.83mM KCl 1.22mM KH_2PO_4 25.5mM $NaHCO_3$ 13mM Glucose 1.2mM $MgSO_4$, 7 H_2O 20mM HEPES 3%BSA Phenol red
Solution 2	120.9mM NaCl 4.83mM KCl 1.22mM KH_2PO_4 25.5mM $NaHCO_3$ 13mM Glucose 1.2mM $MgSO_4$, 7 H_2O 20mM HEPES 3% BSA 0.2mg/ml Trypsin 0.1mg/ml DNAse Phenol red
Solution 3	120.9mM NaCl 4.83mM KCl 1.22mM KH_2PO_4 25.5mM $NaHCO_3$ 13mM Glucose 2.7mM $MgSO_4$, 7 H_2O 20mM HEPES 0.3%BSA 0.52mg/ml SBTI 0.1mg/ml DNAse Phenol red

Solution 4	120.9mM NaCl 4.83mM KCl 1.22mM KH_2PO_4 25.5mM $NaHCO_3$ 13mM Glucose 1.44mM $MgSO_4$, 7 H_2O 16.8mM HEPES 2.52%BSA 0.0832ml/ml STBI 0.016mg/ml DNAse Phenol red

2.1.1.3 Cell Culture media

Cell type	*Medium*
CGN	= Neuronal maintenance medium: Neurobasal A 1% L-Glutamine B27 1x without antioxidant 1% Penicillin/Streptomycin 20mM KCl
Hela S3	DMEM 10% FCS 1% L-Glutamine 1% Penicillin/Streptomycin
N_2A	DMEM 10% FCS 1% L-Glutamine 1% Penicillin/Streptomycin

Whole brain neurons	50% F-12 50% IMDM 10% FCS 1% Penicillin/Streptomycin
U_{251}	DMEM 10% FCS 1% L-Glutamine 1% Penicillin/Streptomycin

2.1.1.4 Antibodies

Name	*Target*	*Type*	*Manufacturer*
Primary Antibodies			
Actin (6 isoforms)	Actin	Monoclonal, mouse	Chemicon
GFAP	Astrocytes	Polyclonal, rabbit	Dako Cytomaton
NeuN	Nucleus of neuron	Monoclonal, mouse	Chemicon
Phospho JNK1/JNK2/3	Phospho JNK1/JNK2/3	Polyclonal, rabbit	Cell signalling
phospho p38	phospho p38	Polyclonal, rabbit	Cell signalling
phospho p42/p44	phospho p42/p44	Polyclonal, rabbit	Cell signalling
6H4	PrP	Monoclonal, mouse	Prionics
Secondary Antibodies			
Name			*Manufacturer*
Goat anti mouse Alexa 568			Molecular Probe
Goat anti rabbit Alexa 488			Molecular Probe
Goat anti mouse HRP			Pharmigen
Goat anti rabbit HRP			DAKO

2.1.2 Kits

	Name	*Manufacturer*
DNA extraction for PCR	High Pure PCR template Preparation kit	Roche
PNGase F	PNGase F kit	New England Biolabs
Protein determination	BCA protein assay reagent	Pierce
Superoxide dismutase assay	Kit SOD Assay Kit-WST	Dojindo
Western blot revelation	Advance western blotting detection kit	Amersham

2.1.3 Plamids

Name	*Vector*	*Insert*	*Source*	*Reference*
pL15TK (mock vector)	Custom-made expression vector (HCMV immediate-early promoter; HSV-TK polyadenylation-signal)	none	A. BÜRKLE	(Kupper, et al., 1990)
pCMV-wtPrP (wt-PrP)	pl15TK	Mouse wt PrP	A. BÜRKLE	(Holscher, et al., 1998)
pCMV-Δ114-121PrP (Δ8TM1-PrP)	pl15TK	Mouse Δ114-121PrP	A. BÜRKLE	(Holscher, et al., 1998)
pcDNA3.1 Δ43-91 (Δocta-PrP)	pcDNA3.1	Mouse Δ43-91PrP	H. SCHÄTZL	(Gilch, et al., 2004)
pCR3-Thy1 (Thy1)	pCR3	Thy-1	D. LEGLER	Unpublished
pDSRed2-C1	pDSRed2-C1	DSRed	D. LEGLER	
pEGFP	pEGFP	EGFP	A. BÜRKLE	

2.1.4 Cells

Cells were routinely tested by Ms Katharina Hüttner (lab technician) for mycoplasma and they were found to be mycoplasma negative.

2.1.4.1 N_2A

The murine neuroblastoma cell line N_2A was purchased from the American Type Culture Collection.

The N_2A subclones (H6, H12, D11, G9 and F1) used have been described (Zhang, et al., 2002).

2.1.4.2 U_{251}

The human glioblastoma cell line U_{251} was purchased from the American Type Culture Collection.

2.1.4.3 HeLa

The human cervical carcinoma cell line HeLa was purchased from Karolinska Institute, Stockholm, Sweden.

2.1.5 Mice

Subcloning of the coding sequences of wt-PrP and Δ8TM1–PrP into the empty vector MoPrP.Xho had been done by Hartmut Niemann (DKFZ, Heidelberg, Germany) (Borchelt, et al., 1996). Microinjection of PrPΔ114-121 MoPrP.Xho in fertilized mouse embryos (C3H x C57BL6) led to two founders called M630 and F902. Generation and some phenotypic characterization of the F902 line has recently been described (Baumann, et al., 2007).

In the present work, the mice were crossed as follows:

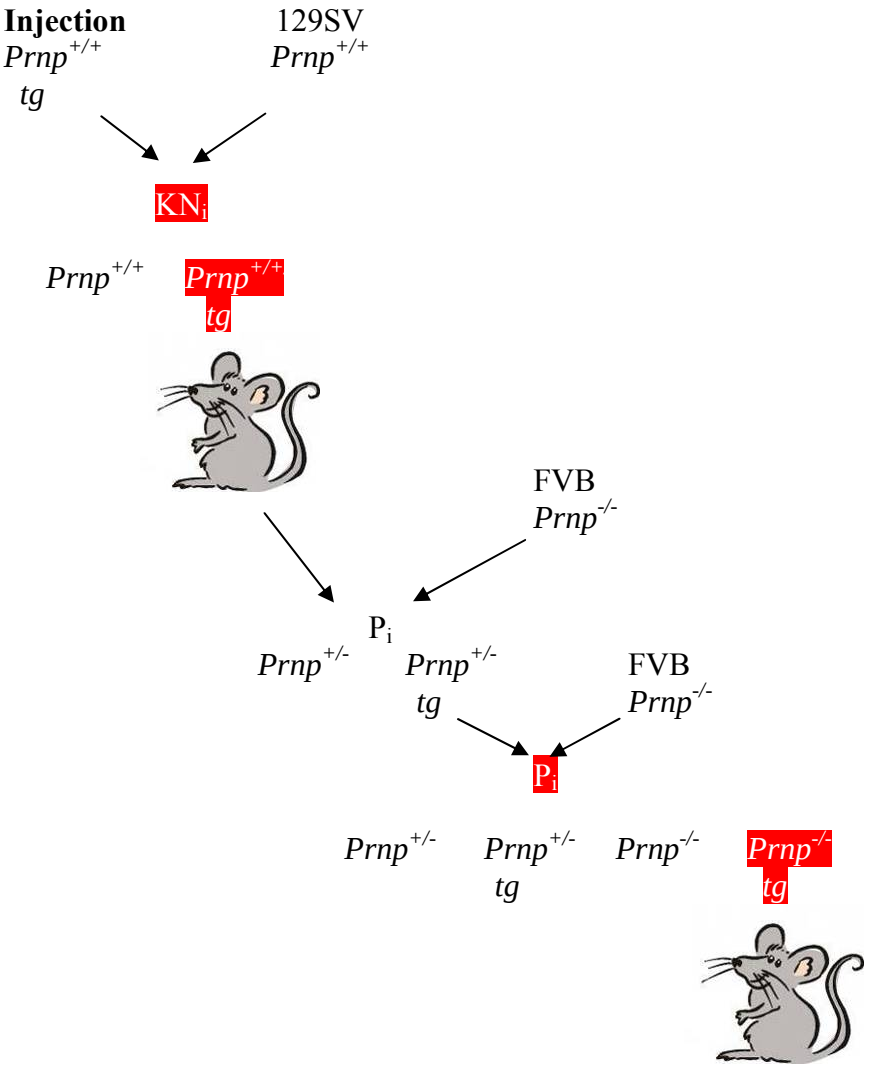

Fig6. **Breeding scheme of tg mice expressing Δ8TM1.** KN_i, P_i i = mouse number. *Tg* = transgenic mouse carrying MoPrPΔ114-121Xho plasmid.

The *Prnp*$^{-/-}$ FVB mice were a generous gift from Prof. J. Collinge.

2.2 Methods

2.2.1 Genotyping of mice

Tails were cut in small pieces and put in 1.5ml tube. DNA extraction was performed according to the protocol from "High Pure PCR template Preparation kit" (Roche) with minor modifications.

Briefly, 200µl Lysis Buffer and 40µl Proteinase K solution were added to tail biopsies, followed by vortexing and incubation of 24 - 48h at 55°C with agitation. When tails were lysed 200µl Binding Buffer and 100µl isopropanol were added, followed by mixing and centrifugation for 3 min at 8,000 *g*. The supernatant was put on a column and a collecting tube and the whole assembly was centrifuged one min at 8,000 *g*. Then 500µl Wash Buffer was added and centrifuged for 1 min at 8,000 *g*. This step was repeated. The filters were put on new tubes and 200µl Elution Buffer prewarmed at 70°C were added. After a centrifugation one min at 8000 *g* each tube contained the DNA solution.

The following primers were used in order to check for the presence of the transgene:

- Primer A: PrP 3´End: GGA TCT TCT CCC GTC GTA ATA GGC
- Primer C: PrP Δ8TM1 5´End: TGT GGC AGG GGG TGG CCT TGG.

The following primers were used in order to check the *Prnp* status:

- Primer P4: PrP 3´End: GGA CCC TTA CTT GTT TCC AAA CGA AAG TT
- Primer P3: PrP 5´End: ATT CGC AGC GCA TCG CCT TCT ATC GC
- Primer P10: PrP neo 5´End: GTA CCC ATA ATC AGT GGA ACA AGC CCA GC.

The primers P4 + P3 reveal the presence of the $Prnp^{-/-}$ status whereas the primers P4 + P10 reveal the $Prnp^{+/+}$ status.

In order to perform the PCR, a reagent mix was prepared. It was containing, per sample, 2µl DNA, 19.4µl H_2O, 2.5µl Hotmaster Taq Buffer 10x, 0.5µl dNTPs 40mM, 0.2µl of each primer 10pmol/µl and 0.2µl Hotmaster Taq. The following PCR programme was used: 5min 94°C, 30sec 94°C, 45sec 70°C, 1min 72°C (the three last 35 times), 10min 72°C, 8°C forever.

PCR products were loaded in loading buffer on 2% agarose gels.

2.2.2 Preparation of brain cells

2.2.2.1 Primary cells from whole brain

Newborn mice (less then two days old) were decapitated. Tails were sampled for genotyping. The whole brain was removed and placed in 1 ml special medium for primary cells. This medium comprised 50% F-12, 50% IMDM, 10% FCS and 1% penicillin/streptomycin. Brain dissociation was performed by using a cannula (0.8 x 40mm, Terumo). Brain was passed several times through this cannula and then the cells were plated on poly-L-lysine-coated 25cm² flasks (Biocoat) in 5ml medium.

2.2.2.2 Cerebellar Granular Neurones (CGN)

Seven-day old mice were decapitated. Tails were sampled for genotyping. The cerebellum was removed, cut in small pieces and placed in 1 ml solution 1. After 2 min centrifugation at 300 *g*, the pellet was resuspended in 1 ml of solution 2 and agitated 15min at 37°C. Then 1 ml of solution 4 was added followed by 6min centrifugation at 300 *g*. The pellet was resuspended in 1 ml of solution 3. Cells were dissociated several times by passing through a cannula (0.8 x 40mm, Temuro) and one ml of Neuronal maintenance medium was added. After 6min centrifugation at 300 *g*, cell pellet was resuspended in 5ml Neuronal maintenance medium. 500µl of cell suspension per well was seeded into PLL-coated 24-well plates and 200µl of cell suspension on PLL coated slide chambers. After one hour medium was exchanged and 2 days later 10µM cytosine arabinoside was added. Cultures were ready for experiments on day 7.

2.2.3 Brain cell culture

2.2.3.1 Primary cells of whole brain

Two days after explantation, medium was exchanged. When the cells were confluent, they were diluted 1:2 (2x25cm² flasks) and if necessary. On the same day, primary brain cell cultures were split and seeded for FACS analysis, immunofluorescence and Western blot. If the cell number was insufficient, the cells were at least seeded for FACS and immunofluorescence and the culture was kept.

2.2.3.2 CGN

After 1 h cell-plating medium was exchanged and two days later 10µM cytosine arabinosid was added. Cultures were ready for experiments on day 7.

2.2.4 Culture of established cell lines

2.2.4.1 N_2A and subclones

N_2A cells were routinely maintained in Dulbecco's Modified Eagle's Medium (DMEM), containing 10% heat-inactivated Fetal Calf Serum, 1% L-glutamine and 1% penicillin/streptomycin at 37°C in 5% CO_2.

2.2.4.2 U_{251}

U_{251} cells were routinely maintained in Dulbecco's Modified Eagle's Medium (DMEM high glucose), containing 10% heat-inactivated Fetal Calf Serum (FCS), 1% L-glutamine and 1% penicillin/streptomycin at 37°C in 5% CO_2.

2.2.4.3 HeLa

HeLa cells were routinely maintained in Dulbecco's Modified Eagle's Medium (DMEM), containing 10% heat-inactivated Fetal Calf Serum, 1% L-glutamine and 1% penicillin/streptomycin at 37°C in 5% CO_2.

2.2.5 Transfection

N_2A cells were transfected with JetPEI following the manufacturer's instructions. JetPEI is a linear polyethylenimine, which leads to compaction of DNA into positively charged particles that interact with anionic proteoglycans at the cell surface and induces endocytosis. Briefly, cells were seeded in 24-well plates. The next day, transfection was performed by applying 1µg DNA (in 50µl NaCl 150mM) to which had been added 2µl JetPEI (in 50µl NaCl 150mM). The whole mix was incubated 30 min at room temperature and then added dropwise onto the cells.

2.2.6 Measurement of mitochondrial membrane potential (TMRE staining)

Tetramethylrhodamine ethyl ester perchlorate (TMRE) was used as a fluorescent probe for the mitochondrial membrane potential (Nicholls and Ward, 2000), as it only accumulates in the negatively charged matrix of mitochondria displaying an electrochemical gradient.

The staining was performed according to the literature (Scaduto and Grotyohann, 1999). Briefly, 1 d post-transfection, medium was exchanged and cells were treated or not with 100µM copper chloride hydrate ($CuCl_2$, Sigma) for 1 day. Then cells were washed with PBS and fresh medium was added. The cells were then incubated with 4µM TMRE for 15min. The cells were washed with PBS and trypsinized (100µl trypsin solution per well). When the cells had detached, 100µl FACS Buffer was added and the cell suspension was collected in small tubes. Then FACScan analysis was performed.

In case of primary cells and CGN, the identical procedure was performed, except for omission of copper treatment. On the day of the experiment, medium was exchanged. The cells were then treated with 4µM TMRE for 15min, washed with PBS and trypsinized (100µl pro well). When the cells had detached, 100µl FACS buffer was added and the cell suspension was collected in small tubes. Then FACScan analysis was performed.

2.2.7 Measurement of Reactive Oxygen Species (H_2DCFDA staining)

2',7'-Dichlorohydrofluorescein diacetate (H_2DCFDA) is a well-established probe for ROS and staining protocols have been published (Sohn, et al., 2002) and (Sauer, et al., 2003). H_2DCFDA is a non-fluorescent dye, which is cleaved in the presence of H_2O_2 and/or peroxidase into the fluorescent compound dichlorohydrofluorescein (DCF) and therefore is a tool to measure intracellular ROS levels.

One day post-transfection, medium was exchanged and cells were treated or not with 100µM $CuCl_2$ for 1 day. Then cells were washed with PBS and fresh medium was added. Cells were then treated with 15µM H_2DCFDA (Molecular Probes) in the presence or in absence of 3mM hydrogen peroxide (H_2O_2, Merck) for 30min. Then cells were washed with PBS and trypsinized (100µl pro well). When the cells did not attached anymore, 100µl FACS buffer were added and the cell suspension was collected in small tubes. Then FACScan analysis was performed.

In case of primary cells and CGN, the identical procedure was performed, except for omission of copper treatment. On the day of the experiment, medium was exchanged. The cells were then treated with 15µM H_2DCFDA in the presence or in absence of 3mM H_2O_2 for 30min. The cells were washed with PBS and trypsinized (100µl pro well). When the cells had detached, 100µl FACS buffer were added and the cell suspension was collected in small tubes. Then FACScan analysis was performed.

2.2.8 Flow-cytometric analysis (FACS)

"Fluorescence-activated cell sorting" (FACS) is a technique to measure the properties of particles as they move in a stream of fluid. The sample is dissociated into single particles in the stream, and as the particles flow in single file through an illuminated volume, light scattering (forward [FSC-H] and side scatter [SSC-H]) and emission of light from excited fluorescent markers (FL-H) are detected by photomultiplier tubes.

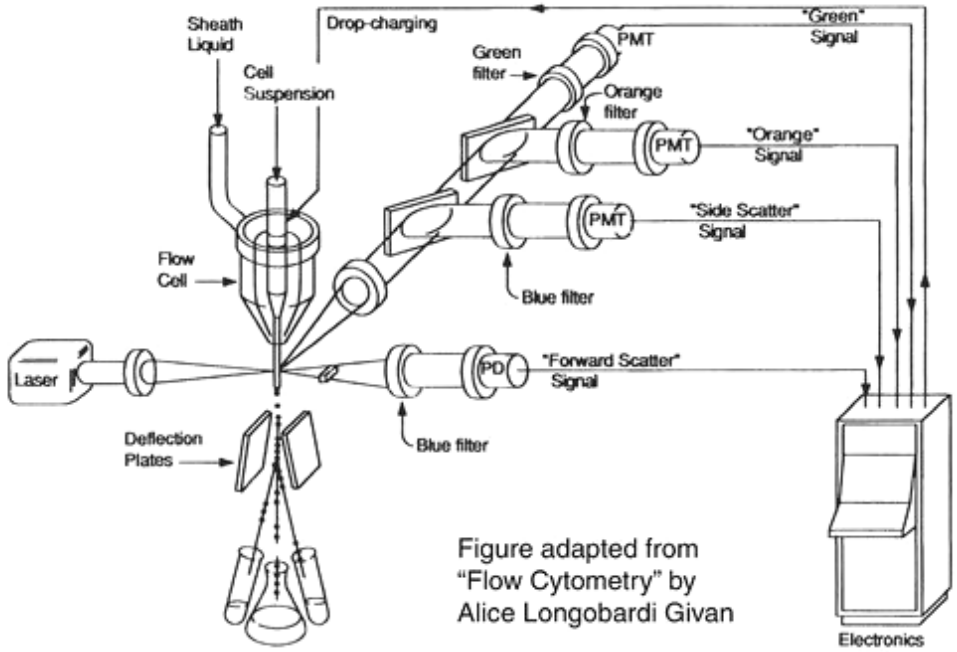

Fig7. **Scheme of FACS machine** (*From*: http://openwetware.org/wiki/BE.109:DNA_engineering/FACS_analysis). Single particles from a cell suspension flow through a laser which gives forward scatter and side scatter. At the same time emissions coming from fluorescent markers are also detected.

Analyses were performed with a FACScan Flow cytometer (Beckton Dickson Biosciences, Mountain View, CA). This flow cytometer was equipped with Cell Quest version 3.3 software and analyses were performed with FlowJo 6.0 programme (TreeStar).

FACS settings:

Cells	FSC	SSC	FL-1 (green)	FL-2 (red)
Transfected N_2A	E-1 3.06 lin	304 1.06 lin	430 log	355 log
Primary cells	E-1 3.04 lin	311 2.39 lin	478 log	315 log
CGN	E-1 3.15 lin	311 2.39 lin	478 log	315 log

2.2.9 Sytox/Hoechst staining

Cells were seeded on 12-well plates and mock transfection or transfection with wt-PrP or Δ8TM1-PrP was carried out 1 d later. On day 3 and 4 cultures were rinsed and stained with 1µl mix solution of Sytox/Hoechst for 10min at 37°C. This mix solution contained Sytox 1mM, Hoechst 0.2g/l in dimethylsulphoxide (DMSO). Images were acquired on a Zeiss Axiovert S100TV microscope.

Sytox stains necrotic cells in green and the Hoechst dye permits distinguishing healthy cells from apoptotic cells via DNA condensation.

2.2.10 Immunofluorescence (IF)

Primary cells were seeded on poly-L-Lysine coated coverslips on the same day as seeding for FACS (see above). As controls, N_2A (neuroblastoma cells) and U_{251} (glioblastoma cells) were also seeded. On the day of FACS analysis, cells were fixed with 4% PFA for 30min at 4°C. The coverslips were rinsed in PBS and the cells were permeabilised with 0.4% Triton X-100 in PBS 15°C at room temperature. Then coverslips were rinsed in PBS three times. Then samples were incubated in the first blocking solution (PBS, 0.05% Tween 20 [also termed PBST], 3% BSA) for 1 h at room temperature. Anti-NeuN antibody detecting neurones (primary antibody # 1; diluted 1:200 in PBST/BSA) was applied to the coverslips overnight at 4°C. The next day, the coverslips were rinsed 3 times in PBS and then secondary antibody (goat-anti-mouse conjugated with Alexa 568) was added at the dilution 1:1000 and incubated 1 h at room temperature in dark. Then coverslips were rinsed 3 times in PBS and second blocking solution (PBST, 5% non-fat dry milk) was added for 1 h at room temperature. Anti-GFAP detecting glial cells (primary antibody #2; diluted 1:200 in PBST/5% non-fat dry milk) was applied to coverslips overnight at 4°C. The next day, coverslips were rinsed 3 times with PBS followed by incubation with secondary antibody (goat-anti-rabbit conjugated with Alexa 488; diluted 1:1,000) for 1 hour at room temperature. After rinsing 3 times in PBS, nuclei were stained with Hoechst (1:20,000) and then the coverslips were mounted with Aqua Poly Mount solution.

In case of chamber slides, the procedure was identical except for adjustment of volumes.

Images were acquired on a Zeiss Axiovert S100TV microscope.

2.2.11 Protein determination (BCA technique)

Protein determination was performed using a colorimetric assay based on reaction between BCA and proteins. In order to establish a standard curve, a serial dilution of BSA was prepared resulting in the following concentration: 0, 0.2, 0.4, 0.6, 0.8, 1.0 and 1.2 mg/ml.

The BCA working solution contained one part of solution B (Cu solution) and 50 parts of solution A (BCA).

5µl of each sample (diluted if necessary) and standard dilution were placed in triplicate in a flat-bottom 96-well plate. Then 100µl of BCA working solution was added. Plates were incubated 30min at 37°C and then absorption was read at 550nm in an ELISA plate reader.

2.2.12 Western blot

2.2.12.1 Transfected cells

Cells were mock-transfected or transfected with wt-PrP, Δ8TM1-PrP or Δocta-PrP. Upon reaching confluency, cells were rinsed three times with PBS and lysed with N_2A lysis buffer for Western Blot for 30 min on ice. Each lysate was collected in a separate tube, followed by determination of protein concentration. Samples were heated in loading buffer for 5min and 50µg of protein was loaded on 12% SDS-PAGE gel and electrophoresed at 20mA for two hours. Western blotting on PVDF membranes was carried out either by wet-transfer or a semi-dry-transfer.

Ponceau S staining of membranes was done to check for transfer efficiency. The membrane was blocked in TBS / 0.05% Tween 20 (TNT) plus 5% non-fat dry milk for 1h at RT and then incubated with first antibody diluted in TNT / 5% non-fat dry milk overnight. The primary antibodies used were 6H4 (1:10,000), phospho-p38, phospho-p42/p44 or phospho-JNK1/JNK2/3 (1:1,000). After three washes with TNT the membranes were incubated with the appropriate secondary antibody (goat anti rabbit or goat anti mouse) coupled with horseradish peroxidase (1: 2,000 in TNT/non-fat dry milk) for 1 h. After three washes with TNT the membranes were incubated with ECL advanced solution and exposed using a LAS-1000 ECL imager.

2.2.12.2 Mouse organs

In parallel to the preparation of CGN the rest of brain was taken off, directly frozen in liquid nitrogen and stored at -80°C. Brain tissues were lysed in lysis buffer-harsh (approximately 10 volumes) supplemented with protease inhibitors. Tissue was dissociated by repeated passage through a cannula. Protein determination and PNGase F digestion was performed as follows: 10µl of each sample was diluted with 90µl MilliQ water and supplemented with 11.1µl glycoprotein denaturating buffer, followed by heating to 95°C for 5 min. Then 11.1µl of G7 reaction buffer, 11.1µl of NP-40 buffer and 2µl PNGase F were added, followed by incubation overnight at 37°C.

After addition of 27µl of 5x protein loading buffer samples were boiled for 5 min, loaded on 12% SDS-PAGE gels and electrophoresed at 20mA for 2h. Then semi-dry transfer was performed on PVDF membranes for 1 h at 20V.

The membrane was blocked in TBST / 5% non-fat dry milk for 30min at room temperature and then incubated with primary antibody 6H4 (1:30,000) in TNT / 5% milk for 45min at room temperature. After three washes with TNT the membranes were incubated with a goat anti-mouse secondary antibody coupled with HRP (1:2,000) in TNT milk for 1 h. After three washes with TNT the membranes were incubated with ECL advanced solution and exposed using a LAS-1000 ECL imager.

2.2.13 SOD assay

The SOD test of Dojudo Molecular Technologies is a colorimetric competition assay based on xanthine/xanthine oxidase as a source of superoxide.

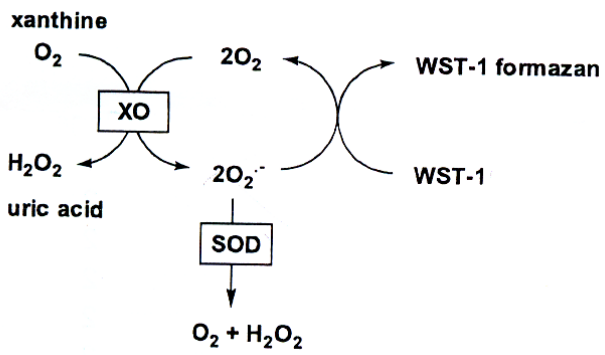

Fig8. **SOD test basis.** WST-1 formazan is yellow.

N_2A cells were seeded in P10 dishes and mock-transfected or transfected with, wt-PrP or Δ8TM1-PrP. One day post-transfection the cells were rinsed three times with PBS and then lysed with 1ml lysis buffer for SOD test on ice for 1 h. Each lysate was collected in a tube and underwent three freeze-thaw cycles using liquid nitrogen. Then protein determination was performed.

Assays were performed according to the manufacturer's instructions. 100µg of protein per sample was used.

2.2.14 Statistical analyses

2.2.14.1 Statistical analyses of the data from transfection assays

Each experiment was done at least in duplicate and the average of those points gave the measure of the day.

Crude data were normalized as follows: The average from all untreated mock mean values was set to be 100%. All other data were expressed as percentage compared to the mock value of the respective experiment.

T-tests were applied on data from FACS and SOD assays. $p<0.05$ was considered significant. Software used was Analyse-it (Analyse-it Software Ltd).

2.2.14.2 Statistical analyses of the data from assays on primary brain cells and CGN

Each experiment was done at in duplicate and the average of those two points gave the measure of the day.

No normalization was done.

Mann-Whitney tests were performed. $p<0.05$ was considered significant. Software used was Analyse-It (Analyse-it Software Ltd).

3 Results

3.1 Transfection assays with N_2A cells

3.1.1 N_2A transfected with empty vector, wt-PrP or Δ8TM1-PrP

In order to investigate the physiological function of PrP and especially the involvement of the TM1 domain of PrP, N_2A cells were transfected with the empty vector (mock transfection), wt-PrP or Δ8TM1-PrP. The mitochondrial membrane potential (ΔΨ), basal intracellular ROS levels and oxidative stress response in these transfected cells were assessed.

3.1.1.1 Impact of PrP (wt or Δ8TM1) overexpression on the mitochondrial membrane potential (ΔΨ)

In order to check the mitochondrial membrane potential (ΔΨ), TMRE was used as a probe. TMRE only accumulates in the negatively charged mitochondrial matrix of mitochondria displaying an electrochemical gradient and so stains functional mitochondria. For quantification FACS analysis were performed.

Untransfected cells were used to gate living cell (circle = R1; Fig. 9a). In all cases the background fluorescence was determined on transfected cells without TMRE (Fig. 9b).

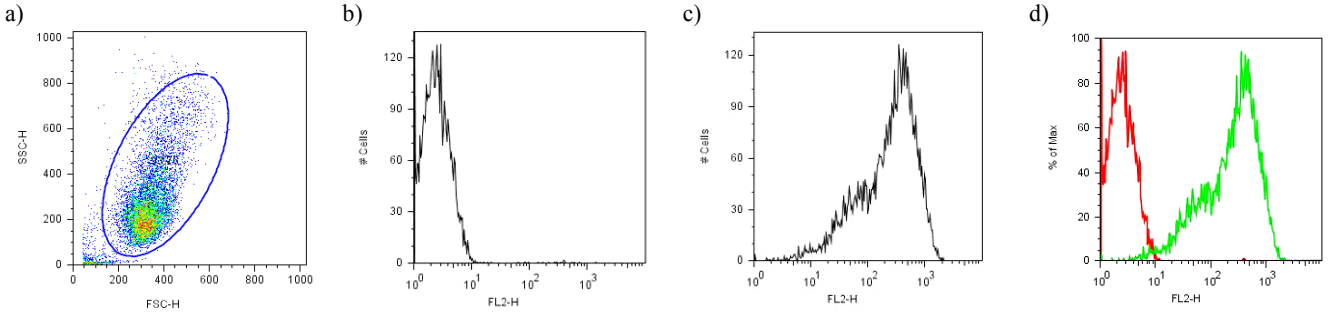

Fig9. **FACS Setting. a)** Living cells gating; **b)** Cells not stained with TMRE, defining the background fluorescence; **c)** Cells stained with TMRE (FL-2); **d)** Overlay b) and c).

In order to be sure to gate PrP-transfected cells, co-transfections were performed as follows: pEGFP with empty vector, pEGFP with wt-PrP or pEGFP with Δ8TM1-PrP. Only cells that were GFP positive were gated (R2), and means for TMRE intensity were calculated.

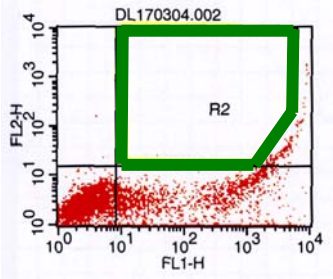

Fig10. **Gating for GFP and TMRE-positive cells (R2)**
FL-1 = green = GFP
FL-2 = red = TMRE.

All experiments were done in triplicate and the average of the 3 mean values was given as a data point. Student's t-Test was performed to determine statistical significance.

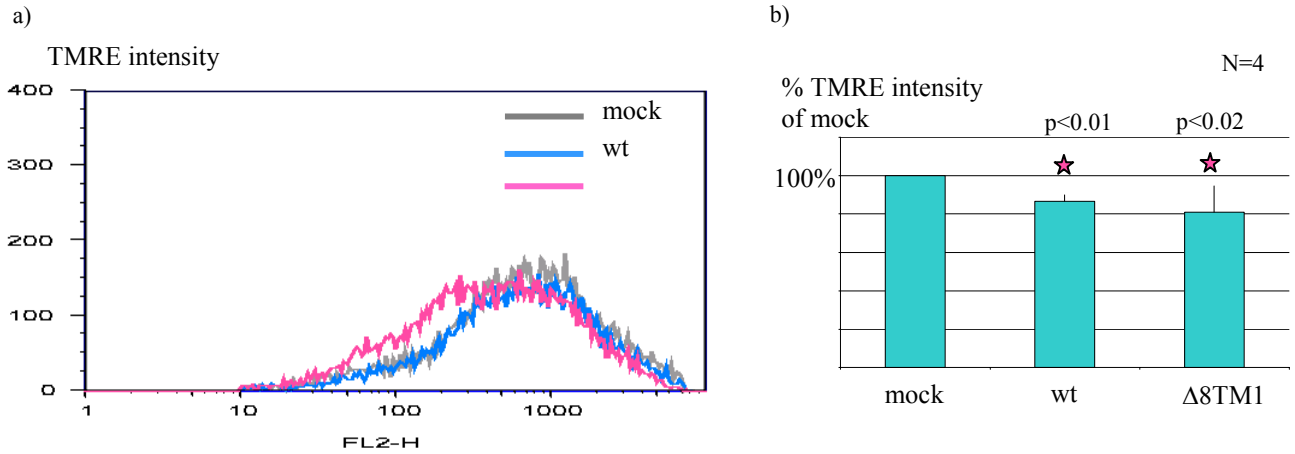

Fig11. **Mitochondrial membrane potential in transfected cells. a)** A representative example of original FACS data for mock, wt-PrP (wt) and Δ8TM1-PrP (Δ8TM1) transfected cells is shown; **b)** Compilation of data from 4 independent experiments. T-test was performed; asterisk denotes $p<0.05$. Note that in PrP (wt and Δ8TM1) overexpressing N_2A cells ΔΨ is significantly reduced compared to mock-transfected cells.

A representative FACS result is shown in Fig.11a. A single peak of TMRE fluorescence is observable in all cases. In the case of Δ8TM1-PrP transfected N_2A the peak is broader and clearly shifted towards the left, which means cells with lower intensity are more abundant.

In Fig.11b the average of mean values of TMRE intensity of four independent experiments for each transfection is plotted and statistical analysis was performed. Both in wt-PrP and Δ8TM1-PrP overexpressing N_2A the mitochondrial membrane potential (ΔΨ) is significantly lower ($p<0.025$ in both cases).

Two hypotheses can be proposed, *i.e.* PrP^c has indeed a regulatory role for $\Delta\Psi$, or the decrease in $\Delta\Psi$ is due to cell death. In order to determine which hypothesis is correct, a Sytox/Hoechst staining was performed on co-transfected cells. Sytox specifically stains necrotic cells. Four days post-transfection no difference between mock, wt-PrP or Δ8TM1-PrP overexpressing cells was observable. This result reinforces the notion that PrP^c has a regulatory for $\Delta\Psi$.

a) mock b) wt-PrP c) Δ8TM1-PrP

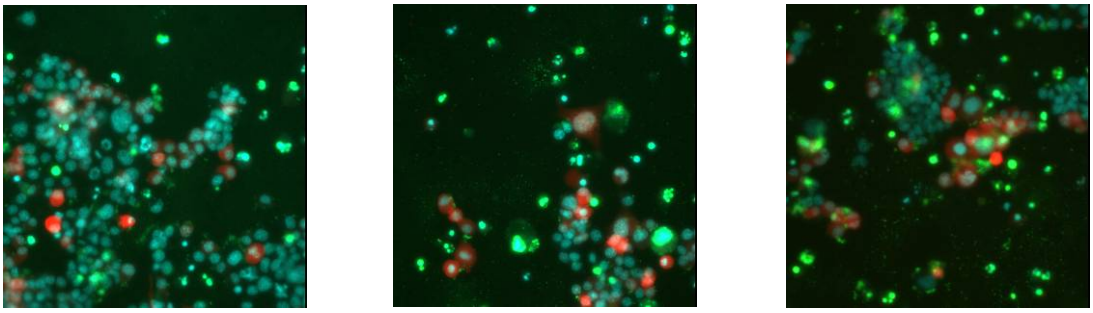

Fig12. **Sytox/Hoechst staining of cultures 4 days post-transfection.** Representative pictures are shown. **a)** mock-transfected cells; **b)** wt-PrP transfected cells, **c)** Δ8TM1-PrP transfected cells. Note that no clear difference exists between a, b, and c for Sytox staining (green).

3.1.1.2 Impact of PrP (wt or Δ8TM1) overexpression on the endogenous ROS level

In order to assess the endogenous (basal) ROS level H_2DCFDA was used as a probe. H_2DCFDA is non-fluorescent but in present of peroxidase and/or H_2O_2 it is cleaved into dihydrofluorescein (DCF), which is fluorescent. For quantification FACS analyses were performed.

Untransfected cultures were used to gate living cells (circle = R1; Fig. 13a). In all cases the background fluorescence was determined on transfected cells without incubation with H_2DCFDA (Fig. 13b).

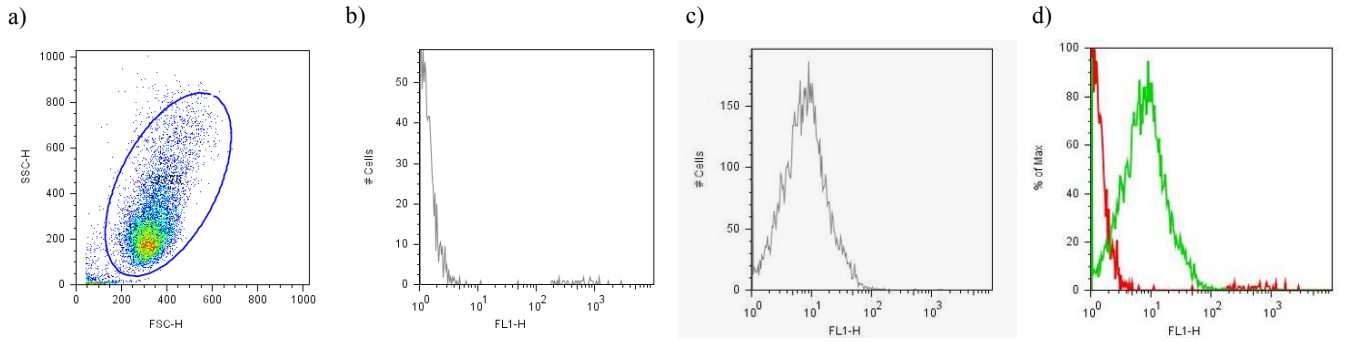

Fig13. **FACS Setting. a)** Gating of living cells; **b)** Cells not stained with H_2DCFDA, defining the background fluorescence; **c)** Cells stained with H_2DCFDA (FL-1); **d)** Overlay b) and c).

Cells were transfected and on the next day stained as described in Materials and Methods. All experiments were done in duplicate and the average of the two mean values was given as a data point. Student's t-Test was performed to determine statistical significance.

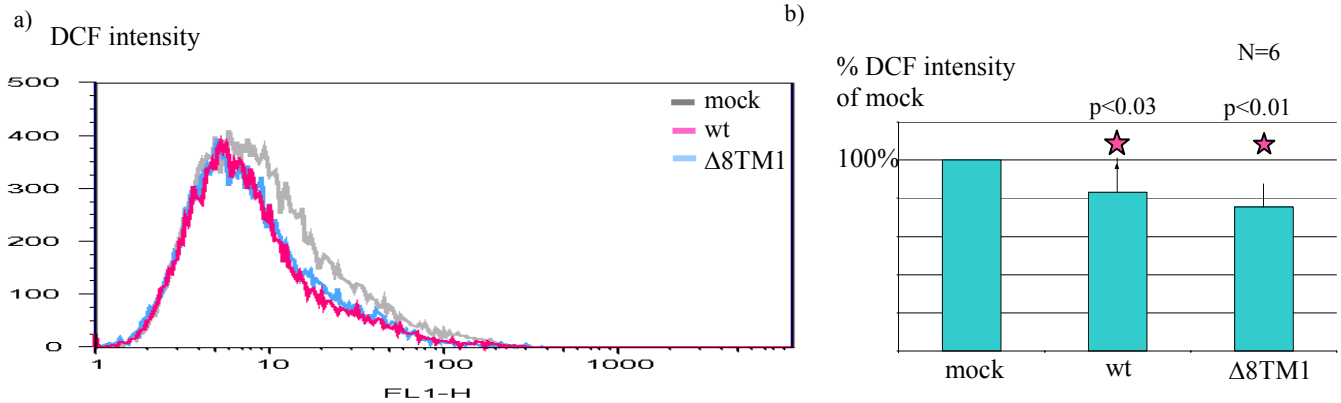

Fig14. **Endogenous ROS levels in transfected cells. a)** A representative example of original FACS data for mock, wt-PrP and Δ8TM1-PrP transfected cells is shown; **b)** Compilation of data from 6 independent experiments. T-test was performed; asterisk denotes $p<0.05$. Note that in PrP (wt or Δ8TM1) overexpressing N_2A cells endogenous ROS levels are siginificantly lower compared to mock-transfected cells.

A representative FACS result is shown in Fig.14a. In all cases a single peak is observable.

In Fig.14b the average of mean values of DCF intensity of 6 independent experiments for each transfection is plotted and statistical analysis was performed. Both in wt-PrP and Δ8TM1-PrP overexpressing N_2A cells the endogenous ROS level is significantly lower ($p<0.04$ in both cases).

3.1.1.3 Impact of PrP (wt or Δ8TM1) overexpression on the oxidative stress response of cells

ROS levels were also measured after challenging the cells with H_2O_2 (3mM 30min), added directly in the medium in the presence of H_2DCFDA (15µM 30min). For quantification FACS analyses were performed.

Untransfected cells were used to gate living cell (R1; Fig. 15a). In all cases the background fluorescence was determined on transfected cells without incubation with H_2DCFDA (Fig. 15b).

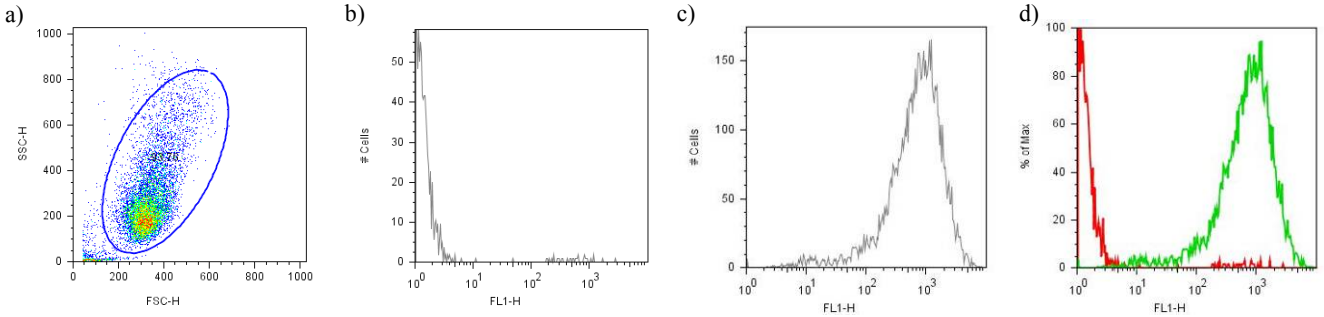

Fig15. **FACS Setting. a)** Gating of living cells; **b)** Cells not stained with H_2DCFDA, defining the background fluorescence; **c)** Cells stained with H_2DCFDA (FL-1) in the presence of H_2O_2; **d)** Overlay b) and c).

Cells were transfected and on the next day stained as described in Materials and Methods. All experiments were done in duplicate and the average of the two means values was given as a data point. Student's t-Test was performed to determine statistical significance.

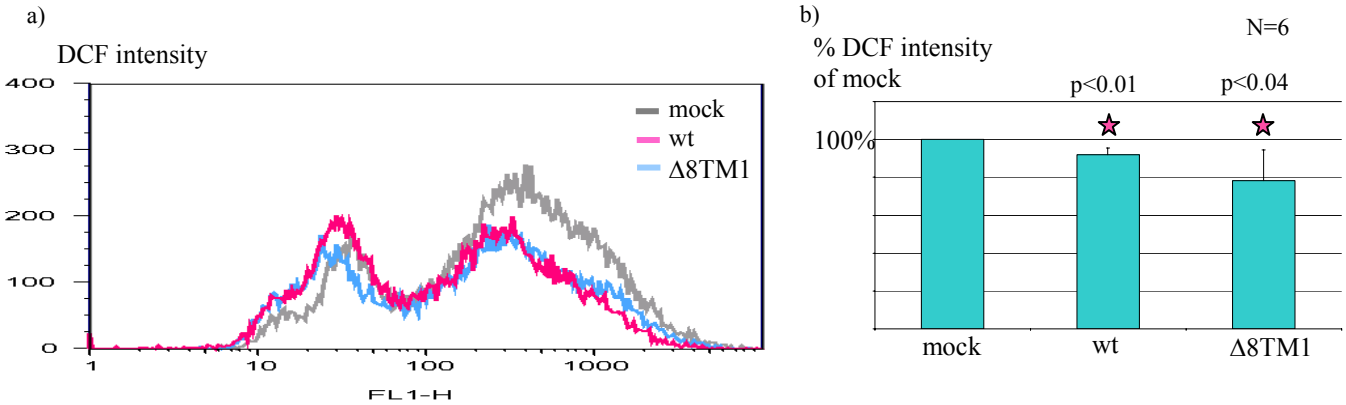

Fig16. **Oxidative stress response of transfected N_2A cells. a)** A representative example of original FACS data for mock, wt-PrP and Δ8TM1-PrP transfected cells is shown; **b)** Compilation of data from 6 independent experiments. T-test was performed, asterisk denotes p<0.05. Note that in PrP (wt or Δ8TM1) overexpressing N_2A cells after induction of oxidative stress the intracellular ROS levels are significantly lower compared to mock-transfected cells.

A representative FACS result is shown in Fig.16a. Surprisingly, in all cases a double peak is observable (see below). In case of mock-transfected N_2A the second peak is bigger whereas in PrP (wt or Δ8TM1) transfected cells both peaks are of equal height.

In Fig.16b the average of mean values of DCF intensity of 6 independent experiments for each transfection is plotted and statistical analysis was performed. Both in wt-PrP and Δ8TM1-PrP overexpressing N_2A cells the intracellular ROS level under oxidative stress is significantly lower ($p<0.05$ in both cases).

As mentioned above, the occurrence of double peaks was surprising and called for an explanation. Was it due to cellular heterogeneity with respect to H_2O_2 diffusion or, alternatively, to some other cellular property? In order to address this question, analogous experiments were done with *tert*-buthylhydroxid peroxide (tBOOH), a compound inducing sustained formation of intracellular ROS, and with buthionine sulfoximin (BSO), a compound depleting cellular glutathione, instead of the rather short-lived H_2O_2. In addition a set of N_2A subclones and also HeLa (human cervical carcinoma) cells were analysed in parallel.

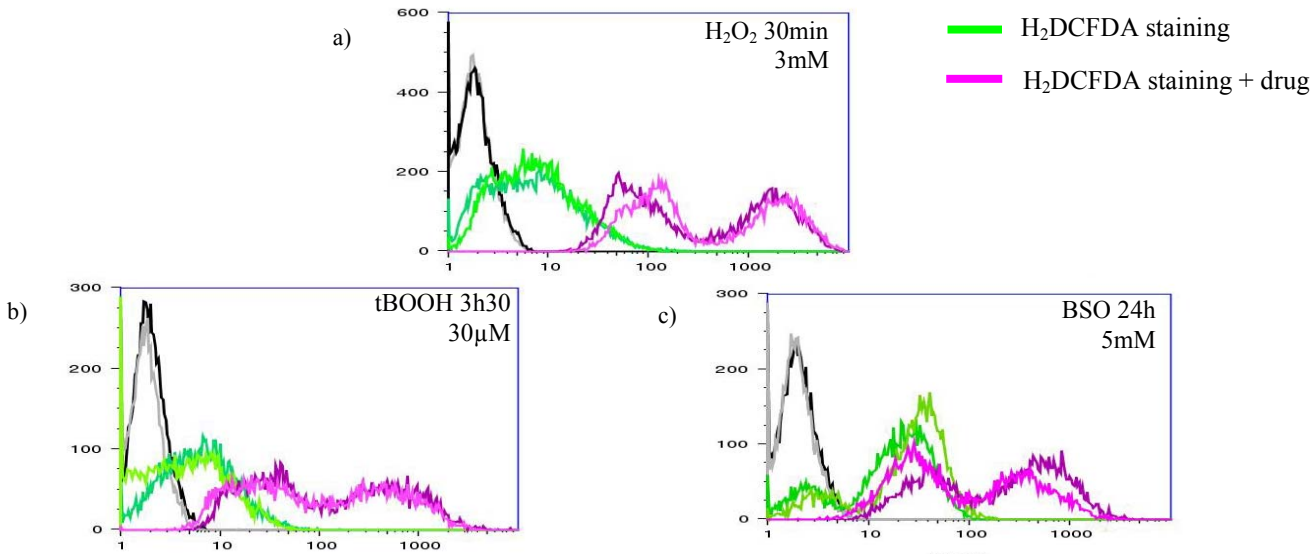

Fig17 **Intracellular ROS levels after exposure of N_2A cells to various inducers of oxidative stress. a)** H_2O_2 treatment; **b)** tBOOH; **c)** BSO. Each condition was run in duplicate and duplicates are displayed in slightly different colour, respectively. Note that upon induction of oxidative stress, the double peak (purple curves) is present in all cases. The green curves represent controls without drug exposure.

Representative FACS results are shown in Fig.17. Unstained cells are in black, endogenous ROS level (H_2DCFDA staining) are in green and ROS level after oxidative stress (H_2DCFDA staining in presence of drug) are in purple.

In all cases a double peak is observable after oxidative stress treatment. Therefore the double peak is not specific to H_2O_2 treatment because some other ROS or ROS enhancer show same result.

As a next step, as set of randomly picked N2A subclones and HeLa cells were analysed.

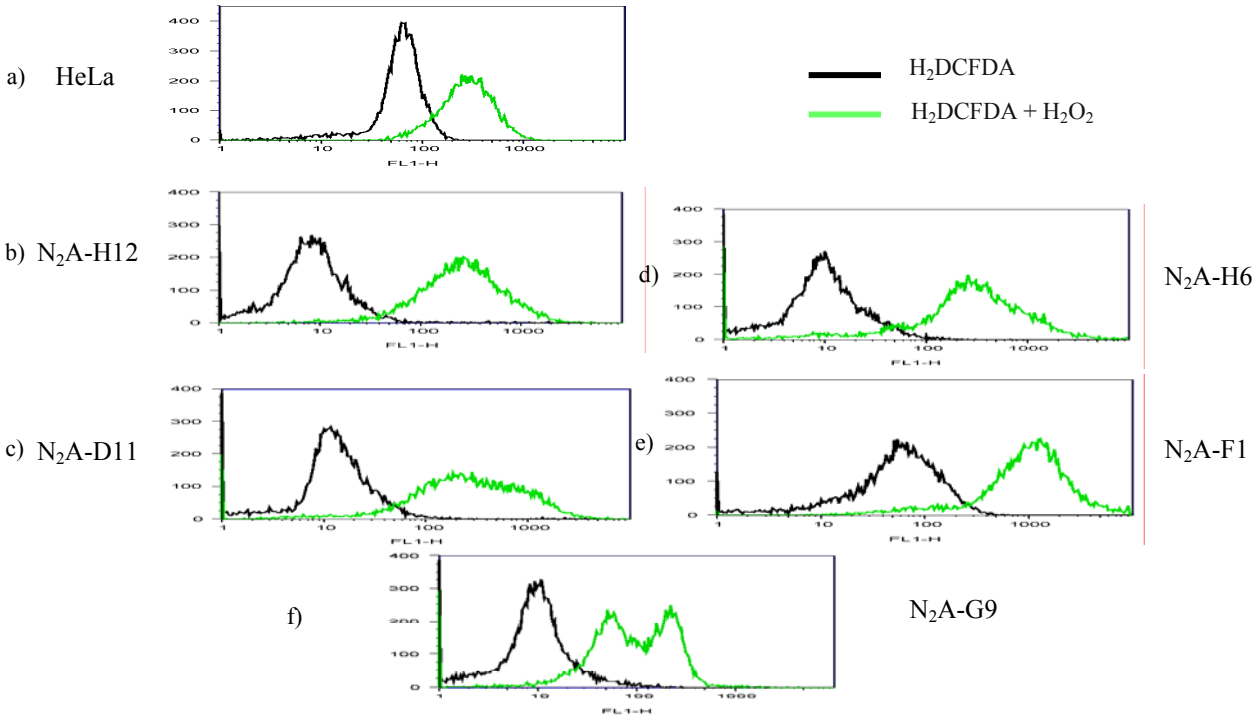

Fig18. **Endogenous ROS and ROS levels after oxidative stress in different cell types. a)** HeLa cells; **b)** N_2a subclone H12; **c)** N_2a subclone D11; **d)** N_2a subclone H6; **e)** N_2a subclone F1; **f)** N_2a subclone G9. Note the variety of patterns obtained.

Representative FACS results are shown in Fig.18. In panels **a** (HeLa), **b** (N_2A-H12), **d** (N_2A-H6) and **e** (N_2A-F1) single, "Gaussian" peaks are observable whereas panel **c** (N_2A-G9) shows a rather broad single peak and panel **f** (N_2A-H12) even a double peak. Therefore the large spread / double peak in the N_2A mass culture is apparently be due to some heterogeneity in the cell population.

Incidentally, the same set of subclones have already been shown to possess different susceptibility to scrapie infection, measured as the efficiency of PrP^{Sc} formation a few weeks after primary infection (Zhang et al., 2002). It was therefore intriguing to search for a possible link between ROS level and PrP^{Sc} susceptibility.

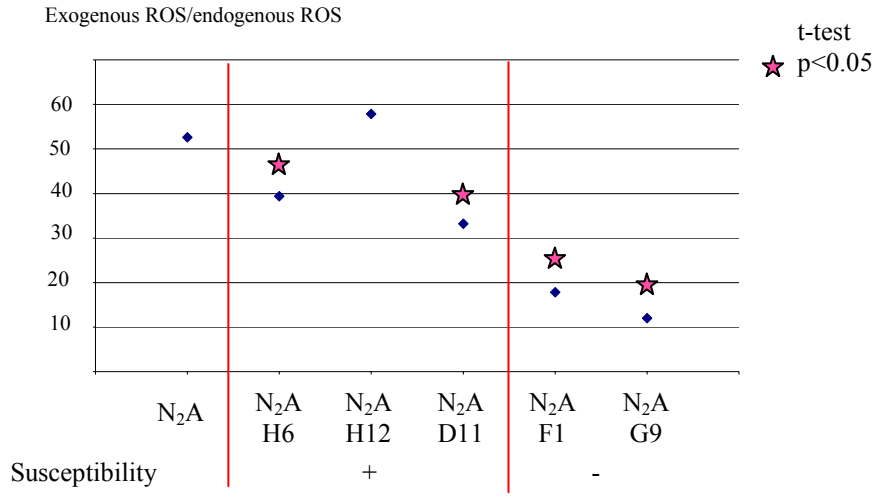

Fig19. **Possible link between susceptibility to scrapie and ROS level.** After subtraction of background signals, the ratio of induced to endogenous ROS levels was determined for N2A mass cultures, three subclones with high scrapie susceptibility and two subclones with low scrapie susceptibility. Statistical analysis was performed using Student's T-test; asterisks denote $p<0.05$. Note that the two low-susceptibility clones display the lowest ratio.

Figure 19 displays the ratios of ROS levels after oxidative stress (termed exogenous ROS) to endogenous (basal) ROS levels for N_2A mass cultures and a set N_2A subclones. Interestingly the ratio of exogenous / endogenous ROS is higher for highly susceptible N_2a subclones than for low-susceptibility cells. For the latter cells this ratio is also quite low compared to N_2A mass cultures. Although the numbers of high and low-susceptibility clones are insufficient for proper statistical analysis, the present data indeed point to some link between ROS levels and susceptibility to efficient prion replication.

3.1.1.4 SOD activity in N_2A cells overexpressing wt-PrP or Δ8TM1-PrP

An explanation for different intracellular ROS level could be a possible SOD-like activity of PrP, as has been proposed in the literature (Brown and Besinger, 1998; Brown, et al., 2001; Brown, et al., 1999); (Sakudo, et al., 2005).

Therefore a colorimetric competition assay based on xanthine/xanthine oxidase as a source of superoxide was performed in N_2A wt-PrP and Δ8TM1-PrP overexpressing cells. The assay principle is depicted in Fig. 20.

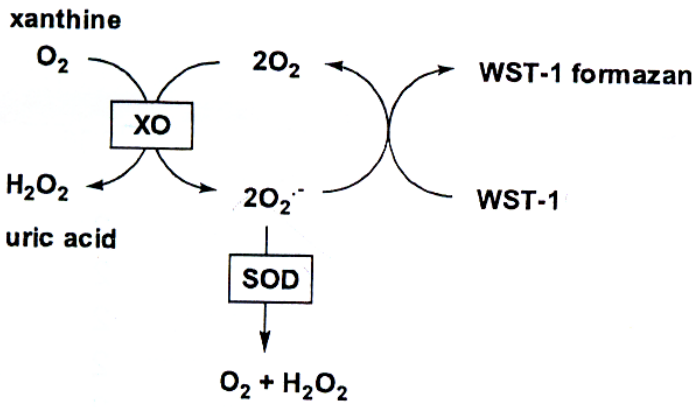

Fig20. **Principle of the SOD activity assay (Dojudo Molecular Technologies).** In the absence of SOD, WST-1 formazan is formed, which is yellow. In presence of SOD this reaction enters in competition with SOD reaction, and less or no WST-1 formazan is formed.

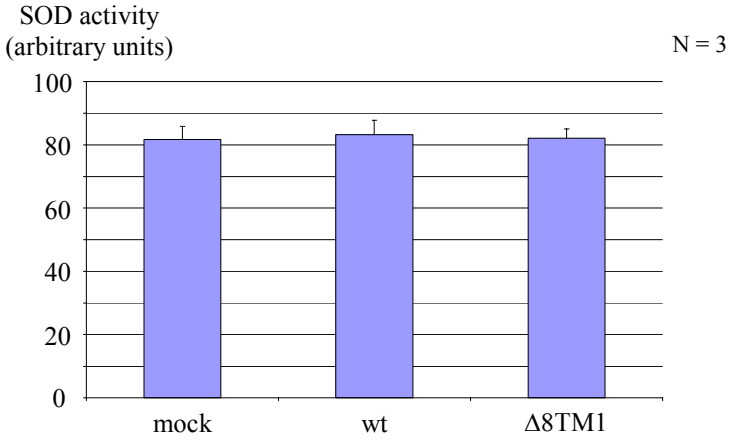

Fig21. **SOD activities in mock, wt-PrP and Δ8TM1-PrP transfected N_2A cells.** Note that there is no evidence for any changes of SOD activity by overexpression of wt-PrP or Δ8TM1-PrP.

Figure 21 show the results of three independent SOD activity assays performed in transfected cells. No difference between mock, wt-PrP and Δ8TM1-PrP transfected cells was observable in this system. The differences in intracellular ROS levels as a consequence of overexpression of the proteins as described above therefore points to some other mechanism in the cascade of cellular responses to oxidant treatment.

3.1.1.5 Transfection efficiency and specificity control

In the context of the present study, the work was focussed on *transient* transfection assays. It was therefore important to determine the transfection efficiency achieved. This was done, both in assays of endogenous ROS and oxidative stress conditions, using pEGFP transfection and subsequent FACS analysis.

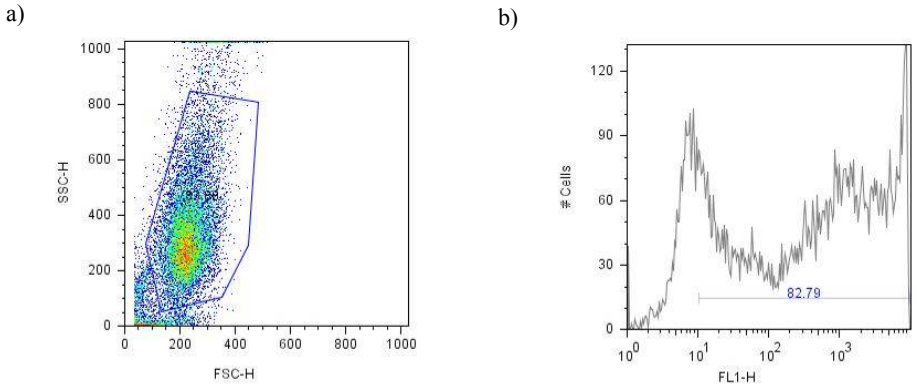

Fig22. **Transfection efficiency. a)** Gating of cells, **b)** Green intensity for pEGFP transfected cells in the gate. More then 80% of these cells are fluorescent.

Figure 22 shows a representative example. According to the results from untransfected controls (data not shown), fluorescence intensities < 10 units in the green channel were considered background. In all experiments performed, at least 60% of gated cells were EGFP-positive, which reflects the typical transfection efficiency in the experiments performed in this study.

Furthermore, in order to exclude any non-specific effects due to overexpression of proteins that are GPI-anchored, N_2A cells were transfected with Thy-1 expression construct. Thy-1 is a GPI-anchored protein commonly used as control for GPI-anchorage effects. Therefore experiments on $\Delta\Psi$, endogenous ROS and the reaction to oxidative stress were repeated for mock and Thy-1 overexpressing cells. The data showed that no differences between mock and Thy-1 transfected cells are observable (Fig. 23). Therefore the effects observed with overexpression of PrP versions are apparently not the mere consequence of overexpressing GPI-anchored proteins.

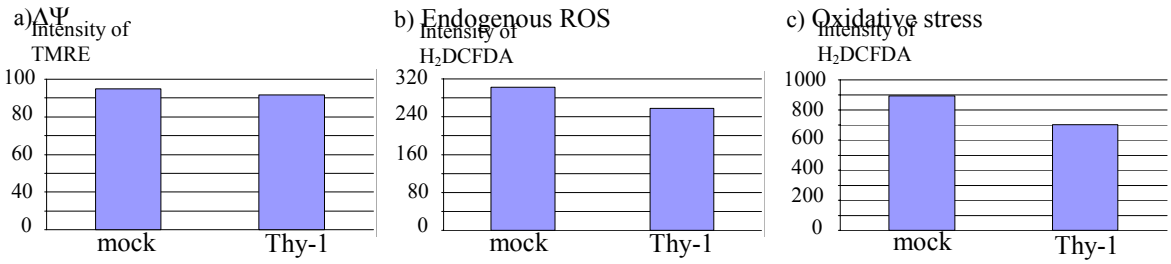

Fig23. **Effect of Thy-1 on ΔΨ, endogenous ROS and reaction to oxidative stress in N_2A. a)** ΔΨ, **b)** Endogenous ROS, **c)** ROS in response to oxidative stress. No difference can be noted between mock and Thy-1 transfected cells.

3.1.2 Effect of copper treatment on mock, wt-PrP and Δ8TM1-PrP transfected N_2A cells

Because PrP can bind copper ions, it was interesting to ask which influence copper might have on ΔΨ, endogenous ROS levels and ROS levels upon oxidative stress induction in PrP overexpressing N_2A.

N_2A were seeded into two 24-well plates on day 1. On day 2, cells were transfected with mock, wt-PrP or Δ8TM1-PrP. Medium was changed on day 3 and copper was added at a saturating concentration (100µM $CuCl_2$) in fresh medium to one of the two plates. On day 4 cells were washed with PBS, fresh medium was added and stainings were performed as described before. FACS analyses were then performed.

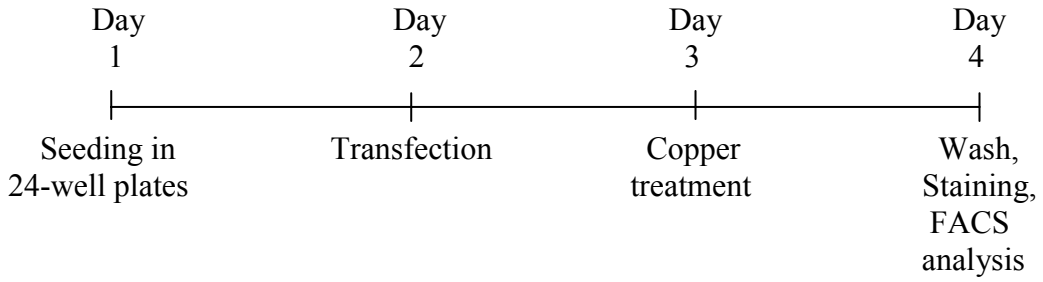

3.1.2.1 Impact of copper treatment on mitochondrial membrane potential (ΔΨ) in mock, wt-PrP or Δ8TM1-PrP overexpressing cells

These experiments were performed 7 times independently and results are expressed as percentage of TMRE intensity for mean value of all mock-transfected cultures in absence of copper treatment (Fig. 24).

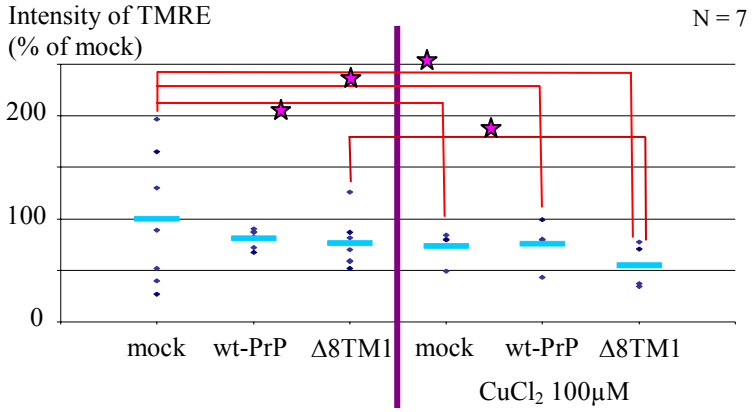

Fig24. **Effect of copper treatment on ΔΨ in transfected N_2A.** After Cu treatment (right-hand side) mock, wt-PrP and Δ8TM1-PrP overexpressing cells show a decrease of ΔΨ compared to mock-transfected cells without treatment. Moreover in the case of Δ8TM1-PrP transfected cells ΔΨ is significantly reduced after copper treatment. Paired t-test was performed. Asterisks denote $p<0.05$. Each blue diamond is a data point and the light blue lines represent the mean values.

After copper treatment mock-transfected, wt-PrP and Δ8TM1-transfected cells show a significant decrease of ΔΨ compared to mock-transfected cells without this treatment. Moreover a significant decrease of ΔΨ could be observed when Δ8TM1-PrP overexpressing cells with copper treatment were compared with the same cells without copper.

3.1.2.2 Impact of copper treatment on the endogenous ROS level in mock, wt-PrP or Δ8TM1-PrP overexpressing cells

These experiments were performed independently 8 times and results are expressed as percentage of DCF fluorescence intensity for mock-transfected cells in the absence of copper treatment (Fig. 25).

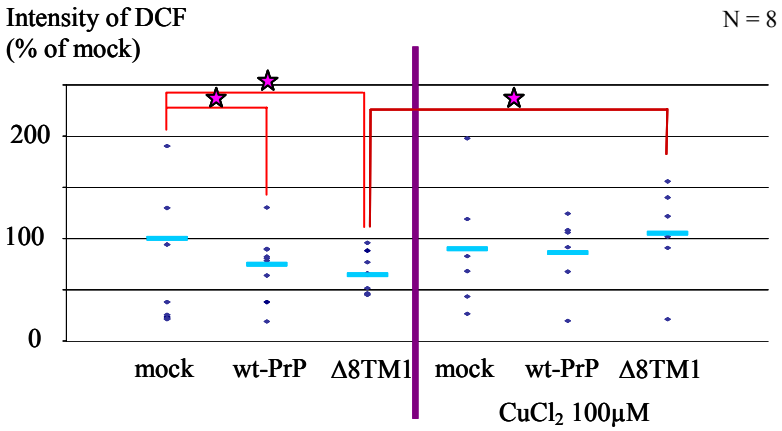

Fig25. **Effect of copper treatment on endogenous ROS in transfected N_2A.** After Cu treatment (right-hand side), Δ8TM1-PrP overexpressing cells show a slight increase of endogenous ROS level compared to mock-transfected cells without treatment. Paired t-tests were performed. Asterisks denote $p<0.05$. Each blue diamond is a data point and the light blue lines represent the mean values.

Both wt-PrP and Δ8TM1-PrP-transfected cells without copper treatment show a significant decrease of endogenous ROS compared to mock-transfected cells without treatment. A significant increase of cellular ROS could be observed when Δ8TM1-PrP overexpressing cells were treated with copper.

3.1.2.3 Impact of copper treatment on the cellular ROS level in response to oxidative stress in mock, wt-PrP or Δ8TM1-PrP overexpressing cells

These experiments were performed 8 times independently and results are expressed as percentage of DCF fluorescence intensity for mock-transfected cells in absence of copper treatment (Fig.26).

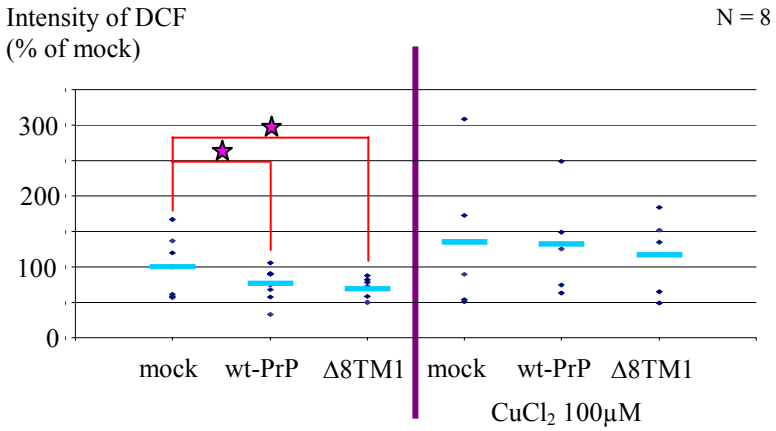

Fig26. **Effect of copper treatment on intracellular ROS upon oxidative stress induction in transfected N_2A.** After Cu treatment in all cases (mock, wt-PrP and Δ8TM1-PrP overexpressing cells) all cultures were exposed to H_2O_2 as described in Materials and Methods and intracellular ROS levels were measured using DCF fluorescence. Paired t-tests were performed. Asterisks denote $p < 0.05$. Each blue diamond is a data point and the light blue lines represent the mean values.

Both wt-PrP and Δ8TM1-PrP transfected cells without copper treatment show a significant decrease of endogenous ROS after oxidative stress compared to mock-transfected cells without treatment. This pattern is conserved after copper treatment, although the differences are not significant here. In all cases the ROS levels are increased after copper treatment.

3.1.3 Impact of Δocta-PrP overexpression in N_2A cells in presence or absence of copper

In view of the effects of copper treatment on PrP-overexpressing N_2A cells and in view of PrP's ability to bind 4 Cu^{2+} ions to its octapeptide region, the experiments were extended to include Δocta-PrP-overexpressing cells. It was expected that the phenotype of this mutant should not be responsive to copper treatment. It should be noted that Figures 27-29 display compilations of the new data combined with all previous data obtained in analogous experiments shown above, in order to increase statistical power.

3.1.3.1 Impact of Δocta-PrP overexpression in the presence or absence of copper on mitochondrial membrane potential (ΔΨ)

The experiments were performed at least 7 times independently and results are expressed as percentage of TMRE intensity of the mock-transfected cells within each individual experiment, respectively (Fig.27).

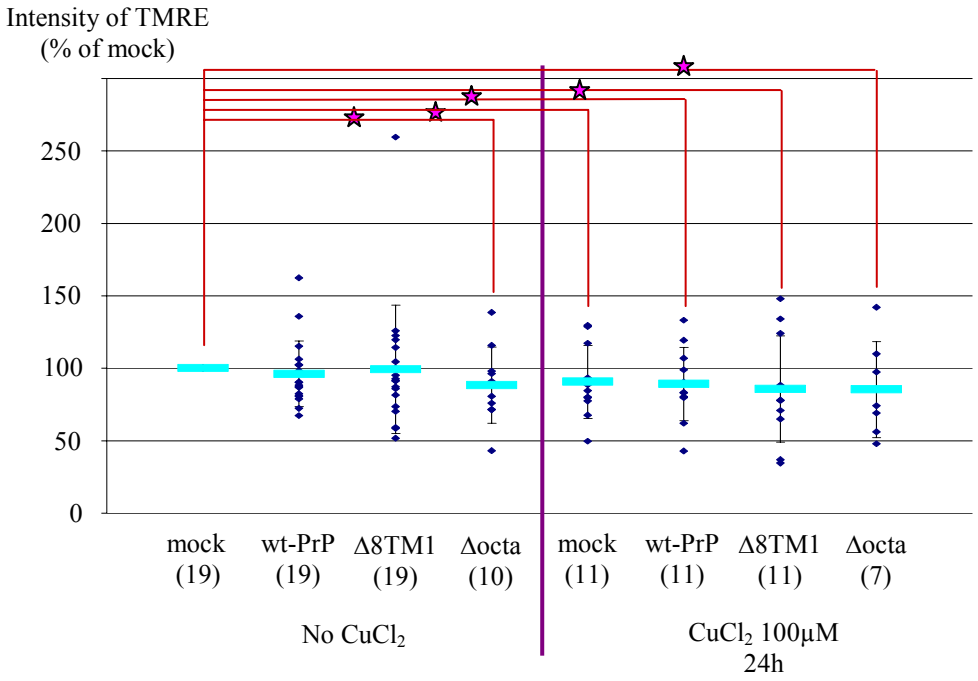

Fig27. **Effect of copper treatment on mitochondrial potential in transfected N_2A.** In the absence of copper treatment Δocta-PrP overexpressing cells show a slight but significant decrease of ΔΨ. After copper treatment ΔΨ is significantly decreased in all cases. T-tests were performed. Asteriks denote $p<0.05$. Each blue diamond is a data point and each light blue dash is the average of all data points. The number of independent experiments is noted in brackets.

Surprisingly Δocta-PrP overexpressing cells showed a phenotype different from mock-transfected cells, *i.e.* in the absence of copper treatment ΔΨ was significantly decreased compared to mock-transfected cells ($p = 0.029$). It should be noted, however, that this aggregate analysis of the effects of wt-PrP and Δ8TM1 did not confirm the more limited data shown in Figs. 11 and 24.

Copper treatment at 100µM for 24h induced a significant ΔΨ decrease in the case of mock, wt-PrP, Δ8TM1-PrP and Δocta-PrP transfected cells with a $p=0.028$ for mock, $p= 0.041$ for wt-PrP, $p= 0.036$ for Δ8TM1-PrP and $p= 0.027$ for Δocta-PrP compared t mock without

copper treatment. Interestingly, copper treatment did not change the already lowered ΔΨin Δocta-PrP overexpressing cells

3.1.3.2 Impact of Δocta-PrP overexpression in the presence or absence of copper on endogenous ROS levels

The experiments were performed at least 6 times independently and results are expressed as percentage of DCF intensity of the mock-transfected cells within each individual experiment, respectively (Fig.28).

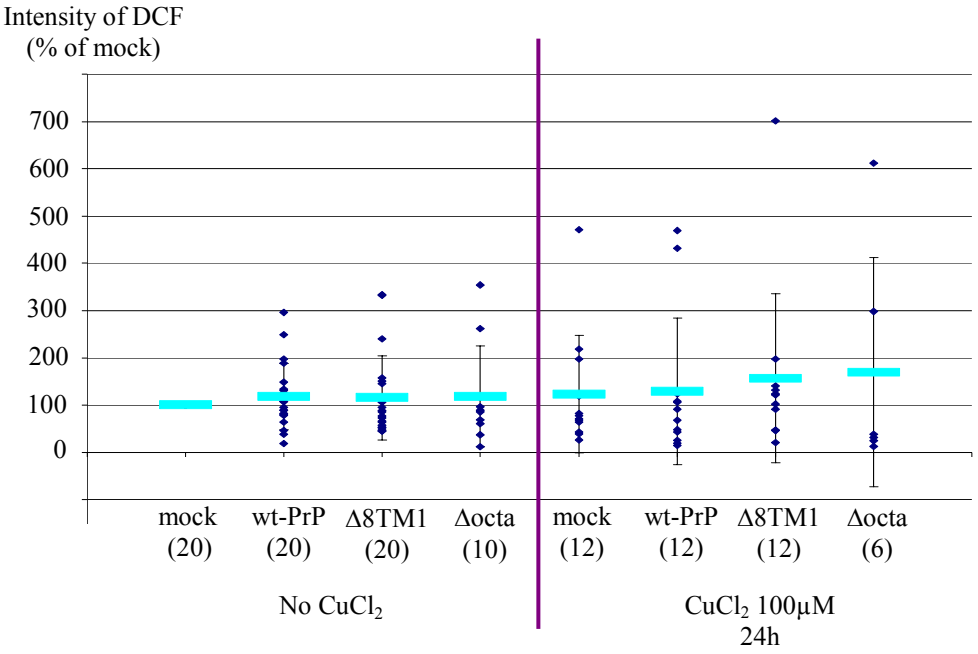

Fig28. **Effect of copper treatment on cellular ROS in transfected N_2A.** No significant difference is observable. T-tests were performed. Each blue diamond is a data point and each light blue dash is the average of all data points. The number of experiments is noted in bracket.

The average of mean value for DCF intensity of all experiments is shown Fig.28. There are no statistically significant differences. It should be noted, however, that this aggregate analysis of the effects of wt-PrP and Δ8TM1 did not confirm the more limited data shown in Figs.14 and 25.

3.1.3.3 Impact of Δocta-PrP overexpression in presence or absence of copper on the cellular ROS level in response to oxidative stress

The experiments were performed at least 6 times independently and results are expressed as percentage of DCF intensity of the mock-transfected cells after H_2O_2 treatment within each individual experiment, respectively (Fig.29).

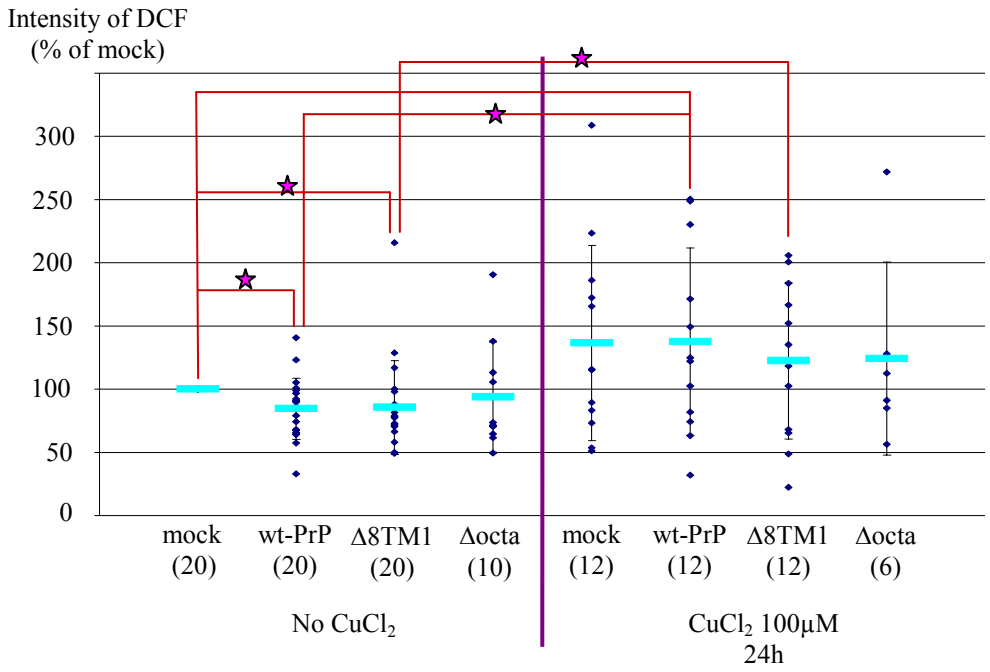

Fig29. **Effect of copper treatment on cellular ROS after oxidative stress in transfected N_2A.** As previously wt-PrP and Δ8TM1-PrP overexpressing cells show a significant decrease of ROS after H_2O_2 treatment whereas Δocta-PrP overexpressing cells show no difference compare to mock-transfected cells. Copper treatment induces a significant increase of the ROS level in wt-PrP and Δ8TM1-PrP overexpressing cells whereas in Δocta-PrP overexpressing cells not. T-test were performed ★ $p<0.05$. Each blue diamond is a data point and each light blue dash is the average of all data points. The number of experiments is noted in bracket.

The average of mean value for DCF intensity of all experiments in presence of H_2O_2 is shown Fig.29.

As previously shown after oxidative stress induced by H_2O_2 treatment the ROS level present in wt-PrP and Δ8TM1-PrP overexpressing cells is significantly reduced compared to mock-transfected cells ($p= 0.003$ and $p=0.04$ respectively). Cells with a Δocta-PrP overexpression do not show any modification of ROS level.

After copper treatment the ROS level in mock-transfected cells show a tendency to increases (p at the borderline = 0.058). The copper treatment induces a significant increase of ROS in wt-PrP and Δ8TM1-PrP overexpressing cells (p= 0.046 for wt-PrP compared to mock, p= 0.012 for the comparison between wt-PrP with and without copper treatment, p=0.021 for the comparison between Δ8TM1-PrP with and without copper treatment). The copper treatment has no effect on Δocta-PrP overexpressing cells.

Δocta-PrP overexpressing cells do not show a return neither to mock values nor to wt-PrP values (for ΔΨ or endogenous ROS or oxidative stress response) in presence or absence of copper treatment.

3.1.4 Implication of phospho-MAPK in oxidative stress response (H_2O_2 treatment) in wt-, Δ8TM1- or Δocta-PrP transfected N_2A

In order to investigate the possible implication of signalling pathways in the cellular phenotypes described above, western blots of lysates from transfected cells exposed H_2O_2 for various time periods (none, 15 min or 30 min or every 5 min.) were probed with phospho-MAPK antibodies (phospho-JNK1/JNK2/3, phospho-p38, phospho-p42/p44). A blot probed with anti-phospho-p38 antibody is shown in Fig. 30.

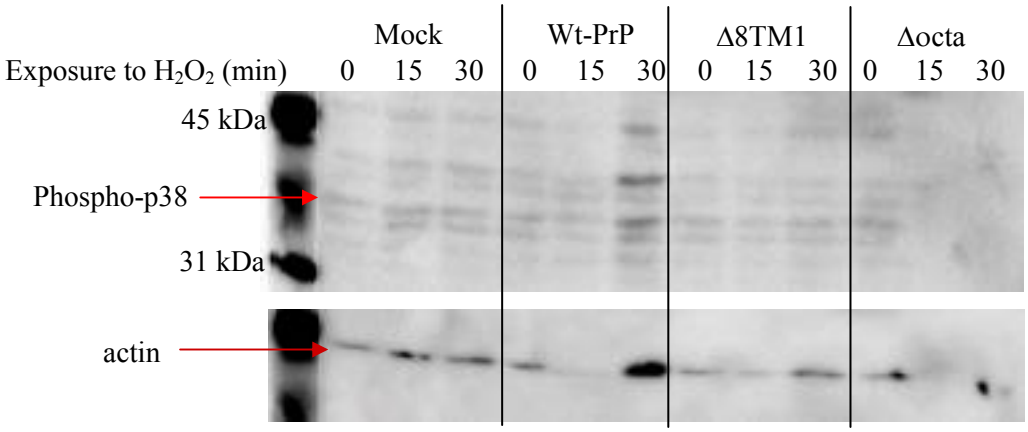

Fig.30. **Western blot of transfected N_2A cells exposed to oxidative stress, stained with an anti-phospho-p38 antibody.** Lysates from transfected N_2A treated with H_2O_2 for 0 min, 15 min or 30 min were loaded.

Each lane corresponds to 50 µg of protein of cellular lysates. Transfected cells were lysed after an exposure to H_2O_2. In the case of wt-PrP after an exposure of 30 minutes to H_2O_2 the band is more intense because of unequal loading. No difference between the different transfected cells and after exposure to H_2O_2 is observable. Therefore the protective effect of PrP is unlikely to implicate phosphorylation of p38.

Fig. 31 displays a western blot stained with anti-phospho-p42/p44 antibody.

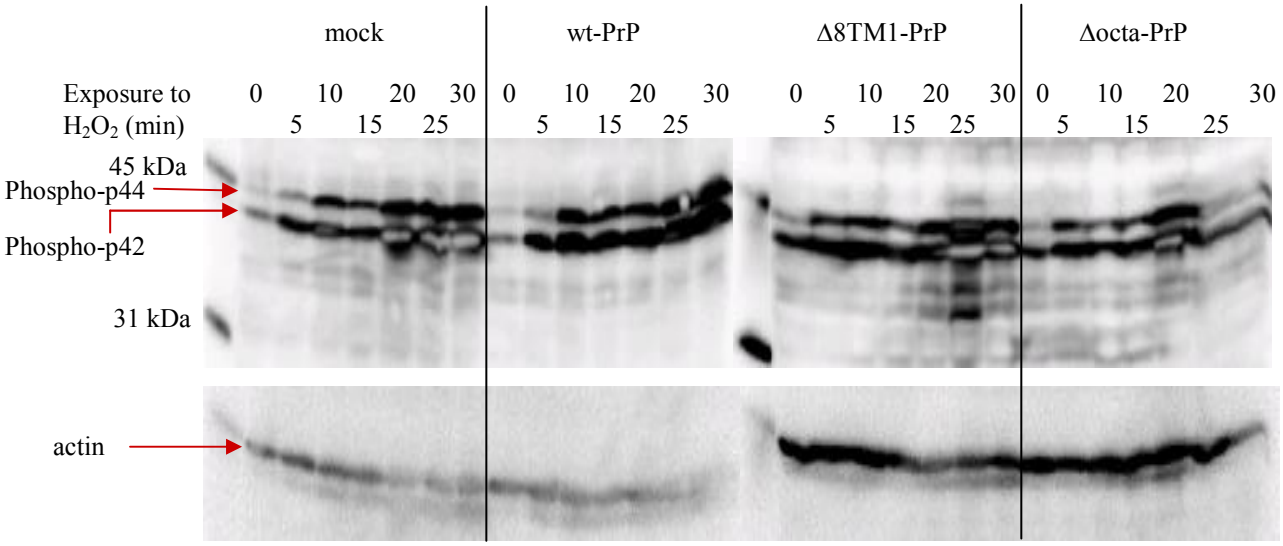

Fig31. **Western blot stained with an anti-phospho-p42/p44 antibody of transfected N_2A after oxidative stress.** Transfected N_2A cells were exposed to H_2O_2 for 0 min, 5 min, 10 min, 15 min, 20 min, 25 min or 30 min and then lysed. 50 µg of proteins from these lysates were loaded. Note that during the exposure to oxidative stress (H_2O_2) the phosphorylation level of p42 and p44 increased proportionally to exposure time. The phosphorylation pattern differs according to the transfected plasmid.

Interestingly, the phosphorylation level of both p42 and p44 increase with increasing duration of H_2O_2 exposure. Phospho-p42 displays increased basal and induced levels compared with phosphor-p44. In the case of mock-transfected cells without H_2O_2 treatment only p42 is phosphorylated and increase with the exposure time till reaching a maximum after 20 min exposure time to H_2O_2. The phosphorylation of p44 begins from 5 min exposure to H_2O_2. Wt-PrP transfected cells showed the same pattern. Intriguingly, in the case of Δ8TM1-PrP transfected cells the basal phosphorylation of p42 is higher. In the case of Δocta-PrP transfected cells the maximal phosphorylation of p42 and p44 is already reached in 20 min and then phosphorylation seems to decrease.

In Fig. 32, the results from quantification of band intensities obtained in 2-5 independent experiments are displayed. The data are expressed as percentage of the mock intensity for a given exposure time to H_2O_2.

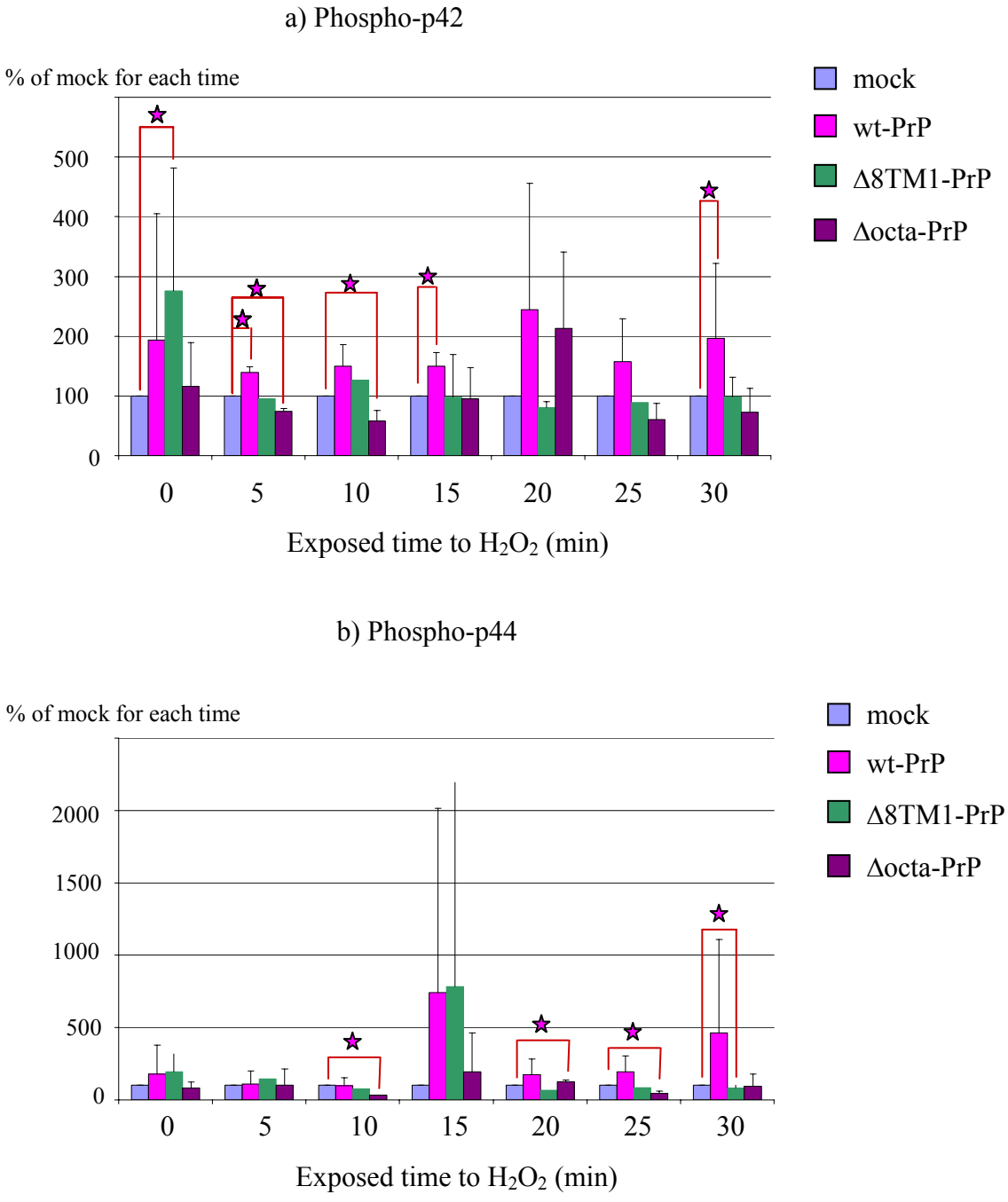

Fig32. **Quantification of western blots of lysates from transfected N_2A after oxidative stress, probed with an anti-phospho-p42/p44 antibody.** a) Quantification of phospho-p42, b) Quantification of phospho-p44. Transfected N_2A were exposed to H_2O_2 during 0 min, 5 min, 10 min, 15 min, 20 min, 25 min or 30 min and then lysed. 50 µg of proteins from these lysates were used. T-tests were performed. Asterisks denote $p<0.05$

Figure 32 shows the phosphorylation of p42 and of p44 of each overexpressing PrP (wt or mutant) in comparison to mock. The basal level of p42 phosphorylation is significantly higher in Δ8TM1-PrP transfected cells. There is a general trend towards increased p42 and p44 phosphorylation in wt-PrP-overexpressing cells and towards decreased phosphorylation in Δocta-PrP-overexpressing cells although statistical significance was not reached at all time points, which was in part due to some outliers.

In conclusion, the activation of the p42/p44 pathway might be implicated in the protective role of PrP against oxidative stress, as phosphorylation tends to be increased in wt-PrP overexpressing cells benefiting from increased protection, but not in Δocta-PrP overexpressing cells in which no protective effect is observable.

Fig. 33 displays a western blot stained with an anti-phospho-JNK/1/JNK2/3 antibody.

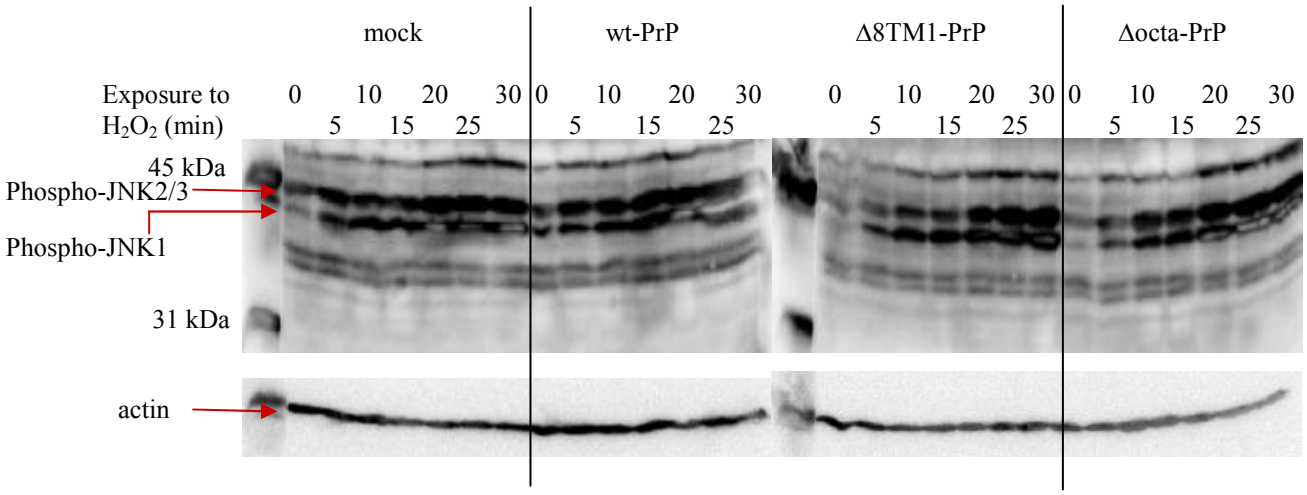

*Fig33.***Western blot of lysates of transfected N_2A after oxidative stress, probed with an anti-phospho-JNK/1/JNK2/3 antibody.**Transfected N_2A were exposed to H_2O_2 for 0 min, 5 min, 10 min, 15 min, 20 min, 25 min or 30 min and then lysed. 50 µg of proteins from these lysates were used. During the exposure to oxidative stress (H_2O_2) the phosphorylation level of JNK1 and JNK2/3 increases progressively. The phosphorylation pattern differs according to the transfected plasmid.

The quantification of the data from 2-5 independent experiments is shown in Fig.34. Results are expressed as percentage of the mock intensity for a given duration of H_2O_2 exposure.

a) Phospho-JNK1

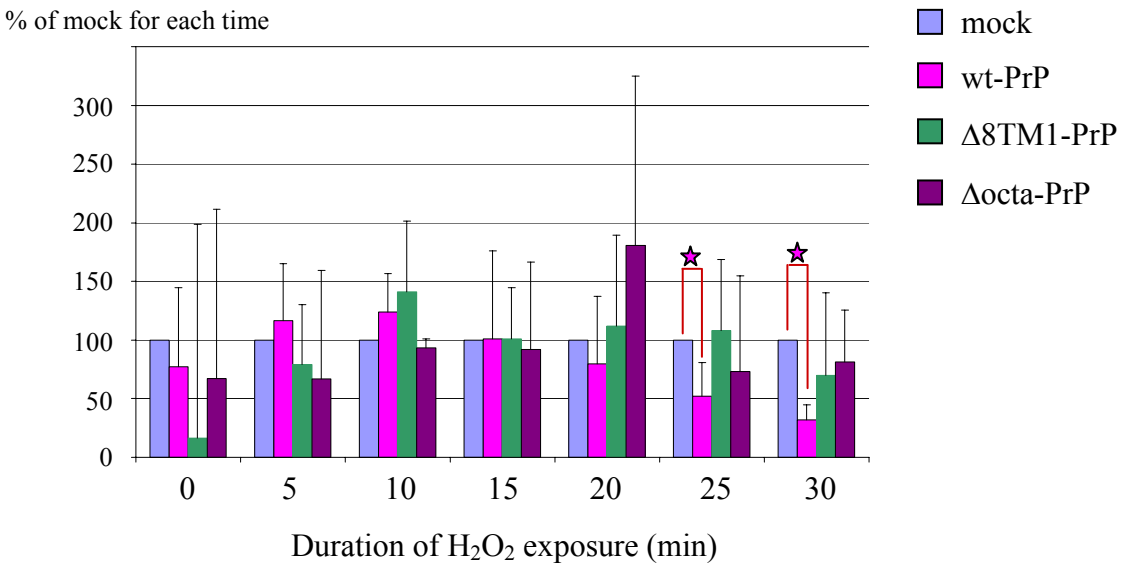

b) Phospho-JNK2/3

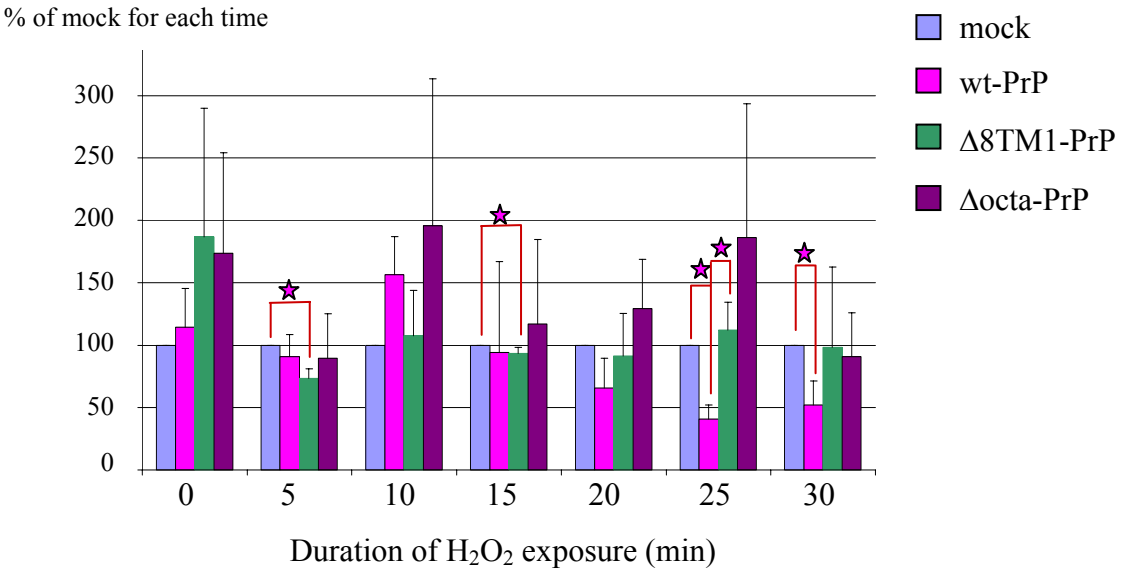

Fig34. **Quantification of western blots stained with an anti-phospho-JNK1/JNK2/3 antibody of transfected N_2A after oxidative stress.** a) Quantification of phospho-JNK1, b) Quantification of phospho-JNK2/3.Transfected N_2A were exposed to H_2O_2 during 0 min, 5 min, 10 min, 15 min, 20 min, 25 min or 30 min and then lysed. 50 µg of proteins from these lysates were used. T-test were performed. Asterisks denote $p<0.05$

Figure 34a summarises the data on phosphorylation of JNK1. After H_2O_2 treatment for 25 min cells overexpressing wt-PrP, but not the mutant versions, show a significant decrease of JNK1 phosphorylation. This reduction of JNK1 phosphorylation in the case of wt-PrP transfected cells is even more prominent after 30 min H_2O_2 treatment.

Figure 34b summarises the data on phosphorylation of JNK2/3. After an exposure to H_2O_2 for 25 min and 30 min cells overexpressing wt-PrP, but not the mutant versions, show a significant decrease of JNK2/3 phosphorylation.

In conclusion, the activation of JNK1 and JNK2/3 might be implicated to some extent in the protective role of PrP against oxidative stress, as their phosphorylation tends to be decreased at later time points during oxidant exposure in wt-PrP overexpressing cells benefiting from increased protection, but not in Δocta-PrP overexpressing cells in which no protective effect is observable. On the other hand, Δ8TM1-PrP overexpressing cells do benefit from increased protection but no not display any significant differences in JNK1 and JNK2/3 phosphorylation compared with mock-transfected cells. This “uncoupling” is in contrast with the effects on p42/p44 signalling described above.

In summary, the MAPK pathway seems to be implicated in the protective effect of PrP against oxidative stress, via generally higher phosphorylation levels of p42 and lower phosphorylation levels of JNK1/JNK2/3 at later time points. The phosphorylation level of p38 MAPK does not seem to be involved.

3.2 Analyses on primary mouse brain cells

The experiments described in Chapter 3.1 have been performed by transiently transfecting cultured N_2A mouse neuroblastoma cells (*Prnp*$^{+/+}$ genotype) with plasmids leading to overexpression of wild-type or mutant PrP versions. As these cells express endogenous PrP^c, some phenotypic effects of mutant PrP versions, especially loss-of-function effects, might be missed. On the other hand, overexpression of proteins in cells may lead to some nonspecific effects. The generation of transgenic mice expressing Δ8TM1-PrP and their breeding into *Prnp*$^{+/+}$, *Prnp*$^{+/-}$, *Prnp*$^{-/-}$ backgrounds, achieved in the context of another project running in the Bürkle group, offered the opportunity to study primary cells from such animals and to circumvent the above-mentioned problems of endogenous PrP^c and of protein overexpression. In addition primary cells are closer to the *in vivo* situation, as the cells maintain their normal diploid karyotype and are not transformed, and are also likely to maintain many features of their state of differentiation in *vivo*. It was therefore decided to carry out similar experiments as those described in Chapter 3.1 in primary mouse brain cells upon short-term growth in cell culture.

3.2.1 Expression of wt-PrP and the transgene Δ8TM1-PrP (tg) in mice

Fig.35 shows the characterisation of the expression of the Δ8TM1-PrP transgene as well as of endogenous PrP^c at protein level. Brain tissue was homogenised and digested with PNGase F in order to remove protein glycosylation and facilitate protein analyses by western blot. Monoclonal antibody 6H4 antibody was used as a probe to detect PrP^c.

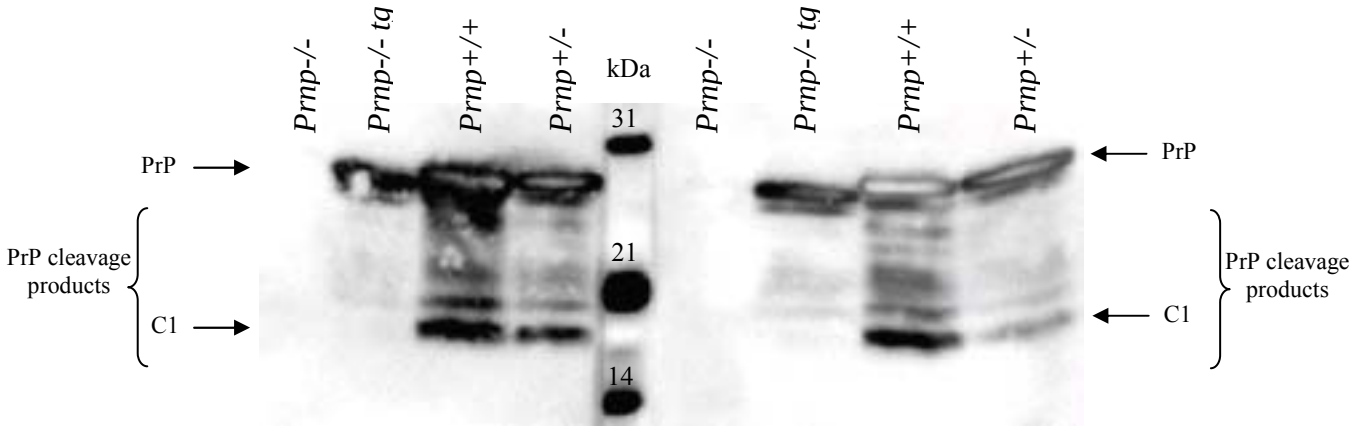

Fig35. **Expression of PrP in the brain of *Prnp*$^{+/+}$, *Prnp*$^{+/-}$, *Prnp*$^{-/-}$ and *Prnp*$^{-/-}$/Δ8TM1-PrP mice.** Blots from two different brains for each genetic background are shown, respectively. No signal is observable in *Prnp*$^{-/-}$ mouse brain. Major bands are detactable in *Prnp*$^{+/+}$, *Prnp*$^{+/-}$ and *Prnp*$^{-/-}$*tg* mouse brains at around 27kDa, which corresponds with the molecular weight of deglycosylated PrP^{c}. Other lower bands result from PrP cleavage, especially the C1 fragment (17kDa) and probably also from non-specific degradation.

In the case of *Prnp*$^{+/+}$ brain, PrP is clearly expressed and cleavage products, including the well-established C1 fragment, are observable. In the case *Prnp*$^{+/-}$ brain extract, the same pattern is observable. In case of *Prnp*$^{-/-}$ no signal at all is observable as expected. In the case of *Prnp*$^{-/-}$/tg brain, the major PrP band migrates slightly faster than endogenous PrP in wild-type mice because of the of 8 amino acid deletion, corresponding to about 1 kDa (N.B. Best seen on the blot on the right-hand side).

It is also apparent that the transgene Δ8TM1-PrP, which is encoded by a single-gene copy integrated into a host chromosome, is underexpressed compared with endogenous PrP^{c}. In a recent joint publication with the Aguzzi group on these mice, the expression level was determined to be about 20% of endogenous PrP^{c} (Baumann, et al., 2007).

3.2.2 Primary cells derived from tg Δ8TM1-PrP and control mice

3.2.2.1 Characterisation of whole-brain cells

Mice were crossed as following *Prnp*$^{+/-}$ x *Prnp*$^{+/-}$*tg* in order to have all possible phenotype in a littermate (Fig.6).

Newborn mice were decapitated and primary brain cell cultures established as described in Materials and Methods. In parallel tails were sampled for genotyping. Brain cells cultures derived from the two transgenic mouse lines (F902, M630) were both used. These primary brain cells were cultured for 2-5 weeks, until a sufficient number of cells was reached to perform, with each culture, FACS and immunofluorescence analysis.

ΔΨ, endogenous ROS levels and oxidative stress response were assessed in these primary cells as described above.

3.2.2.1.1 Immunofluorescence of primary whole-brain cells

Immunofluorescence analyses were performed to determine the composition of these mixed brain cell cultures, *i.e.* the percentage of neurons and glial cells.

Immunofluorescence was performed after FACS analysis (*i.e.* in cultures at least three weeks old). Whole-brain primary cells were cultured on coverslips at least one week and fixed when cells approached confluency.

NeuN antibodies are specific for neurones whereas GFAP antibodies for astrocytes. Hoechst staining was also performed as a reference for the total number of cells present.

Representative photomicrographs are shown in Fig.36.

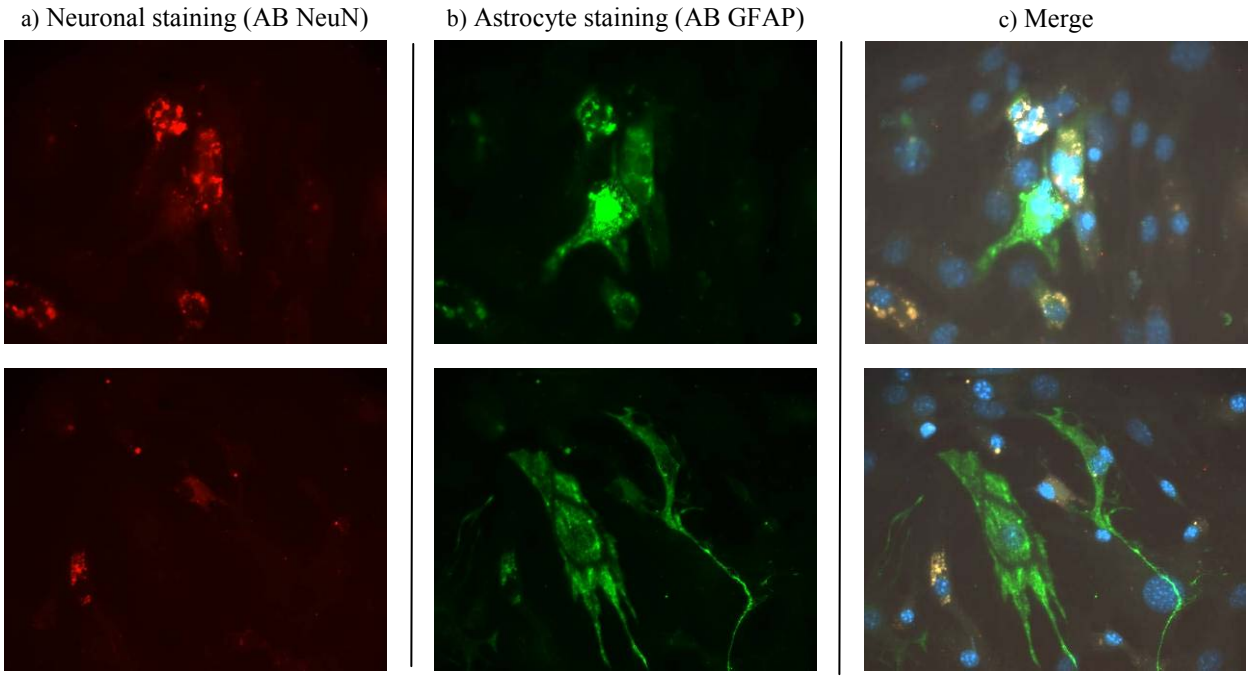

Fig36. **Immunostaining of whole-brain cells neurones and astrocytes.** Two representative examples are shown. Antibody NeuN stains neurones and antibody GFAP astrocytes **a)** NeuN Staining (red); **b)** GFAP staining (green); **c)** Merge of Hoechst (blue), GFAP (green) and NeuN (red) staining.

It was estimated that 30% of total cells are neurones (NeuN positive in red), 40% astrocytes (GFAP positive in green) and 40% other cells (only Hoechst staining, blue).

3.2.2.1.2 FACS setting for primary whole brain cells

3.2.2.1.2.1 FACS setting for the mitochondrial membrane potential (ΔΨ) detection in whole brain primary cells

TMRE staining was performed in order to assess ΔΨ by FACS analysis.

The background was determined on cells without TMRE.

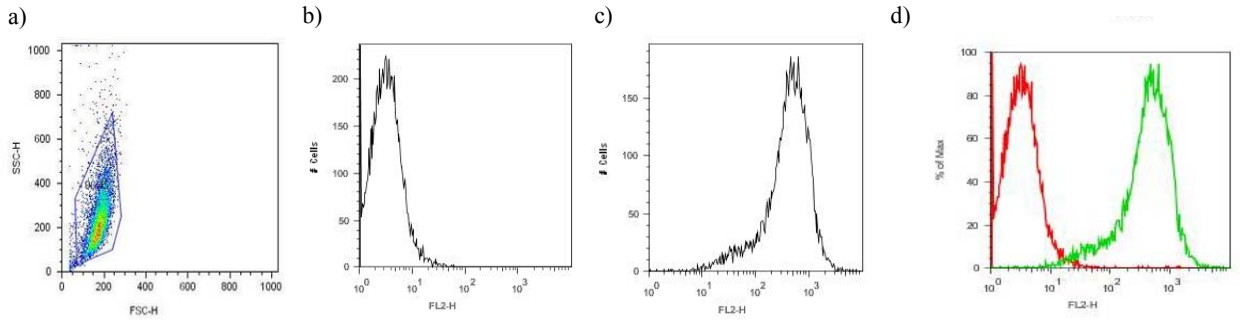

Fig37. **FACS Setting. a)** Gating of living cells; **b)** Cells without TMRE, thus defining the background; **c)** Cells stained with TMRE (FL-2); **d)** Overlay b) and c).

3.2.2.1.2.2 FACS setting for the endogenous ROS measurement in whole-brain primary cells

H_2DCFDA staining was performed in order to check endogenous ROS levels by FACS analysis.

The background was determined on cells without H_2DCFDA.

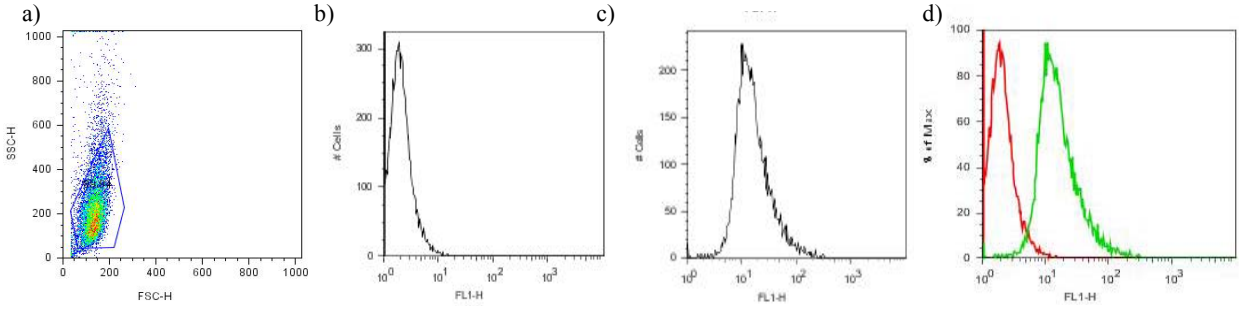

Fig38. **FACS Setting. a)** Gating of living cells; **b)** Cells without H_2DCFDA, thus defining the background; **c)** Cells stained with H_2DCFDA (FL-1); **d)** Overlay b) and c).

3.2.2.1.2.3 FACS setting in order to monitor intracellular ROS in whole-brain primary cells exposed to oxidative stress

H_2DCFDA staining in presence of H_2O_2 was performed in order to monitor the reaction of primary to oxidative stress by FACS analysis.

The background was determined on cells without H_2DCFDA.

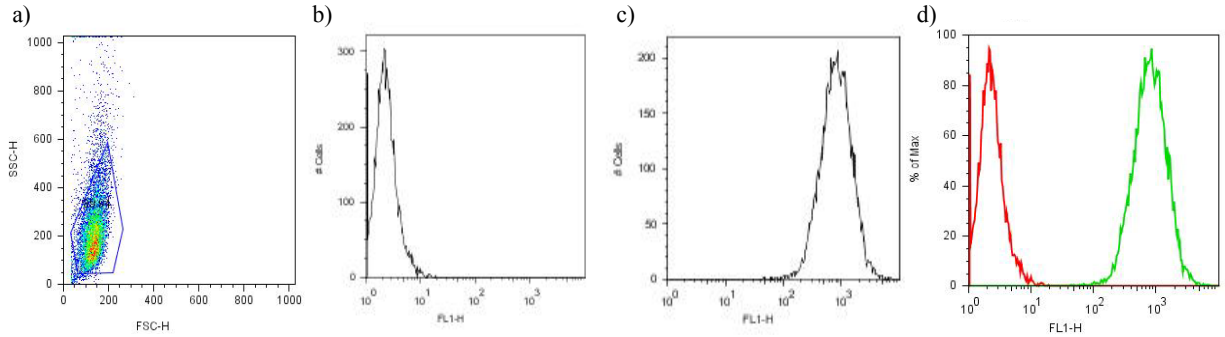

Fig39. **FACS Setting. a)** Gating of living cells; **b)** Cells without H_2DCFDA, thus defining the background; **c)** Cells stained with H_2DCFDA in the presence of H_2O_2 (FL-1); **d)** Overlay b) and c).

3.2.2.2 Effect of culture age of of whole-brain primary cells on ΔΨ, endogenous ROS level and oxidative stress response

In order to check if *in-vitro* ageing of culture could have any influence on the above phenotypic parameters, a set of preliminary experiments was performed on cells from the same culture assayed twice with a one-week delay.

3.2.2.2.1 Impact of in-vitro ageing of cultured cells on ΔΨ

Repeated TMRE staining was performed on cells from the same culture with a one-week delay (Fig.40).

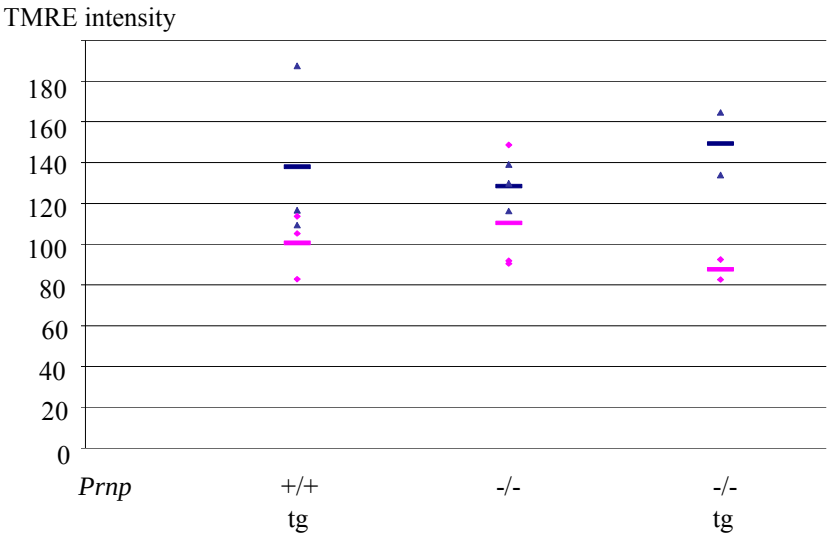

Fig40. **Effect of culture age on mitochondrial membrane potential in primary whole-brain cells.** Each diamond is a data point and each line represents the mean. Data points from the first experiment are plotted in blue and from the second (one week later) in pink.

As strong effect of culture age is obvious from Fig.40, *i.e.* a substantial decrease in $\Delta\Psi$ in those cultures maintained for one more week.

To corroborate these initial findings, a retrospective analysis of a larger data set that had already been generated using cultures of a diverse age range was performed (Fig.41).

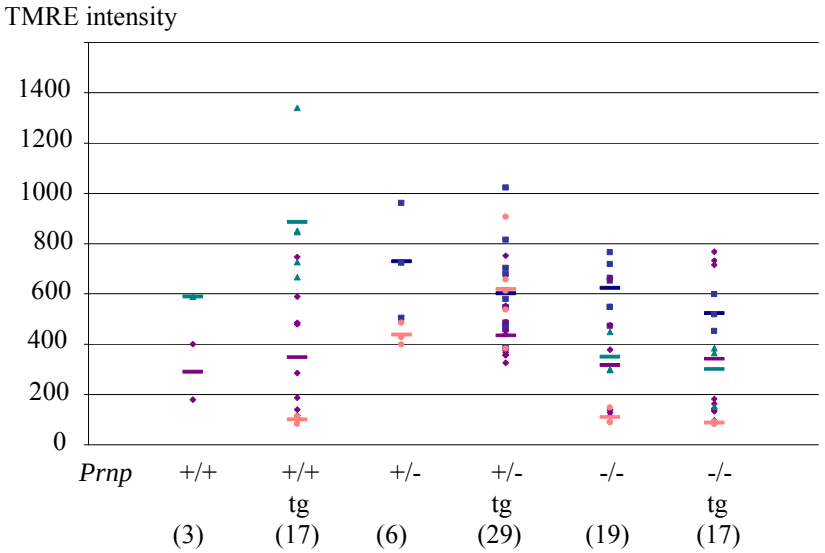

Fig41. **Effect of culture age on mitochondrial membrane potential in primary whole-brain cells.** In blue two weeks old culture, in purple three weeks, in green three and half weeks and in pink four weeks. In dash is the average of all data points per week and in brackets the total of brains used.

It is apparent from Fig.41 that increasing culture age indeed has a big impact on ΔΨ, with a clear tendency towards loss of ΔΨ with age. Therefore use of age-mixed cultures in the context of ΔΨ analyses is not recommendable as the results might be liable to artifacts.

3.2.2.2.2 Impact of ageing of cultured cell on their endogenous ROS level

Because of the big impact of culture age on ΔΨ, data analyses of endogenous ROS level (H_2DCFDA stainings) were plotted depending on age range.

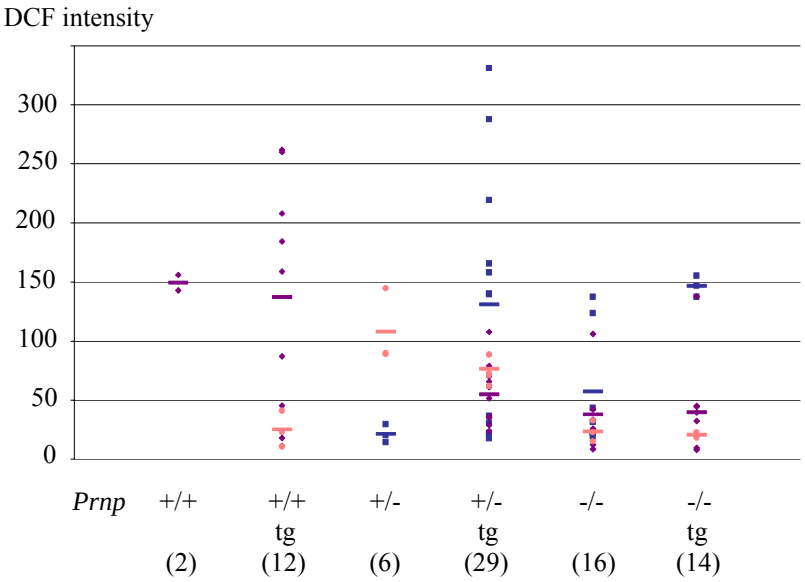

Fig42. **Effect of ageing on endogenous ROS in primary whole brain cells.** In blue two weeks old culture, in purple three weeks and in pink four weeks. In dash is the average of all data points per week and in brackets the total of brains used.

Evolution of endogenous ROS with culture time is shown figure 42. In blue two weeks old culture, in purple three weeks and in pink four weeks. Each genetic background differently evolves.

Such an "aged" mix culture is not representative. The experiments are reproduced with primary brain cells after a culture time comprise between two and three weeks.

3.2.2.2.3 Impact of ageing of cultured cell on their ROS level modulation in response to oxidative stress

Because of the big impact of culture age on ΔΨ, data analyses of endogenous ROS level after oxidative stress (H_2DCFDA stainings and H_2O_2 treatment) were plotted depending on age range.

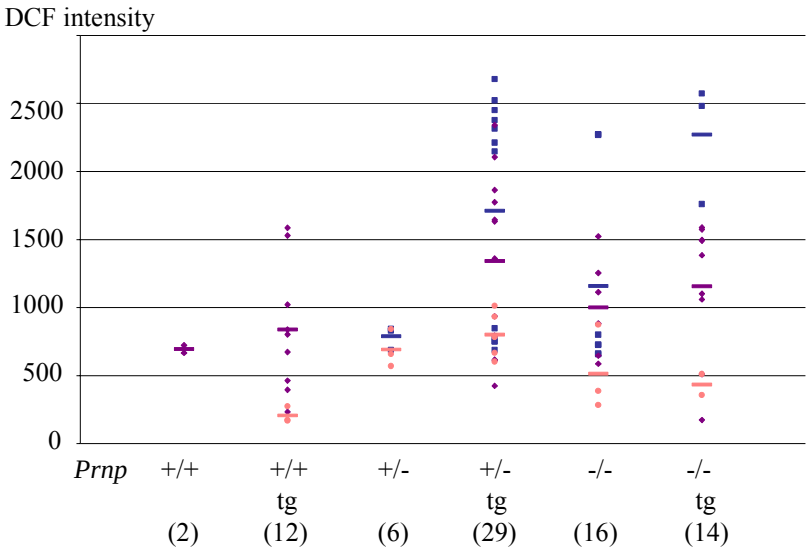

Fig43. **Effect of ageing on oxidative stress response in primary whole brain cells.** In blue two weeks old culture, in purple three weeks and in pink four weeks. In dash is the average of all data points per week and in brackets the total of brains used.

Evolution of ROS level after oxidative stress with culture time is shown figure 43. In blue two weeks old culture, in purple three weeks and in pink four weeks. Each genetic background differently evolves.

Such an "aged" mix culture is not representative. The experiments are reproduced with primary brain cells after a culture time comprise between two and three weeks.

3.2.2.3 Phenotypic analyses performed on whole-brain cell cultures from tg Δ8TM1-PrP mice

In view of the problems encountered with culture age as a confounding factor (see above), the analyses on ΔΨ, basal ROS and oxidative stress-induced ROS were repeated with cultures of well-defined age (2-3 weeks). In addition, the cultures from the two transgenic lines, on *Prnp*$^{+/+}$, *Prnp*$^{+/-}$ and *Prnp*$^{-/-}$ background, respectively, were analysed separately, to rule out chromosomal integration site of the transgene as a confounding factor.

3.2.2.3.1 Mitochondrial membrane potential (ΔΨ) of primary whole-brain cells derived from tg lines F902 and M630 and littermate controls

TMRE staining and FACS analysis were performed in order to assess ΔΨ. Figs.50 and 51 display the data for tg lines F902 and M630, respectively.

Line F902

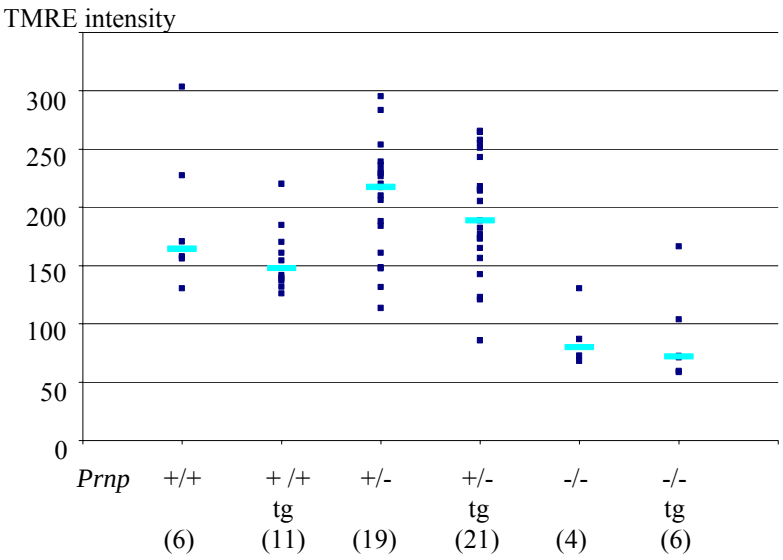

Fig44. **Mitochondrial membrane potential in primary whole-brain cells derived from tg line F902.** Each blue square is a data point and the light blue lines represent the medians of the respective data points. The number of mice from which brain cell cultures were established is indicated in brackets. No statistically significant effect is observable in any of the three *Prnp* genotypes.

Line M630

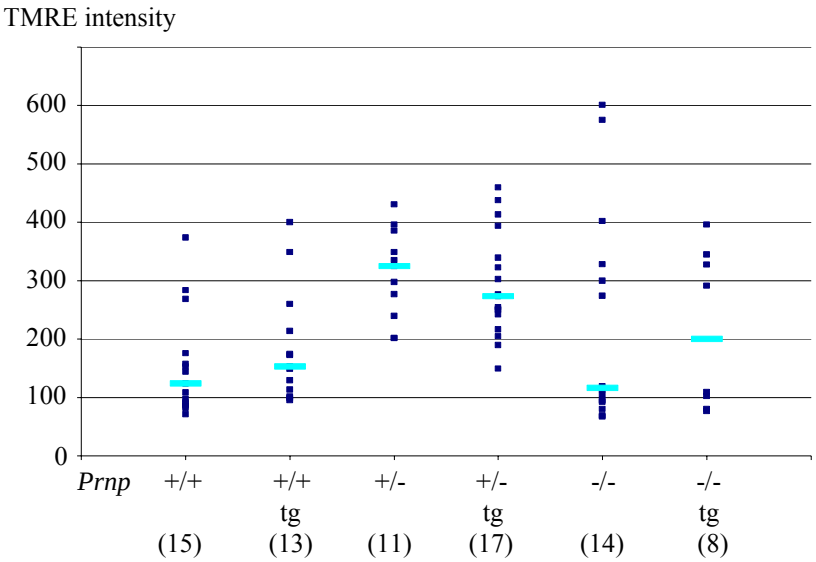

Fig45. **Mitochondrial membrane potential in primary whole-brain cells derived from tg line M630.** Each blue square is a data point and the light blue lines represent the medians of the respective data points. The number of mice from which brain cell cultures were established is indicated in brackets. No statistically significant effect is observable in any of the three *Prnp* genotypes.

The data were statistically analysed using the Mann-Whitney test. No significant effect due to the presence of the transgene Δ8TM1-PrP was observed in either of the two tg lines. It should be noted that comparisons between $Prnp^{+/+}$, $Prnp^{+/-}$ and $Prnp^{-/-}$ mice are not valid because the mice were of different genetic backgrounds. The oocyte donors for microinjections were C3H x C57BL6 hybrids and due to the subsequent breeding the tg lines there various genomic contributions from FVB vs. 129SV associated with the *Prnp* genotypes; see Chapter 2.1.5). The only legitimate comparisons, therefore, are between littermates with or without transgene.

3.2.2.3.2 Endogenous ROS level of primary whole-brain cells derived from tg lines F902 and M630 and littermate controls

H_2DCFDA staining and FACS analysis were performed in order to assess endogenous ROS levels. Figs.52 and 53 display the data for tg lines F902 and M630, respectively.

Line F902

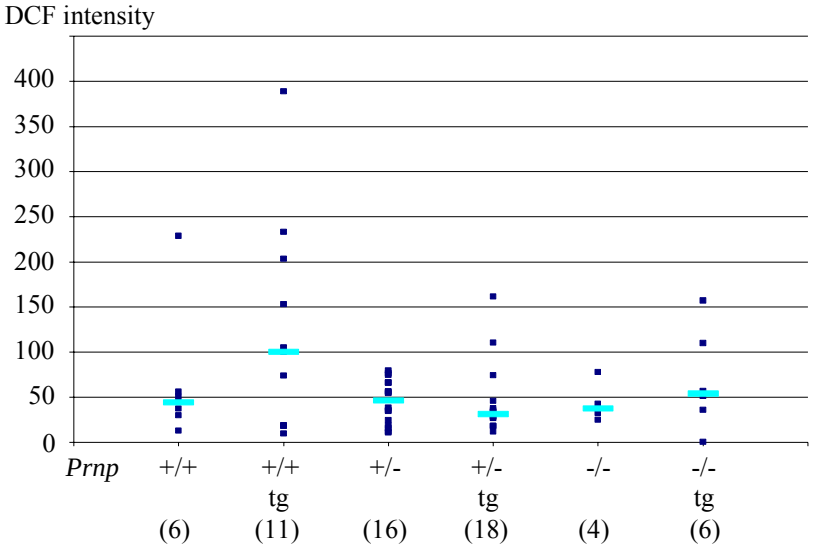

Fig46. **Endogenous ROS level in primary whole-brain cells derived from tg line F902.** Each blue square is a data point and the light blue lines represent the medians of the respective data points. The number of mice from which brain cell cultures were established is indicated in brackets. No statistically significant effect is observable in any of the three *Prnp* genotypes.

Line M630

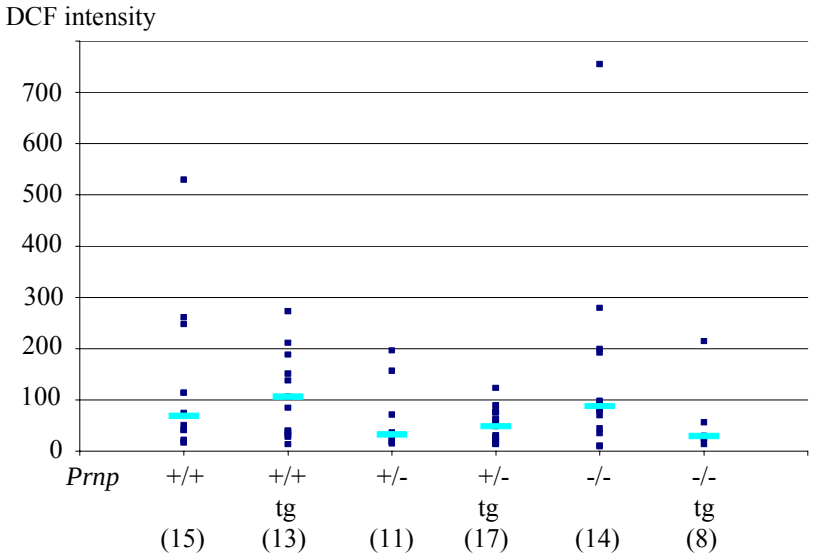

Fig47. **Endogenous ROS level in primary whole-brain cells derived from tg line M630.** Each blue square is a data point and the light blue lines represent the medians of the respective data points. The number of mice from which brain cell cultures were established is indicated in brackets. No statistically significant effect is observable in any of the three *Prnp* genotypes.

The data were statistically analysed using the Mann-Whitney test. No significant effect due to the presence of the transgene Δ8TM1-PrP was observed in either of the two tg lines. (N.B. For reasons mentioned above, the only legitimate comparisons are between littermates with or without transgene.)

3.2.2.3.3 ROS level after induction of oxidative stress in primary-whole brain cells derived from tg lines F902 and M630 and littermate controls

H_2DCFDA staining in presence of H_2O_2 and subsequent FACS analysis were performed in order to check intracellular ROS level under conditions of oxidative stress. Figs.48 and 49 display the data for tg lines F902 and M630, respectively.

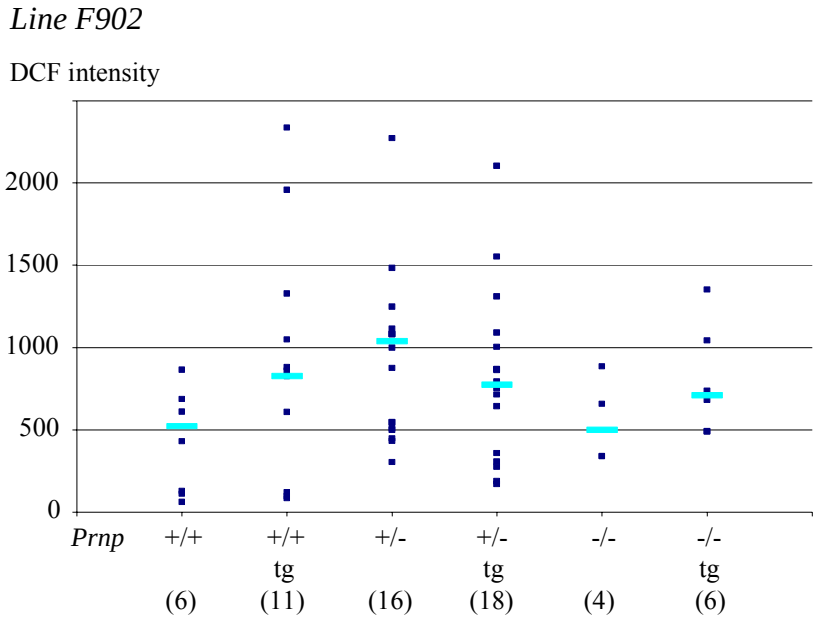

Fig48. **Intracellular ROS level after oxidative stress in primary whole-brain cells derived from tg line F902.** Each blue square is a data point and the light blue lines represent the medians of the respective data points. The number of mice from which brain cell cultures were established is indicated in brackets. No statistically significant effect is observable in any of the three *Prnp* genotypes.

The data were statistically analysed using the Mann-Whitney test. No significant effect due to the presence of the transgene Δ8TM1-PrP was observed in either of the two tg lines. (N.B. For reasons mentioned above, the only legitimate comparisons are between littermates with or without transgene.)

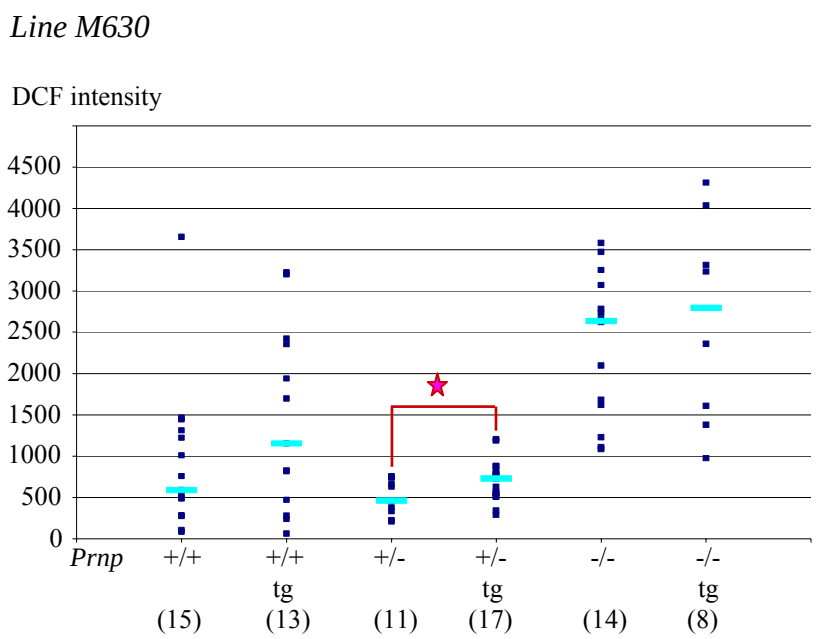

Fig49. **Intracellular ROS level after oxidative stress in primary whole-brain cells derived from tg line M630.** Each blue square is a data point and the light blue lines represent the medians of the respective data points. The number of mice from which brain cell cultures were established is indicated in brackets. Asterisk denotes $p<0.05$ by Mann-Whitney test.

No transgene-induced effect is observable in $Prnp^{+/+}$ and $Prnp^{-/-}$ primary cells. However, in the $Prnp^{+/-}$ genotype, the transgene-positive cells show significant increase ($p=0.0407$, Mann-Whitney test) of endogenous ROS after oxidative stress compared to cells from $Prnp^{+/-}$ littermates. (N.B. For reasons mentioned above, the only legitimate comparisons are between littermates with or without transgene.)

3.2.3 CGN (Cerebellar Granular Neurones) derived from control and transgenic Δ8TM1-PrP mice

In view of the big spread of the data points depicted in Figs. 44-49 that may well preclude detection of putative real differences between transgenic cells and controls, it was reasoned that a potential problem could be the heterogeneity of the cultures derived from whole brain as to cell type. Such heterogeneity was expected and confirmed (see 3.2.2.1.1.1). An alternative procedure

was to establish cultures of cerebellar granular cells (CGN), known to comprise mostly neuronal cells, and repeat the analyses of ΔΨ, basal ROS levels and ROS levels under oxidative stress. A this point the work was restricted to the tg mouse line F902, as this line had been characterised most extensively in the framework of a cooperative project (Baumann, et al., 2007).

3.2.3.1 Characterisation of cellular composition of CGN cultures derived from tg line F902

Immunofluorescence analysis with the neurone-specific NeuN antibody was performed on CGN cultures after PFA fixation in order to determine the percentage of neurones in these cultures (Fig.50).

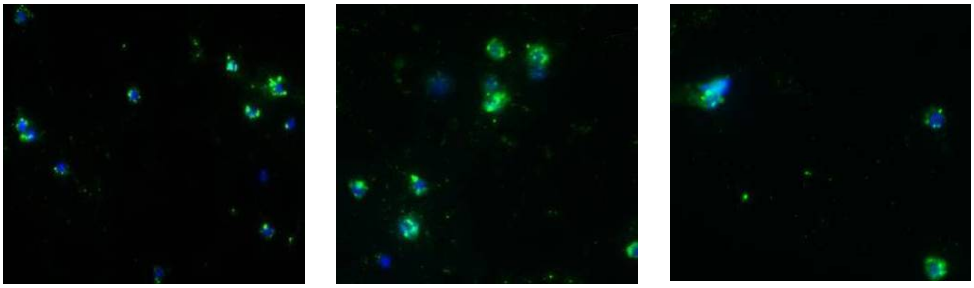

Fig50. **Immunostaining of CGN with a neuronal specific antibody.** Three representative examples are shown. Neurones are stained with antibody NeuN (green) and nuclei with Hoechst (blue). Photomicrographs represent a merge of Hoechst and NeuN staining. More then 95% of culture are neurons.

About 95% of cells were NeuN-positive, confirming that the CGN cultures were almost purely neuronal cultures, as expected.

3.2.3.2 Mitochondrial membrane potential (ΔΨ) of CGN derived from the F902 line of tg Δ8TM1-PrP

TMRE staining and FACS analysis were performed in order to assess ΔΨ (Fig. 51).

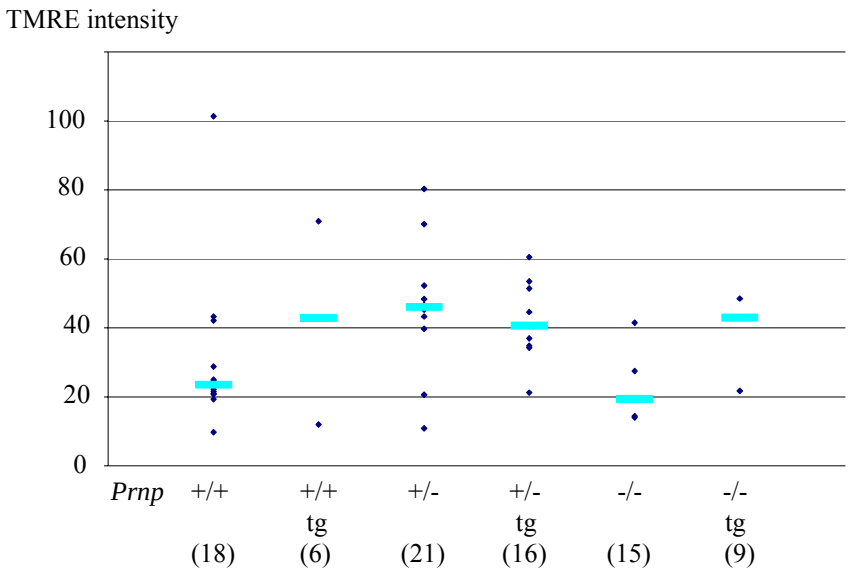

Fig51. **Mitochondrial membrane potential in CGN.** Each blue diamond is a data point and the light blue lines represent the medians of the respective data points. The number of mice from which cultures were established is indicated in brackets. No statistically significant effect is observable in any of the three *Prnp* genotypes.

In none of genotypes (*Prnp*$^{+/+}$, *Prnp*$^{+/-}$, *Prnp*$^{-/-}$) could any statistically significant difference be observed between the presence or absence of the transgene Δ8TM1-PrP. (N.B. For reasons mentioned above, the only legitimate comparisons are between littermates with or without transgene.) In conclusion the transgene Δ8TM1-PrP does not seem to have any effect on the regulation of mitochondrial membrane potential CGN cultures.

3.2.3.3 Endogenous ROS level in CGN derived from the F902 line of tg Δ8TM1-PrP

H_2DCFDA staining and FACS analysis were performed in order to assess endogenous ROS levels (Fig.52).

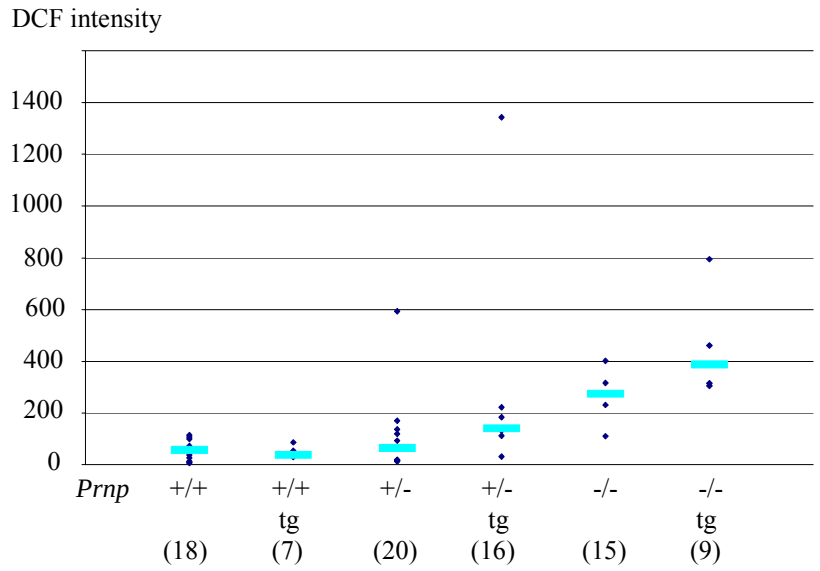

Fig52. **Endogenous ROS level in CGN.** Each blue diamond is a data point and the light blue lines represent the medians of the respective data points. The number of mice from which cultures were established is indicated in brackets. No statistically significant effect is observable in any of the three *Prnp* genotypes.

Here it is interesting to note that the data points display a wide spread except for $Prnp^{+/+}$ (with or without the transgene).

In none of genotypes ($Prnp^{+/+}$, $Prnp^{+/-}$, $Prnp^{-/-}$) could any statistically significant difference be observed between the presence or absence of the transgene Δ8TM1-PrP. (N.B. For reasons mentioned above, the only legitimate comparisons are between littermates with or without transgene.) In conclusion the transgene Δ8TM1-PrP does not seem to have any impact on endogenous ROS levels in CGN cultures.

3.2.3.4 ROS level after oxidative stress in CGN derived from F902 founder of tg Δ8TM1-PrP and control mice

H_2DCFDA staining in the presence of H_2O_2 and FACS analysis were performed in order to assess endogenous ROS levels (Fig.53).

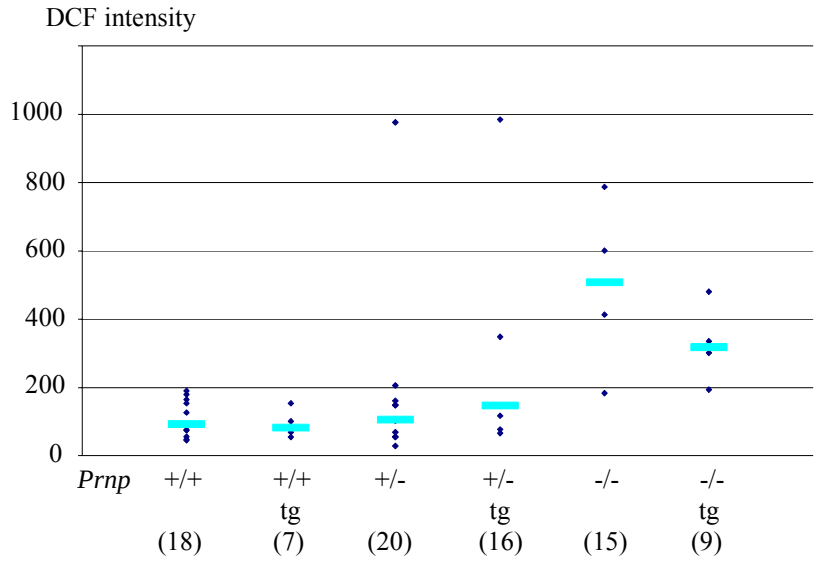

Fig53. **Intracellular ROS levels after oxidative stress induction in CGN.** Each blue diamond is a data point and the light blue lines represent the medians of the respective data points. The number of mice from which cultures were established is indicated in brackets. No statistically significant effect is observable in any of the three *Prnp* genotypes.

Once again, it is interesting to note that the data points display a wide spread except for *Prnp*$^{+/+}$ (with or without the transgene) as was the case for endogenous ROS levels (see above).

In none of genotypes (*Prnp*$^{+/+}$, *Prnp*$^{+/-}$, *Prnp*$^{-/-}$) could any statistically significant difference be observed between the presence or absence of the transgene Δ8TM1-PrP. (N.B. For reasons mentioned above, the only legitimate comparisons are between littermates with or without transgene.) In conclusion the transgene Δ8TM1-PrP does not seem to have any impact on intracellular ROS levels after induction of oxidative stress in CGN cultures.

4 Discussion

Most of the studies on prion protein have been focused on the scrapie isoform and tried to find ways of how to interfere with the posttranslational conversion process that makes PrP^{res} out of PrP^{c}, in an attempt to provide a cure or at least a halt of disease progression. In contrast, relative little research work has been invested on the cellular isoform.

The aim of the present work was to contribute to a better understanding of the physiological role of the cellular isoform of PrP and, in particular, of the role of the TM1 domain, the region of PrP which is most highly conserved throughout evolution.

The first approach chosen to investigate the contribution of the TM1 domain to the physiological roles of PrP was overexpression of wild-type and mutant PrP versions in mouse N_2A neuroblastoma cells. N_2A cells were transiently transfected with expression constructs for wt-PrP, Δ8TM1-PrP, Δocta-PrP or the empty vector ("mock"). The phenotypic analyses included measurements of the mitochondrial membrane potential ($\Delta\Psi$), the levels of endogenous reactive oxygen species (ROS) and ROS level after induction of oxidative stress by H_2O_2 exposure of the cells. Measuring $\Delta\Psi$ was interesting, as it reflects mitochondrial function. On the one hand the production of ATP, which occurs in active mitochondria and requires the presence of a mitochondrial membrane potential, is crucial for cell survival and proper cellular function. On the other hand mitochondria are probably the most important cellular site for endogenous ROS production, and this has also been linked with $\Delta\Psi$. Finally phenomena like mitochondrial uncoupling or imminent cell death are associated with a decrease in $\Delta\Psi$.

As is shown in Figs.16, 26 and 29 the ROS level after oxidative stress was reduced both in wt-PrP and Δ8TM1-PrP overexpressing cells. This protective, antioxidant effect had already been known in the literature for wt-PrP, but it is a new finding for Δ8TM1-PrP. That means this protective effect is *not* linked to the TM1 domain of PrP.

The double peak observable in Fig.16a is due to cellular heterogeneity in the mass population of N_2A, as demonstrated by the different subclones and also HeLa cells in Fig.18. As is shown Fig.17, three different oxidant compounds, *i.e.* H_2O_2, tBOOH and BSO, showed the same pattern, which rules out any compound-specific effect as an explanation for the observed heterogeneity.

A possible candidate mechanism underlying the antioxidant effect of PrP is an SOD-like activity of PrP, originally proprosed by Brown and colleagues (Brown and Besinger, 1998), (Brown, et al., 1999). However, as is shown Fig.21, the experiments performed in the framework of

the present study did not show any increase in the total cellular SOD activity, in line with data by Hutter and colleagues, showing that PrP^c itself has no SOD-like activity (Hutter, et al., 2003).

The next step was to investigate if copper could influence PrP^c functions. Copper is a well known ligand of PrP. Apart from a specialised copper binding domain, *i.e.* the octarepeat region, copper can also bind to histidines 99/111((Jones, et al., 2004), (Thompsett, et al., 2005)). As is shown in Fig.24 after a 24 h exposure of the cells to copper (100 μM), ΔΨ was decreased. Copper treatment also influenced endogenous ROS in Δ8TM1-PrP overexpressing cells (Fig.25). Copper had no impact on ROS level after oxidative stress (Fig.26). Additional experiments and aggregate analysis, however, did not confirm those initial results.

As PrP could bind copper mostly on its octarepeat region, these experiments were repeated with wt-PrP, Δ8TM1-PrP, Δocta-PrP or the empty vector transfection. Surprisingly, the phenotype of Δocta-PrP-transfected cells was different from mock-transfected cells: Overexpression of wt-PrP and Δ8TM1-PrP had no impact of ΔΨ whereas Δocta-PrP induced a decrease of ΔΨ (Fig.27). After copper treatment in all cases ΔΨ was decreased, which, in principle, might be explained as some kind of copper toxicity. However, this hypothesis could be excluded by microscopical inspection of the cells and viability tests (data not shown).

Fig.28 shows the aggregate data on the effect of PrP (wt or mutant) overexpression on endogenous ROS. It is apparent that overexpression of PrP has no impact on endogenous, basal ROS levels.

Fig.29 shows a protective effect of wt-PrP (already known from the literature) and Δ8TM1-PrP (new finding and as in Fig.16) which does not exist with Δocta-PrP. The protective effect of PrP^c involves its octarepeat region and *not* its TM1 domain. Copper treatment of these transfected cells leads to an increase of the ROS level.

As PrP does not seem to have any impact on the basal ROS level or to possess any SOD-like activity, its protective effect against oxidative stress calls for some other explanation, such as involvement in cellular signalling pathways.

As the MAPK pathway is involved in many signalling cascades all and as PrP has been reported to interact with many proteins involved in signalling, attention was focussed on three major MAP kinases, *i.e.* p38, c-Jun N-terminal Kinase (JNK) and Extracellular Regulated Kinase (ERK). It is also well known that JNK activation (phosphorylation) plays a key role in response to oxidative stress because its phosphorylation induces to protection against it or regulate apoptosis. More generally, p38 is known to be involved in apoptosis; JNK1 and JNK2/3 also called JNK/SAPK are involved in apoptosis, differentiation and inflammation response as well as in growth. Finally ERK1/ERK2, also called p42/p44, are involved in growth, differentiation and

development. An exposure to H_2O_2 and / or to other oxidative stress induces the stimulation of JNK and p38 pathways.

The prion protein is a GPI-anchored protein and such proteins are prominent in lipid rafts and caveolae where the membrane is enriched in cholesterol and glycolipids and in which a lot of signalling molecules are localized such as G-protein-coupled receptors and the Src family of tyrosine kinases (Src, Lyn, Fyn, Yes, Lck, Blk and Hck). PrP^c enriched in caveolae can active Fyn kinase, which leads to ERK1/2 activation (Toni, et al., 2006). Furthermore PrP signalling can induce a ROS production through NADPH oxidase recruitment and ERK1/2 phosphorylation (Schneider, et al., 2003). PrP 90-231 is also known to activate ERK1/2 (Thellung, et al., 2007). Moreover, in primary microglial cells the β-amyloid fibril or PrP peptide 106-126 activate inflammatory cascades and more specially Lyn and Syk kinases (Combs, et al., 1999). Activation of Lyn and Syk leads to an increase of calcium and to the activation of PKC and PYK2, which also activate ERK1/2. The pathway of signal transduction implicated in survival is activated in primary cerebellar granule neurones grown in PrP-coated tissue culture plates (Chen, et al., 2003). PKA, Scr kinases, PI3 kinases/AKT, MAPK (ERK) were activated, Bcl2 level was increased and Bax level was lower. The interaction between STI-1 and PrP has two major effect, *i.e.* neurogenesis through MAPK and neuroprotection through cAMP dependent PKA (Lopes, et al., 2005).

The data obtained in the present work showed the following: Phospho-p38 is not involved in the pathway which leads to the protective effect of PrP against oxidative stress (Fig.30). In contrast, the protective effect of PrP^c against oxidative stress seems to be linked to increased phosphorylation of p42 (Figs. 31 and 32). Interestingly, in Δ8TM1-PrP transfected cells the basal phosphorylation level of p42 is already increased compared to mock-transfected cells. In conclusion, the p42/p44 pathway seems to be involved in the protective function of PrP. As shown Figs. 33 and 34, the protective role of wt-PrP seems to be linked to a lower phosphorylation level of JNK2/3 and JNK1, in later phases of oxidant exposure.

In summary, the protective effect of PrP seems to involve the MAPK pathways via higher phosphorylation of p42 and lower phosphorylation of JNK1/JNK2/3.

PrP^c have also two possible cleavage sites. The α-cleavage occurs between the amino acids 110 and 111 by an ADAM protease and produces two fragments, *i.e.* C1 and N1. The β-cleavage occurs at the cell surface around or in the octarepeat region of PrP and produces two fragments, *i.e.* C2 and N2. Watt and colleagues (Watt and Hooper, 2005) were the first to show a link between ROS and β-cleavage. Very recent publications (Watt, et al., 2007) showed an involvement of the β-cleavage in the protective role of PrP against oxidative stress. H_2O_2 can induce β-cleavage of PrP at the plasma membrane. The same group also showed that tethering of the N-terminus of PrP

compromises it β-cleavage, which leads to an increase of ROS and the susceptibility to H_2O_2 and copper (Zeng, et al., 2003).

The complex relationships between PrP versions, H_2O_2, copper, MAPK and cytoprotection can be are summarised graphically in the schematic drawings shown in Fig. 54. Panel A shows the basic domain structure of PrP and the locations of the α and β cleavage sites. Panels B-D describe the proposed sequence of events following oxidant treatment of cells overexpression wt-PrP, Δ8TM1-PrP and Δocta-PrP, respectively.

a) Basic domain structure of PrP

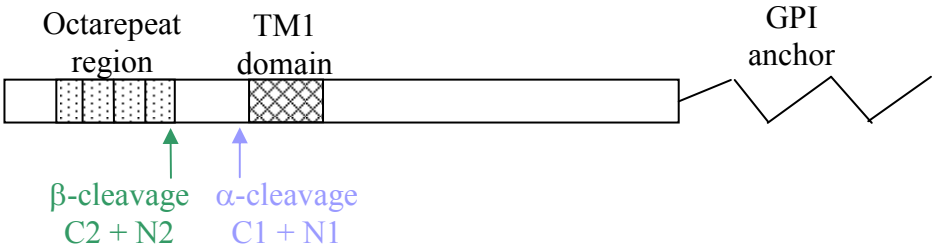

b) Model for wt-PrP

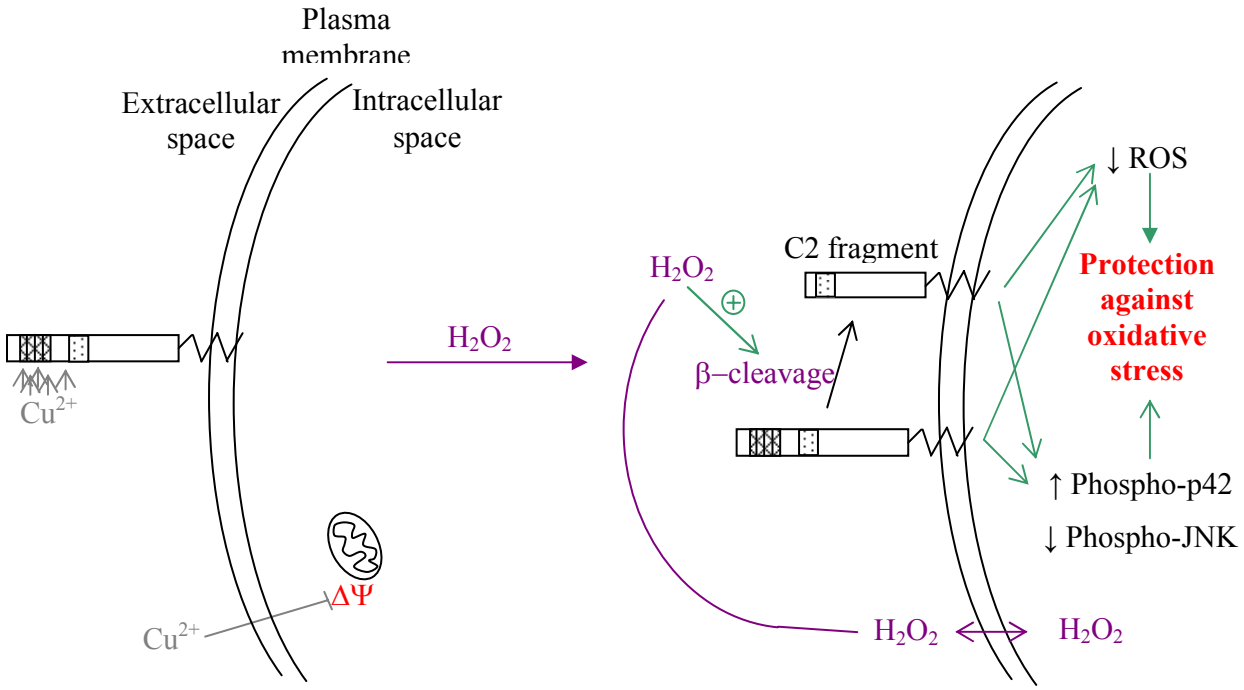

WT-PrP

c) Model for Δ8TM1-PrP

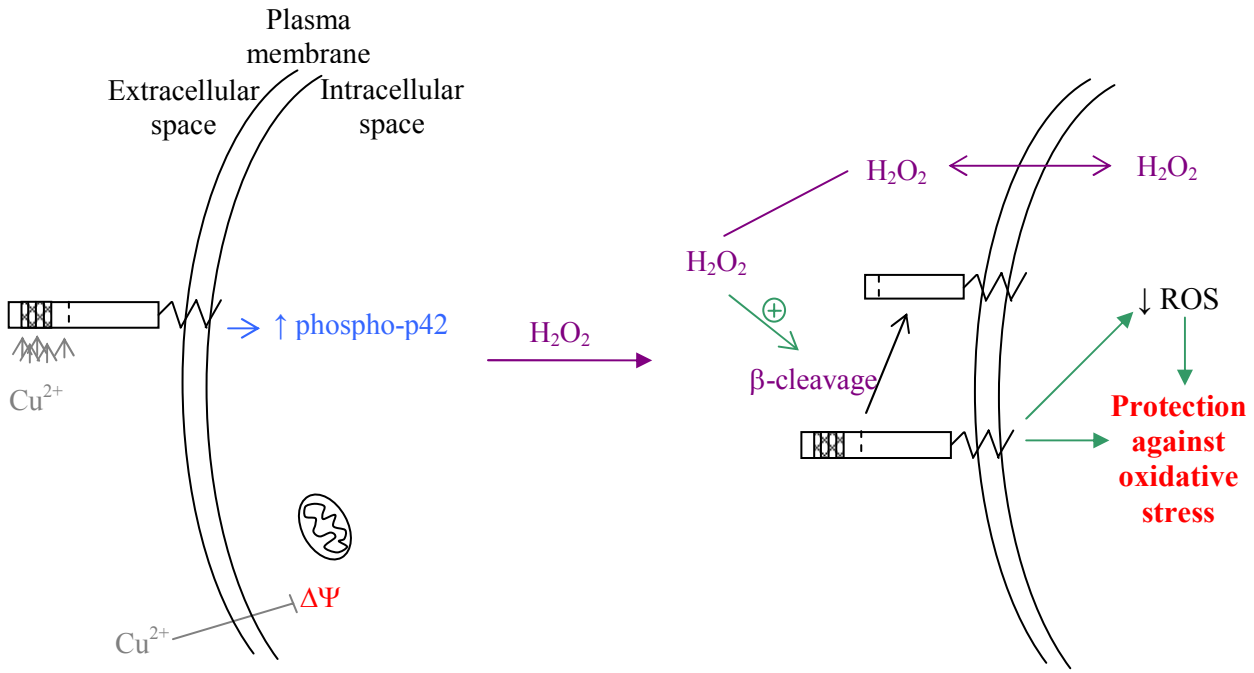

Δ8TM1-PrP

d) Model for Δocta-PrP

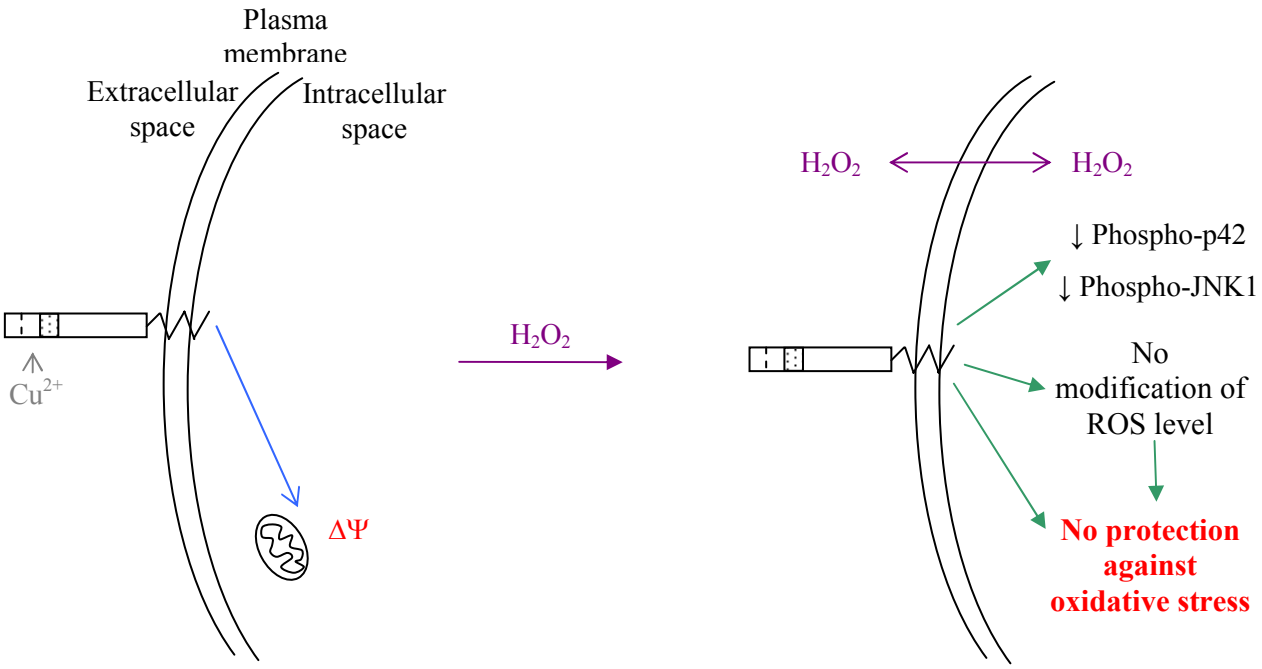

Δocta-PrP

Fig54. **Schematic drawing of the complex relationships between PrP versions, H_2O_2, copper, MAPK and cytoprotection**. a) Basic domain structure of PrP and the locations of the α and β cleavage sites; b) – d) Proposed sequence of events following oxidant treatment of cells overexpressing wt-PrP, Δ8TM1-PrP and Δocta-PrP, respectively.

All previous experiments have been performed with transiently overexpressing N_2A cells with $Prnp^{+/+}$ genotype. These cells already express PrP^c, which can overshadow some phenotypic effects of mutant PrP versions, especially loss-of-function effects. The generation of transgenic mice expressing Δ8TM1-PrP and their breeding into $Prnp^{+/+}$, $Prnp^{+/-}$, $Prnp^{-/-}$ backgrounds, achieved in the context of another project running in the Bürkle group, offered the opportunity to study primary cells from such animals.

As is shown Fig.35 and in Baumann et al. (Baumann, et al., 2007) the transgene Δ8TM1-PrP is weakly expressed in mouse brain.

First whole-brain primary cells were used. Culture age, *i.e.* the time between explantation of the brain cells and FACS analysis, has a big impact on ΔΨ, endogenous ROS level and ROS level after oxidative stress on these cells, as is shown Figs.40 to Fig.43. Therefore it was decided to exclusively use cells that had been in culture for two to three weeks after explantation. Moreover, the cell cultures were separated according to the tg lines F902 or M630, in order to exclude any confounding effects of the chromosomal intergration site of the transgene.

As the genetic background of the animals was mixed and was different for the three *Prnp* genotypes ($Prnp^{+/+}$, $Prnp^{+/-}$, $Prnp^{-/-}$), comparisons were only valid between transgenic mice and non-transgenic littermates of the same genotype. No difference was observable in any for the parameters studied (Fig.44-45 for ΨΔ, Fig.46-47 for endogenous ROS and Fig.48-49 for ROS after H_2O_2 treatment), except for an increase in ROS induced by oxidative stress in transgenic mice of the line M630 on $Prnp^{+/-}$ background (Fig. 49). In Figs. 44 to 49 the patterns of datapoints observed differ between lines M630 or F902, which may well be due to differences in the chromosomal integration site and/or regulation of the transgene.

In an attempt to reduce the large spread of the experimental data obtained with whole-brain primary cells, which was possibly due to the heterogeneity of diverse cell types present in those cultures, further experiments were done with Cerebellar Granular Neurones (CGN), as this type of culture typically yields a very high proportion of neurones.

As shown Figs.51 to 53 the transgene Δ8TM1-PrP had no effect on the mitochondrial membrane potential, endogenous ROS or any protective effect after oxidative stress in CGN cultures. A plausible explanation is the relative underexpression of the transgene.

Interestingly, in the experiments shown in figures 51 to 53, the spread of the datapoints was consistently and dramatically reduced for the cultures of $Prnp^{+/+}$ genetic background. These experiments were performed on different days, thus demonstrating that the methodology used was accurate and stable. Therefore, the large spread observed in other case should reflect biological variation rather than technical instability. For example, in cases of $Prnp^{+/-}$ and $Prnp^{-/-}$ genotypes

(Figures 51 to 53) error bars are rather big. This could be due to the diversity of genetic background (see Fig. 6). Another explanation could be a haploinsufficiency of the wt-PrP copy left in the *Prnp*$^{+/-}$ background, which might preclude readjustment of some delicate balance between endogenous and exogenous PrP.

Unfortunately, in the present work no comparison was possible between the three *Prnp* genotypes, as explained above. It would have been interesting to investigate the effect of the transgene as a function of different genotypes, because reports from the literature indicate some interesting differences. For example, mitochondrial numbers and morphology are changed in *Prnp*$^{-/-}$ mice (Miele, et al., 2002), whereas baseline mitochondrial respiration and mitochondrial membrane potential are not changed (Lobao-Soares, et al., 2005). Moreover *Prnp*$^{-/-}$ mice suffer from more extensive injury and cell death after hypoxic brain damage (McLennan, et al., 2004) and after traumatic brain injury (Hoshino, et al., 2003). Cultured cell from Zürich-1 *Prnp*$^{-/-}$ mice are more sensitive to toxic substances such as copper or superoxide and their copper metabolism is altered (Brown, et al., 1997a; Brown, et al., 1998a). Markers of oxidative stress are upregulated in *Prnp*$^{-/-}$ mice (Wong, et al., 2001) and antioxidant defence in these mice is out of balance (Klamt, et al., 2001). In their brains and derived cell cultures p53 expression is altered and the expression of BAX, Bcl2 and ERK are enhanced (Brown, et al., 2002).

5 Conclusion and Outlook

One major conclusion of this study is that PrP^c has a protective function against oxidative stress induced for example by H_2O_2 treatment but does not seem to be implicated either in the regulation of the mitochondrial membrane potential nor in the endogenous ROS level.

This protection involves the octarepeat region of PrP^c but not its TM1 domain. The MAPK pathways seem to be involved in this protective role as is indicated by an increased phosphorylation of p42 and a decreased phosphorylation of JNK1/JNK2/3.

It could be interesting to create a double mutant in which both the octarepeat region and the Δ8TM1 domain are lacking and to repeat the experiments. Which impact will it have on mitochondrial membrane potential, endogenous ROS and especially on ROS level after oxidative stress and on the MAPK pathway, in the presence or absence of copper treatment? If any effect will be observable in the presence of copper it would point to a role for the two histidines (His99 and His111) that can also bind copper ((Jones, et al., 2004), (Thompsett, et al., 2005)).

Another interesting question would be the effect of oxidant treatment on mitochondrial membrane potential in PrP (wt or mutants) overexpressing N_2A cells. Is, in case of oxidative stress, the protective effect of PrP linked to the mitochondrial membrane potential? Will, in this condition more or less calcium be released? Is there any involvement of uncoupling proteins (UCP)? UCP are a family of proteins located in the inner mitochondrial membrane. They can dissociate oxidative phosphorylation from the respiratory chain and so induced heat production and a decrease of ROS production (Pecqueur, et al., 2001). In mammalians, the UCP family comprises 5 members. UCP1 is specifically expressed in brown adipose tissue, UCP2 in neurones and glia cells, UCP3 in skeletal muscle cells, and UCP 4 and UCP5 in the nervous system.

In order to confirm the involvement of MAPK, additional western blots should be done after treatment with specific MAPK inhibitors such as U0126, PD98059, SB203580 or SP600125. U0126 inhibits MEK1 and MEK2, which normally phosphorylate ERK1 and ERK2. PD98059 specially inhibits MEK1, SB203580 is specific for p38 and SP600125 for JNK.

Some other proteins such as Fyn and other Src kinases or STI-1 might be also involved in this protective effect. Therefore additional analyses should be done focussed on these proteins.

Because N_2A cells express endogenous PrP, other cells on a *Prnp*$^{-/-}$ background could be also used to repeat the experiments. In this case any effect would only result from the PrP version encoded by the transfected plasmid.

In primary cells and CGN derived from mice carrying or not the transgene Δ8TM1-PrP, no effect was observable between the absence and the presence of the transgene. A likely explanation is the low level of expression. This problem might be overcome by creating new lines of transgenic mice with increased transgene Δ8TM1-PrP gene copy number. It would be also useful to include only animals sharing the same genetic background in order to rule out any effect resulting from any other gene apart from the transgene. An alternative solution could be infecting *Prnp*$^{-/-}$ CGN with retroviral vectors carrying expression cassettes for wt or mutant PrP versions.

Another interesting question is to explain why in the same experiments CGN with different *Prnp* genotype displayed hugely different error bars, *e.g.* in ROS levels after H_2O_2 treatment (Fig. 53). In order to determine if this was due to the *Prnp* genotype or the general genetic background (FVB vs. 129SV) the following experiments could be done: repetition of the previous experiments with CGN derived from *Prnp*$^{+/+}$ FVB mice crossed with *Prnp*$^{-/-}$ FVB mice, *Prnp*$^{+/+}$ FVB mice crossed with *Prnp*$^{+/+}$ FVB mice and *Prnp*$^{-/-}$ FVB mice crossed with *Prnp*$^{-/-}$ FVB mice. This would guarantee that the genetic background from all other genes is really identical, and any phenotypic difference, including the spread of the experimental data, should then be due to the *Prnp* genotype.

As it has been shown that *in vivo*, PrP can modulate intracellular calcium response to H_2O_2 through its octarepeat region and Fyn signalling (Krebs, et al., 2007) it could be interesting to monitor and compare calcium influx in primary cells derived from mice carrying or not the Δ8TM1-PrP transgene and this on different *Prnp* background.

Finally, transgenic mice on the same genetic background could be used for microarray analysis, in order to search for any modification (up or down regulation) in gene expression patterns between *Prnp*$^{-/-}$, *Prnp*$^{-/-}$ *tg,* and *Prnp*$^{+/-}$.

6 Literature

Aguzzi, A., (2006). 'Prion diseases of humans and farm animals: epidemiology, genetics, and pathogenesis'. *J Neurochem*, 97 (6):1726-1739.

Aguzzi, A., Glatzel, M., Montrasio, F., Prinz, M. and Heppner, F.L., (2001). 'Interventional strategies against prion diseases'. *Nat Rev Neurosci*, 2 (10):745-749.

Aguzzi, A. and Polymenidou, M., (2004). 'Mammalian prion biology. One century of evolving concepts'. *Cell*, 116 (2):313-327.

Archibald, S., (2004). 'Prion protein found outside the CNS'. *Lancet Neurol*, 3 (1):8.

Bai, G., Rama Rao, K.V., Murthy, C.R., Panickar, K.S., Jayakumar, A.R. and Norenberg, M.D., (2001). 'Ammonia induces the mitochondrial permeability transition in primary cultures of rat astrocytes'. *J Neurosci Res*, 66 (5):981-991.

Basler, K., Oesch, B., Scott, M., Westaway, D., Walchli, M., Groth, D.F., McKinley, M.P., Prusiner, S.B. and Weissmann, C., (1986). 'Scrapie and cellular PrP isoforms are encoded by the same chromosomal gene'. *Cell*, 46 (3):417-428.

Baumann, F., Pahnke, J., Brabeck, C., Kloz, U., Niemann, H.H., Bürkle, A., Tolnay, M., Rülicke, T. and Aguzzi, A., (2007a). 'Identification of functional domains within the prion protein PrP in transgenic mice'.

Bendheim, P.E., Brown, H.R., Rudelli, R.D., Scala, L.J., Goller, N.L., Wen, G.Y., Kascsak, R.J., Cashman, N.R. and Bolton, D.C., (1992). 'Nearly ubiquitous tissue distribution of the scrapie agent precursor protein'. *Neurology*, 42 (1):149-156.

Borchelt, D.R., Davis, J., Fischer, M., Lee, M.K., Slunt, H.H., Ratovitsky, T., Regard, J., Copeland, N.G., Jenkins, N.A., Sisodia, S.S. and Price, D.L., (1996). 'A vector for expressing foreign genes in the brains and hearts of transgenic mice'. *Genet Anal*, 13 (6):159-163.

Boyd, C.S. and Cadenas, E., (2002). 'Nitric oxide and cell signaling pathways in mitochondrial-dependent apoptosis'. *Biol Chem*, 383 (3-4):411-423.

Brown, D.R., (2001). 'Prion and prejudice: normal protein and the synapse'. *Trends Neurosci*, 24 (2):85-90.

Brown, D.R. and Besinger, A., (1998). 'Prion protein expression and superoxide dismutase activity'. *Biochem J*, 334 (Pt 2):423-429.

Brown, D.R., Clive, C. and Haswell, S.J., (2001). 'Antioxidant activity related to copper binding of native prion protein'. *J Neurochem*, 76 (1):69-76.

Brown, D.R., Nicholas, R.S. and Canevari, L., (2002). 'Lack of prion protein expression results in a neuronal phenotype sensitive to stress'. *J Neurosci Res*, 67 (2):211-224.

Brown, D.R., Qin, K., Herms, J.W., Madlung, A., Manson, J., Strome, R., Fraser, P.E., Kruck, T., von Bohlen, A., Schulz-Schaeffer, W., Giese, A., Westaway, D. and Kretzschmar, H., (1997a). 'The cellular prion protein binds copper in vivo'. *Nature*, 390 (6661):684-687.

Brown, D.R., Schmidt, B. and Kretzschmar, H.A., (1998a). 'Effects of copper on survival of prion protein knockout neurons and glia'. *J Neurochem*, 70 (4):1686-1693.

Brown, D.R., Schmidt, B. and Kretzschmar, H.A., (1998b). 'A prion protein fragment primes type 1 astrocytes to proliferation signals from microglia'. *Neurobiol Dis*, 4 (6):410-422.

Brown, D.R., Schulz-Schaeffer, W.J., Schmidt, B. and Kretzschmar, H.A., (1997b). 'Prion protein-deficient cells show altered response to oxidative stress due to decreased SOD-1 activity'. *Exp Neurol*, 146 (1):104-112.

Brown, D.R., Wong, B.S., Hafiz, F., Clive, C., Haswell, S.J. and Jones, I.M., (1999). 'Normal prion protein has an activity like that of superoxide dismutase'. *Biochem J*, 344 Pt 1:1-5.

Büeler, H., Fischer, M., Lang, Y., Bluethmann, H., Lipp, H.P., DeArmond, S.J., Prusiner, S.B., Aguet, M. and Weissmann, C., (1992). 'Normal development and behaviour of mice lacking the neuronal cell-surface PrP protein'. *Nature*, 356 (6370):577-582.

Burns, C.S., Aronoff-Spencer, E., Legname, G., Prusiner, S.B., Antholine, W.E., Gerfen, G.J., Peisach, J. and Millhauser, G.L., (2003). 'Copper coordination in the full-length, recombinant prion protein'. *Biochemistry*, 42 (22):6794-6803.

Chattopadhyay, M., Walter, E.D., Newell, D.J., Jackson, P.J., Aronoff-Spencer, E., Peisach, J., Gerfen, G.J., Bennett, B., Antholine, W.E. and Millhauser, G.L., (2005). 'The Octarepeat Domain of the Prion Protein Binds Cu(II) with Three Distinct Coordination Modes at pH 7.4'. *J Am Chem Soc*, 127 (36):12647-12656.

Chen, S., Mange, A., Dong, L., Lehmann, S. and Schachner, M., (2003). 'Prion protein as trans-interacting partner for neurons is involved in neurite outgrowth and neuronal survival'. *Mol Cell Neurosci*, 22 (2):227-233.

Chen, S.G., Teplow, D.B., Parchi, P., Teller, J.K., Gambetti, P. and Autilio-Gambetti, L., (1995). 'Truncated forms of the human prion protein in normal brain and in prion diseases'. *J Biol Chem*, 270 (32):19173-19180.

Chernoff, Y.O., Lindquist, S.L., Ono, B., Inge-Vechtomov, S.G. and Liebman, S.W., (1995). 'Role of the chaperone protein Hsp104 in propagation of the yeast prion-like factor [psi+]'. *Science*, 268 (5212):880-884.

Colling, S.B., Collinge, J. and Jefferys, J.G., (1996). 'Hippocampal slices from prion protein null mice: disrupted Ca(2+)-activated K+ currents'. *Neurosci Lett*, 209 (1):49-52.

Colling, S.B., Khana, M., Collinge, J. and Jefferys, J.G., (1997). 'Mossy fibre reorganization in the hippocampus of prion protein null mice'. *Brain Res*, 755 (1):28-35.

Collinge, J., (2001). 'Prion diseases of humans and animals: their causes and molecular basis'. *Annu Rev Neurosci*, 24:519-550.

Collinge, J., Whittington, M.A., Sidle, K.C., Smith, C.J., Palmer, M.S., Clarke, A.R. and Jefferys, J.G., (1994). 'Prion protein is necessary for normal synaptic function'. *Nature*, 370 (6487):295-297.

Collins, P.S., Lawson, V.A. and Masters, P.C., (2004). 'Transmissible spongiform encephalopathies'. *Lancet*, 363 (9402):51-61.

Combs, C.K., Johnson, D.E., Cannady, S.B., Lehman, T.M. and Landreth, G.E., (1999). 'Identification of microglial signal transduction pathways mediating a neurotoxic response to amyloidogenic fragments of beta-amyloid and prion proteins'. *J Neurosci*, 19 (3):928-939.

Coustou, V., Deleu, C., Saupe, S. and Begueret, J., (1997). 'The protein product of the het-s heterokaryon incompatibility gene of the fungus Podospora anserina behaves as a prion analog'. *Proc Natl Acad Sci U S A*, 94 (18):9773-9778.

de Almeida, C.J., Chiarini, L.B., da Silva, J.P., PM, E.S., Martins, M.A. and Linden, R., (2005). 'The cellular prion protein modulates phagocytosis and inflammatory response'. *J Leukoc Biol*, 77 (2):238-246.

Derkatch, I.L., Bradley, M.E., Hong, J.Y. and Liebman, S.W., (2001). 'Prions affect the appearance of other prions: the story of [PIN(+)]'. *Cell*, 106 (2):171-182.

Derkatch, I.L., Chernoff, Y.O., Kushnirov, V.V., Inge-Vechtomov, S.G. and Liebman, S.W., (1996). 'Genesis and variability of [PSI] prion factors in Saccharomyces cerevisiae'. *Genetics*, 144 (4):1375-1386.

Droge, W., (2002). 'Free radicals in the physiological control of cell function'. *Physiol Rev*, 82 (1):47-95.

Ettaiche, M., Pichot, R., Vincent, J.P. and Chabry, J., (2000). 'In vivo cytotoxicity of the prion protein fragment 106-126'. *J Biol Chem*, 275 (47):36487-36490.

Ford, M.J., Burton, L.J., Li, H., Graham, C.H., Frobert, Y., Grassi, J., Hall, S.M. and Morris, R.J., (2002). 'A marked disparity between the expression of prion protein and its message by neurones of the CNS'. *Neuroscience*, 111 (3):533-551.

Forloni, G., Angeretti, N., Chiesa, R., Monzani, E., Salmona, M., Bugiani, O. and Tagliavini, F., (1993). 'Neurotoxicity of a prion protein fragment'. *Nature*, 362 (6420):543-546.

Fuhrmann, M., Bittner, T., Mitteregger, G., Haider, N., Moosmang, S., Kretzschmar, H. and Herms, J., (2006). 'Loss of the cellular prion protein affects the Ca2+ homeostasis in hippocampal CA1 neurons'. *J Neurochem*, 98 (6):1876-1885.

Gabriel, J.M., Oesch, B., Kretzschmar, H., Scott, M. and Prusiner, S.B., (1992). 'Molecular cloning of a candidate chicken prion protein'. *Proc Natl Acad Sci U S A*, 89 (19):9097-9101.

Gains, M.J., Roth, K.A. and LeBlanc, A.C., (2006). 'Prion protein protects against ethanol-induced Bax-mediated cell death in vivo'. *Neuroreport*, 17 (9):903-906.

Gilch, S., Nunziante, M., Ertmer, A., Wopfner, F., Laszlo, L. and Schatzl, H.M., (2004). 'Recognition of lumenal prion protein aggregates by post-ER quality control mechanisms is mediated by the preoctarepeat region of PrP'. *Traffic*, 5 (4):300-313.

Griffith, J.S., (1967). 'Self-replication and scrapie'. *Nature*, 215 (105):1043-1044.

Gunter, T.E. and Pfeiffer, D.R., (1990). 'Mechanisms by which mitochondria transport calcium'. *Am J Physiol*, 258 (5 Pt 1):C755-786.

Harris, D.A., Falls, D.L., Johnson, F.A. and Fischbach, G.D., (1991). 'A prion-like protein from chicken brain copurifies with an acetylcholine receptor-inducing activity'. *Proc Natl Acad Sci U S A*, 88 (17):7664-7668.

Harris, D.A., Huber, M.T., van Dijken, P., Shyng, S.L., Chait, B.T. and Wang, R., (1993a). 'Processing of a cellular prion protein: identification of N- and C-terminal cleavage sites'. *Biochemistry*, 32 (4):1009-1016.

Harris, D.A., Lele, P. and Snider, W.D., (1993b). 'Localization of the mRNA for a chicken prion protein by in situ hybridization'. *Proc Natl Acad Sci U S A*, 90 (9):4309-4313.

Hegde, R.S., Mastrianni, J.A., Scott, M.R., DeFea, K.A., Tremblay, P., Torchia, M., DeArmond, S.J., Prusiner, S.B. and Lingappa, V.R., (1998). 'A transmembrane form of the prion protein in neurodegenerative disease'. *Science*, 279 (5352):827-834.

Hegde, R.S., Tremblay, P., Groth, D., DeArmond, S.J., Prusiner, S.B. and Lingappa, V.R., (1999). 'Transmissible and genetic prion diseases share a common pathway of neurodegeneration'. *Nature*, 402 (6763):822-826.

Herms, J.W., Korte, S., Gall, S., Schneider, I., Dunker, S. and Kretzschmar, H.A., (2000). 'Altered intracellular calcium homeostasis in cerebellar granule cells of prion protein-deficient mice'. *J Neurochem*, 75 (4):1487-1492.

Holscher, C., Delius, H. and Burkle, A., (1998). 'Overexpression of nonconvertible PrPc delta114-121 in scrapie-infected mouse neuroblastoma cells leads to trans-dominant inhibition of wild-type PrP(Sc) accumulation'. *J Virol*, 72 (2):1153-1159.

Horiuchi, M., Yamazaki, N., Ikeda, T., Ishiguro, N. and Shinagawa, M., (1995). 'A cellular form of prion protein (PrPC) exists in many non-neuronal tissues of sheep'. *J Gen Virol*, 76 (Pt 10):2583-2587.

Hornshaw, M.P., McDermott, J.R., Candy, J.M. and Lakey, J.H., (1995). 'Copper binding to the N-terminal tandem repeat region of mammalian and avian prion protein: structural studies using synthetic peptides'. *Biochem Biophys Res Commun*, 214 (3):993-999.

Hoshino, S., Inoue, K., Yokoyama, T., Kobayashi, S., Asakura, T., Teramoto, A. and Itohara, S., (2003). 'Prions prevent brain damage after experimental brain injury: a preliminary report'. *Acta Neurochir Suppl*, 86:297-299.

Hutter, G., Heppner, F.L. and Aguzzi, A., (2003). 'No superoxide dismutase activity of cellular prion protein in vivo'. *Biol Chem*, 384 (9):1279-1285.

Jones, C.E., Abdelraheim, S.R., Brown, D.R. and Viles, J.H., (2004). 'Preferential Cu2+ coordination by His96 and His111 induces beta-sheet formation in the unstructured amyloidogenic region of the prion protein'. *J Biol Chem*, 279 (31):32018-32027.

Klamt, F., Dal-Pizzol, F., Conte da Frota, M.J., Walz, R., Andrades, M.E., da Silva, E.G., Brentani, R.R., Izquierdo, I. and Fonseca Moreira, J.C., (2001). 'Imbalance of antioxidant defense in mice lacking cellular prion protein'. *Free Radic Biol Med*, 30 (10):1137-1144.

Kowaltowski, A.J. and Vercesi, A.E., (1999). 'Mitochondrial damage induced by conditions of oxidative stress'. *Free Radic Biol Med*, 26 (3-4):463-471.

Krebs, B., Dorner-Ciossek, C., Schmalzbauer, R., Vassallo, N., Herms, J. and Kretzschmar, H.A., (2006). 'Prion protein induced signaling cascades in monocytes'. *Biochem Biophys Res Commun*, 340 (1):13-22.

Krebs, B., Wiebelitz, A., Balitzki-Korte, B., Vassallo, N., Paluch, S., Mitteregger, G., Onodera, T., Kretzschmar, H.A. and Herms, J., (2007). 'Cellular prion protein modulates the intracellular calcium response to hydrogen peroxide'. *J Neurochem*, 100 (2):358-367.

Kristiansen, M., Messenger, M.J., Klohn, P.C., Brandner, S., Wadsworth, J.D., Collinge, J. and Tabrizi, S.J., (2005). 'Disease-related prion protein forms aggresomes in neuronal cells leading to caspase activation and apoptosis'. *J Biol Chem*, 280 (46):38851-38861.

Kupper, J.H., de Murcia, G. and Burkle, A., (1990). 'Inhibition of poly(ADP-ribosyl)ation by overexpressing the poly(ADP-ribose) polymerase DNA-binding domain in mammalian cells'. *J Biol Chem*, 265 (31):18721-18724.

Kuwahara, C., Takeuchi, A.M., Nishimura, T., Haraguchi, K., Kubosaki, A., Matsumoto, Y., Saeki, K., Yokoyama, T., Itohara, S. and Onodera, T., (1999). 'Prions prevent neuronal cell-line death'. *Nature*, 400 (6741):225-226.

Laine, J., Marc, M.E., Sy, M.S. and Axelrad, H., (2001). 'Cellular and subcellular morphological localization of normal prion protein in rodent cerebellum'. *Eur J Neurosci*, 14 (1):47-56.

Li, A., Sakaguchi, S., Atarashi, R., Roy, B.C., Nakaoke, R., Arima, K., Okimura, N., Kopacek, J. and Shigematsu, K., (2000a). 'Identification of a novel gene encoding a PrP-like protein expressed as chimeric transcripts fused to PrP exon 1/2 in ataxic mouse line with a disrupted PrP gene'. *Cell Mol Neurobiol*, 20 (5):553-567.

Li, A., Sakaguchi, S., Shigematsu, K., Atarashi, R., Roy, B.C., Nakaoke, R., Arima, K., Okimura, N., Kopacek, J. and Katamine, S., (2000b). 'Physiological expression of the gene for PrP-like protein, PrPLP/Dpl, by brain endothelial cells and its ectopic expression in neurons of PrP-deficient mice ataxic due to Purkinje cell degeneration'. *Am J Pathol*, 157 (5):1447-1452.

Lobao-Soares, B., Bianchin, M.M., Linhares, M.N., Carqueja, C.L., Tasca, C.I., Souza, M., Marques, W., Jr., Brentani, R., Martins, V.R., Sakamoto, A.C., Carlotti, C.G., Jr. and Walz, R., (2005). 'Normal brain mitochondrial respiration in adult mice lacking cellular prion protein'. *Neurosci Lett*, 375 (3):203-206.

Lopes, M.H., Hajj, G.N., Muras, A.G., Mancini, G.L., Castro, R.M., Ribeiro, K.C., Brentani, R.R., Linden, R. and Martins, V.R., (2005). 'Interaction of cellular prion and stress-inducible protein 1 promotes neuritogenesis and neuroprotection by distinct signaling pathways'. *J Neurosci*, 25 (49):11330-11339.

Mallucci, G.R., Ratte, S., Asante, E.A., Linehan, J., Gowland, I., Jefferys, J.G. and Collinge, J., (2002). 'Post-natal knockout of prion protein alters hippocampal CA1 properties, but does not result in neurodegeneration'. *Embo J*, 21 (3):202-210.

Manson, J., West, J.D., Thomson, V., McBride, P., Kaufman, M.H. and Hope, J., (1992). 'The prion protein gene: a role in mouse embryogenesis?' *Development*, 115 (1):117-122.

Manson, J.C., Hope, J., Clarke, A.R., Johnston, A., Black, C. and MacLeod, N., (1995). 'PrP gene dosage and long term potentiation'. *Neurodegeneration*, 4 (1):113-114.

McLennan, N.F., Brennan, P.M., McNeill, A., Davies, I., Fotheringham, A., Rennison, K.A., Ritchie, D., Brannan, F., Head, M.W., Ironside, J.W., Williams, A. and Bell, J.E., (2004). 'Prion protein accumulation and neuroprotection in hypoxic brain damage'. *Am J Pathol*, 165 (1):227-235.

Miele, G., Jeffrey, M., Turnbull, D., Manson, J. and Clinton, M., (2002). 'Ablation of cellular prion protein expression affects mitochondrial numbers and morphology'. *Biochem Biophys Res Commun*, 291 (2):372-377.

Milhavet, O. and Lehmann, S., (2002). 'Oxidative stress and the prion protein in transmissible spongiform encephalopathies'. *Brain Res Brain Res Rev*, 38 (3):328-339.

Millhauser, G.L., (2004). 'Copper binding in the prion protein'. *Acc Chem Res*, 37 (2):79-85.

Mironov, A., Jr., Latawiec, D., Wille, H., Bouzamondo-Bernstein, E., Legname, G., Williamson, R.A., Burton, D., DeArmond, S.J., Prusiner, S.B. and Peters, P.J., (2003). 'Cytosolic prion protein in neurons'. *J Neurosci*, 23 (18):7183-7193.

Moore, R.C., Lee, I.Y., Silverman, G.L., Harrison, P.M., Strome, R., Heinrich, C., Karunaratne, A., Pasternak, S.H., Chishti, M.A., Liang, Y., Mastrangelo, P., Wang, K., Smit, A.F., Katamine, S., Carlson, G.A., Cohen, F.E., Prusiner, S.B., Melton, D.W., Tremblay, P., Hood, L.E. and Westaway, D., (1999). 'Ataxia in prion protein (PrP)-deficient mice is associated with upregulation of the novel PrP-like protein doppel'. *J Mol Biol*, 292 (4):797-817.

Morel, E., Fouquet, S., Chateau, D., Yvernault, L., Frobert, Y., Pincon-Raymond, M., Chambaz, J., Pillot, T. and Rousset, M., (2003). 'The cellular prion protein PrPc is expressed in human enterocytes in cell-cell junctional domains'. *J Biol Chem*.

Moser, M., Colello, R.J., Pott, U. and Oesch, B., (1995). 'Developmental expression of the prion protein gene in glial cells'. *Neuron*, 14 (3):509-517.

Mouillet-Richard, S., Ermonval, M., Chebassier, C., Laplanche, J.L., Lehmann, S., Launay, J.M. and Kellermann, O., (2000). 'Signal transduction through prion protein'. *Science*, 289 (5486):1925-1928.

Nagy, G., Koncz, A. and Perl, A., (2003). 'T cell activation-induced mitochondrial hyperpolarization is mediated by Ca2+- and redox-dependent production of nitric oxide'. *J Immunol*, 171 (10):5188-5197.

Nicholls, D.G. and Ward, M.W., (2000). 'Mitochondrial membrane potential and neuronal glutamate excitotoxicity: mortality and millivolts'. *Trends Neurosci*, 23 (4):166-174.

Nicholson, E.M., Mo, H., Prusiner, S.B., Cohen, F.E. and Marqusee, S., (2002). 'Differences between the prion protein and its homolog Doppel: a partially structured state with implications for scrapie formation'. *J Mol Biol*, 316 (3):807-815.

Nishida, N., Tremblay, P., Sugimoto, T., Shigematsu, K., Shirabe, S., Petromilli, C., Erpel, S.P., Nakaoke, R., Atarashi, R., Houtani, T., Torchia, M., Sakaguchi, S., DeArmond, S.J., Prusiner, S.B. and Katamine, S., (1999). 'A mouse prion protein transgene rescues mice deficient for the prion protein gene from purkinje cell degeneration and demyelination'. *Lab Invest*, 79 (6):689-697.

Nunziante, M., Gilch, S. and Schatzl, H.M., (2003). 'Prion diseases: from molecular biology to intervention strategies'. *Chembiochem*, 4 (12):1268-1284.

O'Donovan, C.N., Tobin, D. and Cotter, T.G., (2001). 'Prion protein fragment PrP-(106-126) induces apoptosis via mitochondrial disruption in human neuronal SH-SY5Y cells'. *J Biol Chem*, 276 (47):43516-43523.

Pan, T., Li, R., Wong, B.S., Liu, T., Gambetti, P. and Sy, M.S., (2002). 'Heterogeneity of normal prion protein in two- dimensional immunoblot: presence of various glycosylated and truncated forms'. *J Neurochem*, 81 (5):1092-1101.

Pan, T., Wong, P., Chang, B., Li, C., Li, R., Kang, S.C., Wisniewski, T. and Sy, M.S., (2005). 'Biochemical fingerprints of prion infection: accumulations of aberrant full-length and N-terminally truncated PrP species are common features in mouse prion disease'. *J Virol*, 79 (2):934-943.

Paushkin, S.V., Kushnirov, V.V., Smirnov, V.N. and Ter-Avanesyan, M.D., (1997). 'In vitro propagation of the prion-like state of yeast Sup35 protein'. *Science*, 277 (5324):381-383.

Pecqueur, C., Couplan, E., Bouillaud, F. and Ricquier, D., (2001). 'Genetic and physiological analysis of the role of uncoupling proteins in human energy homeostasis'. *J Mol Med*, 79 (1):48-56.

Prusiner, S.B., (1982). 'Novel proteinaceous infectious particles cause scrapie'. *Science*, 216 (4542):136-144.

Rachidi, W., Vilette, D., Guiraud, P., Arlotto, M., Riondel, J., Laude, H., Lehmann, S. and Favier, A., (2003). 'Expression of prion protein increases cellular copper binding and antioxidant enzyme activities but not copper delivery'. *J Biol Chem*, 278 (11):9064-9072.

Rivera-Milla, E., Oidtmann, B., Panagiotidis, C.H., Baier, M., Sklaviadis, T., Hoffmann, R., Zhou, Y., Solis, G.P., Stuermer, C.A. and Malaga-Trillo, E., (2006). 'Disparate evolution of prion protein domains and the distinct origin of Doppel- and prion-related loci revealed by fish-to-mammal comparisons'. *Faseb J*, 20 (2):317-319.

Rivera-Milla, E., Stuermer, C.A. and Malaga-Trillo, E., (2003). 'An evolutionary basis for scrapie disease: identification of a fish prion mRNA'. *Trends Genet*, 19 (2):72-75.

Roucou, X., Giannopoulos, P.N., Zhang, Y., Jodoin, J., Goodyer, C.G. and LeBlanc, A., (2005). 'Cellular prion protein inhibits proapoptotic Bax conformational change in human neurons and in breast carcinoma MCF-7 cells'. *Cell Death Differ*, 12 (7):783-795.

Sakaguchi, S., Katamine, S., Nishida, N., Moriuchi, R., Shigematsu, K., Sugimoto, T., Nakatani, A., Kataoka, Y., Houtani, T., Shirabe, S., Okada, H., Hasegawa, S., Miyamoto, T. and Noda, T., (1996). 'Loss of cerebellar Purkinje cells in aged mice homozygous for a disrupted PrP gene'. *Nature*, 380 (6574):528-531.

Sakudo, A., Lee, D.C., Li, S., Nakamura, T., Matsumoto, Y., Saeki, K., Itohara, S., Ikuta, K. and Onodera, T., (2005). 'PrP cooperates with STI1 to regulate SOD activity in PrP-deficient neuronal cell line'. *Biochem Biophys Res Commun*, 328 (1):14-19.

Sales, N., Rodolfo, K., Hassig, R., Faucheux, B., Di Giamberardino, L. and Moya, K.L., (1998). 'Cellular prion protein localization in rodent and primate brain'. *Eur J Neurosci*, 10 (7):2464-2471.

Sauer, H., Wefer, K., Vetrugno, V., Pocchiari, M., Gissel, C., Sachinidis, A., Hescheler, J. and Wartenberg, M., (2003). 'Regulation of intrinsic prion protein by growth factors and TNF-alpha: the role of intracellular reactive oxygen species'. *Free Radic Biol Med*, 35 (6):586-594.

Sayre, L.M., Perry, G. and Smith, M.A., (1999). 'Redox metals and neurodegenerative disease'. *Curr Opin Chem Biol*, 3 (2):220-225.

Scaduto, R.C., Jr. and Grotyohann, L.W., (1999). 'Measurement of mitochondrial membrane potential using fluorescent rhodamine derivatives'. *Biophys J*, 76 (1 Pt 1):469-477.

Schneider, B., Mutel, V., Pietri, M., Ermonval, M., Mouillet-Richard, S. and Kellermann, O., (2003). 'NADPH oxidase and extracellular regulated kinases 1/2 are targets of prion protein signaling in neuronal and nonneuronal cells'. *Proc Natl Acad Sci U S A*, 100 (23):13326-13331.

Shields, S.B. and Franklin, S.J., (2007). 'Investigation of the affinity and selectivity of avian prion hexarepeat peptides for physiological divalent metal ions'. *J Inorg Biochem*.

Shmerling, D., Hegyi, I., Fischer, M., Blattler, T., Brandner, S., Gotz, J., Rulicke, T., Flechsig, E., Cozzio, A., von Mering, C., Hangartner, C., Aguzzi, A. and Weissmann, C., (1998). 'Expression of amino-terminally truncated PrP in the mouse leading to ataxia and specific cerebellar lesions'. *Cell*, 93 (2):203-214.

Simonian, N.A. and Coyle, J.T., (1996). 'Oxidative stress in neurodegenerative diseases'. *Annu Rev Pharmacol Toxicol*, 36:83-106.

Simonic, T., Duga, S., Strumbo, B., Asselta, R., Ceciliani, F. and Ronchi, S., (2000). 'cDNA cloning of turtle prion protein'. *FEBS Lett*, 469 (1):33-38.

Smaili, S.S., Hsu, Y.T., Carvalho, A.C., Rosenstock, T.R., Sharpe, J.C. and Youle, R.J., (2003). 'Mitochondria, calcium and pro-apoptotic proteins as mediators in cell death signaling'. *Braz J Med Biol Res*, 36 (2):183-190.

Smaili, S.S., Hsu, Y.T., Youle, R.J. and Russell, J.T., (2000). 'Mitochondria in Ca2+ signaling and apoptosis'. *J Bioenerg Biomembr*, 32 (1):35-46.

Sohn, I.P., Ahn, H.J., Park, D.W., Gye, M.C., Jo do, H., Kim, S.Y., Min, C.K. and Kwon, H.C., (2002). 'Amelioration of mitochondrial dysfunction and apoptosis of two-cell mouse embryos after freezing and thawing by the high frequency liquid nitrogen infusion'. *Mol Cells*, 13 (2):272-280.

Sparkes, R.S., Simon, M., Cohn, V.H., Fournier, R.E., Lem, J., Klisak, I., Heinzmann, C., Blatt, C., Lucero, M., Mohandas, T. and et al., (1986). 'Assignment of the human and mouse prion protein genes to homologous chromosomes'. *Proc Natl Acad Sci U S A*, 83 (19):7358-7362.

Spielhaupter, C. and Schatzl, H.M., (2001). 'PrPC directly interacts with proteins involved in signaling pathways'. *J Biol Chem*, 276 (48):44604-44612.

Stewart, R.S. and Harris, D.A., (2005). 'A transmembrane form of the prion protein is localized in the Golgi apparatus of neurons'. *J Biol Chem*, 280 (16):15855-15864.

Stuermer, C.A., Langhorst, M.F., Wiechers, M.F., Legler, D.F., Von Hanwehr, S.H., Guse, A.H. and Plattner, H., (2004). 'PrPc capping in T cells promotes its association with the lipid raft proteins reggie-1 and reggie-2 and leads to signal transduction'. *Faseb J*, 18 (14):1731-1733.

Taraboulos, A., Jendroska, K., Serban, D., Yang, S.L., DeArmond, S.J. and Prusiner, S.B., (1992). 'Regional mapping of prion proteins in brain'. *Proc Natl Acad Sci U S A*, 89 (16):7620-7624.

Thannickal, V.J. and Fanburg, B.L., (2000). 'Reactive oxygen species in cell signaling'. *Am J Physiol Lung Cell Mol Physiol*, 279 (6):L1005-1028.

Thellung, S., Villa, V., Corsaro, A., Pellistri, F., Venezia, V., Russo, C., Aceto, A., Robello, M. and Florio, T., (2007). 'ERK1/2 and p38 MAP kinases control prion protein fragment 90-231-induced astrocyte proliferation and microglia activation'. *Glia*, 55 (14):1469-1485.

Thompsett, A.R., Abdelraheim, S.R., Daniels, M. and Brown, D.R., (2005). 'High affinity binding between copper and full-length prion protein identified by two different techniques'. *J Biol Chem*, 280 (52):42750-42758.

Tobler, I., Gaus, S.E., Deboer, T., Achermann, P., Fischer, M., Rulicke, T., Moser, M., Oesch, B., McBride, P.A. and Manson, J.C., (1996). 'Altered circadian activity rhythms and sleep in mice devoid of prion protein'. *Nature*, 380 (6575):639-642.

Toni, M., Spisni, E., Griffoni, C., Santi, S., Riccio, M., Lenaz, P. and Tomasi, V., (2006). 'Cellular prion protein and caveolin-1 interaction in a neuronal cell line precedes fyn/erk 1/2 signal transduction'. *J Biomed Biotechnol*, 2006 (5):69469.

Vassallo, N., Herms, J., Behrens, C., Krebs, B., Saeki, K., Onodera, T., Windl, O. and Kretzschmar, H.A., (2005). 'Activation of phosphatidylinositol 3-kinase by cellular prion protein and its role in cell survival'. *Biochem Biophys Res Commun*, 332 (1):75-82.

Watt, N.T. and Hooper, N.M., (2005). 'Reactive oxygen species (ROS)-mediated beta-cleavage of the prion protein in the mechanism of the cellular response to oxidative stress'. *Biochem Soc Trans*, 33 (Pt 5):1123-1125.

Watt, N.T., Routledge, M.N., Wild, C.P. and Hooper, N.M., (2007). 'Cellular prion protein protects against reactive-oxygen-species-induced DNA damage'. *Free Radic Biol Med*, 43 (6):959-967.

Westaway, D., DeArmond, S.J., Cayetano-Canlas, J., Groth, D., Foster, D., Yang, S.L., Torchia, M., Carlson, G.A. and Prusiner, S.B., (1994). 'Degeneration of skeletal muscle, peripheral nerves, and the central nervous system in transgenic mice overexpressing wild-type prion proteins'. *Cell*, 76 (1):117-129.

White, A.R., Collins, S.J., Maher, F., Jobling, M.F., Stewart, L.R., Thyer, J.M., Beyreuther, K., Masters, C.L. and Cappai, R., (1999). 'Prion protein-deficient neurons reveal lower glutathione reductase activity and increased susceptibility to hydrogen peroxide toxicity'. *Am J Pathol*, 155 (5):1723-1730.

Whittington, M.A., Sidle, K.C., Gowland, I., Meads, J., Hill, A.F., Palmer, M.S., Jefferys, J.G. and Collinge, J., (1995). 'Rescue of neurophysiological phenotype seen in PrP null mice by transgene encoding human prion protein'. *Nat Genet*, 9 (2):197-201.

Wickner, R.B., (1994). '[URE3] as an altered URE2 protein: evidence for a prion analog in Saccharomyces cerevisiae'. *Science*, 264 (5158):566-569.

Wickner, R.B., (1997). 'A new prion controls fungal cell fusion incompatibility'. *Proc Natl Acad Sci U S A*, 94 (19):10012-10014.

Wong, B.S., Liu, T., Li, R., Pan, T., Petersen, R.B., Smith, M.A., Gambetti, P., Perry, G., Manson, J.C., Brown, D.R. and Sy, M.S., (2001). 'Increased levels of oxidative stress markers detected in the brains of mice devoid of prion protein'. *J Neurochem*, 76 (2):565-572.

Wopfner, F., Weidenhofer, G., Schneider, R., von Brunn, A., Gilch, S., Schwarz, T.F., Werner, T. and Schatzl, H.M., (1999). 'Analysis of 27 mammalian and 9 avian PrPs reveals high conservation of flexible regions of the prion protein'. *J Mol Biol*, 289 (5):1163-1178.

Zahn, R., Guntert, P., von Schroetter, C. and Wuthrich, K., (2003). 'NMR structure of a variant human prion protein with two disulfide bridges'. *J Mol Biol*, 326 (1):225-234.

Zahn, R., Liu, A., Luhrs, T., Riek, R., von Schroetter, C., Lopez Garcia, F., Billeter, M., Calzolai, L., Wider, G. and Wuthrich, K., (2000). 'NMR solution structure of the human prion protein'. *Proc Natl Acad Sci U S A*, 97 (1):145-150.

Zeng, F., Watt, N.T., Walmsley, A.R. and Hooper, N.M., (2003). 'Tethering the N-terminus of the prion protein compromises the cellular response to oxidative stress'. *J Neurochem*, 84 (3):480-490.

Zhang, Y., Poirier, G.G. and Burkle, A., (2002). 'In-situ analysis of cellular poly(ADP-ribose) production in scrapie-infected mouse neuroblastoma cells'. *Histochem J*, 34 (6-7):357-363.

7 CV

Muriel MALAISÉ
Kapperlersgutweg 2A
78462 KONSTANZ
GERMANY
Tel: +49 7531 365 346
+49 171 3464275
e-mail: muriel.malaise@uni-konstanz.de
Born: 2nd September 1977

Work experience:

2003- 2007: PhD student, University of Konstanz (Germany), group of Prof. Alexander BÜRKLE, supervisor: Prof. BÜRKLE; topic: Functional analysis of TM1 mutant of Prion protein *in vivo* and *in vitro*: 4 years.

2002-2003: IGBMC (Illkirch, France), group of Dr. WASYLYK Bohdan, supervisor: Dr. WASYLYK: Study of a novel post-translational modification (SUMOylation) of transcription factor Net: 12 month.

2001-2002: IGBMC (Illkirch, France), group of Prof. KEDINGER Claude, supervisor: Dr. BOEUF Hélène; topic: Study of cytokine LIF (Leukemia Inhibitory Factor) on mouse embryonic stem cells (ES): pluripotency, apoptosis and other endpoints: 9 month.

1996: Laboratoire de Pharmacologie et Physiopathologie Cellulaires URA - CNRS 600, Illkirch, France (training 3 weeks): Drug effects on pregnant rats.

Formation:

2006: Certificate for animal research from University of Konstanz (Germany).

2003: "Diplôme d'Etudes Approfondies" (DEA) of molecular cellular biology from Université Louis Pasteur (ULP) (Strasbourg, FRANCE).

2002: "Maîtrise de Biologie Cellulaire & Physiologique", ULP; courses: eucaryotic genomes: plasticity and modification (GEE), molecular pharmacology and pharmacometry (PMP), physiology and integrated biology (PBI).
Course of CEIPE: Legal aspects of the protection of Intellectual Property.

2001: "Maîtrise de Biochimie" (ULP), options: animal developmental biology (BDA), systems pharmacology (PHS), molecular phytopathology (PPM) and molecular virology (VIR).

1999: "Licence de Biochimie" (ULP.

1998: DEUG de BPC (biophysicochimie) (ULP).

1995: "Baccalauréat S option Mathématiques + épreuve biologie en anglais" (Strasbourg, France).

Conference presentations:

6 oral presentations, 5 of which were at international meetings (EU PRIONS Partners meeting 2004, 2005, DGPT 2005, Transregio SFB 2005).

4 posters at international meetings (PRION 2005, PRION 2006, ELSO 2002, Transregio SFB 2004).

Publications:

Malaisé M, Schätzl H, Bürkle A. "The octarepeat region of Prion protein, but not the TM1 domain, is important for the antioxidant effect of Prion protein.", **submitted**.

Kunzmann A, Liu D, Annett K, Malaisé M, Thaa B, Barnett Y., Bürkle A. "Flow-cytometric assessment of cellular poly(ADP-ribosyl)ation capacity in peripheral blood lymphocytes. ", Immun Ageing 2006 Jul 19;3:8.

Duval D, Malaisé M, Reinhardt B, Kedinger C, Boeuf H. "A p38 inhibitor allows to dissociate differentiation and apoptotic processes triggered upon LIF withdrawal in mouse embryonic stem cells.", Cell Death Differ. 2004 Mar;11(3):331-41.

8 Acknowledgements

I want to thank:

- Andreas, for his presence, support and patience also on difficult days;
- My parents, without whom nothing would be possible, for their love and support in all cases;

- Prof. Dr. Alexander BÜRKLE for the opportunity to do my PhD in his lab. He always encouraged me and I enjoyed our discussions. I also appreciated the freedom I had to pursue my line of work so independently;
- Prof. Dr. Markus GROETTRUP and Dr. Daniel LEGLER to initiate me and allow me to use their FACS and also their group for them welcome, help and kindness;
- Prof. Dr. Marcel LEIST for his valuable suggestions and assistance with doing a lab rotation with Lundbeck (Copenhagen, Denmark) in order to learn CGN preparation;
- And finally all my colleagues, the present and the former, for the atmosphere. I want to thank especially Veronica, Katharina for her technical supports, Claudia for her daily non scientist support and the "prion-Group": Jens, Nathalie and Tina for constructive discussions.

This work was supported by the Deutsche Forschungsgemeinschaft through the "TransRegio-SFB 11 Konstanz-Zürich, Structure and function of membrane proteins" (TP C10) as well as funding by the EU Commission through the FP6 Network of Excellence "NeuroPrion" / subproject PrioGen.

9 Manuscript submitted

Submitted to Free Radical Biology and Medicine

THE OCTAREPEAT REGION OF PRION PROTEIN, BUT NOT THE TM1 DOMAIN, IS IMPORTANT FOR THE ANTIOXIDANT EFFECT OF PRION PROTEIN

Muriel Malaisé[1], Hermann Schätzl[2], and Alexander Bürkle[1]

[1]Chair of Molecular Toxicology, Department of Biology, University of Konstanz, D-78457 Konstanz, Germany; [2]Institute of Virology, Prion Research Group, Technical University Munich, D-81675 Munich, Germany

Running head: Antioxidant effect of PrP

Address correspondence to: Prof Alexander Bürkle, Department of Biology, Box X911, University of Konstanz, 78457 Konstanz, Germany, FAX +49-7531 88 4033, E-mail: alexander.buerkle@uni-konstanz.de

Acknowledgements

We thank Prof. Dr. Marcus Groettrup and Dr. Daniel Legler (Chair of Immunology, Department of Biology, University of Konstanz, D-78457 Konstanz, Germany) for introducing us the method und using their FACS We gratefully acknowledge funding by the Deutsche Forschungsgemeinschaft through the "TransRegio-SFB 11 Konstanz-Zürich, Structure and function of membrane proteins" (TP C10) as well as funding by the EU Commission through the FP6 Network of Excellence "NeuroPrion" / subproject PrioGen.

ABSTRACT

The cellular prion protein (PrP^c) plays an essential role in the pathogenesis of several inherited and transmissible neurodegenerative diseases. Despite many studies, only putative functions for PrP^c immerged as binding and internalisation of metals (copper), superoxide dismutase-like activity, regulation of cellular antioxidant activities and signal transduction. The transmembrane (TM1) region of PrP^c (codons 110-135) is interesting because of its high conservation, its hydrophobic amino acids array and the neurotoxicity of peptides derived from this region. A set of deletion mutants centred on the codons 114-121 of PrP^c were constructed in order to elucidate the physiological role of the TM1 domain. Here our aim is to try to elucidate a possible role of PrP^c in antioxidative defence *in vitro*. For this purpose the impact of wt-PrP and Δ8TM1-PrP overexpression in N_2A mouse neuroblastoma cells on intracellular reactive oxygen species (ROS) level was checked. After oxidative stress the endogenous ROS production was lower in overexpressing wt-PrP or Δ8TM1-PrP cells. After a copper treatment wt-PrP or Δ8TM1-PrP overexpressing cells shown same increase of ROS level as in mock transfected cells whereas endogenous ROS level after oxidative stress in Δocta-PrP overexpressing cells is not sensitive to copper treatment. Moreover the mitochondrial membrane potential was lowered in all transfected cells. We conclude that the protective effect of PrP^c against oxidative stress implicated its octarepeat region but not its TM1 domain.

Keywords: antioxidant / prion protein / copper / signalling / ROS detection / mitochondrial membrane potential

INTRODUCTION

Transmissible Spongiform Encephalopathies (TSEs), also termed prion diseases, are neurodegenerative lethal diseases occurring in various mammalian species [1], [2]. TSEs are characterized by spongiform changes, neuronal death, astrogliosis and accumulation of a disease-associated, pathogenic isoform of prion protein (PrP), termed PrP^{Sc}, which arises from a normal, cellular isoform termed PrP^{c} in a posttranslational process involving refolding [2],[4, 5]. PrP^{c} is encoded by the *PRNP* gene on human chromosome 20 and mouse chromosome 2 [3], [4]. This gene is highly conserved during evolution [5], [6], [7]. The known PrP^{c} 3D structure differs from that proposed for PrP^{Sc}. PrP^{c} contains a long flexible amino terminal tail (amino acids [aa] 23-128) followed by three α-helices and 2 β-sheets [8]. PrP^{c} contains an octarepeat region (amino acids 51-91) and a highly hydrophobic region also called transmembrane domain (TM1) (aa 110-135). PrP^{c} can be glycosylated on Asn180 and Asn196 and comprises a disulfide bridge between Cys178 and Cys213. PrP^{c} is a glycosyl-phosphatidyl-inositol (GPI)-linked glycoprotein, which is enriched in detergent-resistant membranes. The very high degree of conservation of the TM1 region is indicative of an essential contribution to the physiological function of PrP^{c}. This region extends from aa 110 through 135 and comprises an array of hydrophobic amino acids. It is also a highly flexible and unstructured portion of PrP^{c} as shown by NMR analysis of recombinant PrP [8].

Previously we showed that expression of a deletion mutant of 8 aa in the TM1 domain (PrPΔ114-121) is sufficient to inhibit PrP^{Sc} accumulation in prion-infected neuroblastoma cells in a *trans*-dominant fashion [9]. Recently, we generated transgenic mice expressing the same deletion mutant [10]. These mice (termed $PrP_{\Delta pHC}$ in ref. 12) do not show any obvious phenotype. However, crossing $PrP_{\Delta pHC}$ mice on a $Prnp^{-/-}$ background with transgenic mice carrying pathogenic PrPΔ94-134 or PrPΔ32-134 transgenes ("Shmerling mice") led to enhanced toxicity of PrP Δ94-134 transgene whereas it diminished toxicity of the PrP Δ32-134 [10].

A variety of putative functions have been proposed for PrP^c, such as immunoregulation [11], [12], signal transduction [11], [13], [14], [17], binding of copper and other metals and their sequestration [15], [16], [17], [18], synaptic transmission [19], either induction of or protection against apoptosis [20], [21], [22], superoxide dismutase (SOD)-like activity [23], [24], [25], or regulation of cellular antioxidant activities [29], [30], [26], [27]. The ability of PrP^c to bind copper via its octarepeat region and via two independent histidine residues (His99 and His111) [28], [29] might play an important role in its function(s). PrP^c could act as a sensor for oxidative stress [35], [36], [30], [30] and trigger intracellular anti-stress signaling events. A function of PrP^c as an SOD-like activity has been proposed [26, 27, 29] but other groups either have been unable to confirm this [25] or have proposed some indirect mechanism [31].

Intriguingly there is a clear link between transition-metal binding and neurodegenerative diseases, including prion diseases [32]. In some cases this metal binding seems either to protect against oxidation or enhance it by disturbing free radical homeostasis [33], [34]. The principal ROS are the superoxide anion (O_2^-•), hydrogen peroxide (H_2O_2) and the hydroxyl radical (OH•). Ionizing radiation or some chemicals are potent inducers of ROS but ROS are also continually produced from endogenous sources in the cell. Two major mechanisms of ROS production are (i) the incomplete reduction of O_2 in the respiratory chain at the mitochondria (complexes I and III), and (ii) the "oxidative burst" mediated by NADPH oxidases. ROS have both physiological and pathological functions. They play an essential role in intracellular signaling [35], but excessive ROS levels leads to oxidative stress and ultimately to cell death. For example H_2O_2 acts as a second messenger for cell signaling and can activate components of signaling cascades that are involved in cell survival, proliferation, differentiation and also cell death [36], [37]. On the other hand, H_2O_2 is recognized as an important mediator of oxidative stress in neurons [30]. There is also ample evidence in support of oxidative stress being a driving force of the aging process, as was predicted by the 'free-radical theory of aging' first proposed half a century ago by Denham Harman [38], [39], [40] and [41].

The mitochondrial membrane potential ($\Delta\Psi$) arises from proton translocation from the mitochondrial matrix to the mitochondrial intermembrane space through the electron transport chain. $\Delta\Psi$ reflects the mitochondrial activity of the cell. Mitochondrial activity can generate ROS by occasional escapes of electrons from the respiratory chain. Hyperpolarisation of the inner mitochondrial membrane (*i.e.*, increased $\Delta\Psi$) facilitates ROS production, which in turn induces a decrease of $\Delta\Psi$ by the induction of uncoupling protein 2 (UCP2) and so the equilibrium is maintained. Persistent overproduction of ROS will lead to calcium influx and cytochrome c release into the cytoplasm, thus triggering apoptosis [45].

The aim of the present study was to investigate a possible role of the highly conserved TM1 domain of PrP^c (i) on the cellular response to exogenous oxidative stress, (ii) on endogenous ROS levels and (iii) on mitochondrial membrane potential ($\Delta\Psi$). We chose N_2A mouse neuroblastoma cells as an experimental system, as these cells have extensively been used in research on PrP^c and on prions. N_2A cells were transfected with expression constructs either encoding wild-type (wt) mouse PrP^c or with the deletion mutant PrPΔ114-121, carrying an 8-aa deletion in the TM1 region of PrP [9]. In order to assess cellular ROS levels we used 2',7'-dichlorohydrofluorescein diacetate (H_2DCFDA) as a probe suitable for quantitative analysis by flow cytometry (FACS), and tetramethylrhodamine ethyl ester perchlorate (TMRE) in order to monitor changes in $\Delta\Psi$.

EXPERIMENTAL PROCEDURES

cDNA Constructs

The expression plasmid pL15TK [42] (empty vector, used for mock transfections) was the basis for creating pCMV-wtPrP [9] (henceforth termed wt-PrP), pCMV-Δ114-121PrP [9] (henceforth termed

Δ8TM1-PrP). Plasmid pcDNA3.1Δ43-91 (henceforth termed Δocta-PrP) was described before [43]. Plasmids pCR3-Thy1and pEGFP were used as controls.

Cell culture

The murine neuroblastoma cell line N_2A and its subclones (H6, H12, D11, G9 and F1) were cultured as described [44]. The human cervical carcinoma cell line HeLa was cultured in DMEM, 10% FCS, 1% L-Glutamine, 1% Penicillin/Streptomycin.

Transfection

N_2A cells were transiently transfected using JetPEI reagent (Qbiogene) according to the manufacturer's instructions. Briefly N_2A were seeded in 24-well plates. The next day, transfections were performed. 1µg DNA dissolved in 50µl of 150mM NaCl was combined with 2µl JetPEI reagent pre-diluted in 50µl of 150mM NaCl. The whole mix was incubated 30min at RT and then added onto cells drop-wise.

Endogenous ROS and reaction to oxidative stress monitoring by FACS analysis

The use of H_2DCFDA as ROS staining and modified staining methods have been described by Sohn et al. [45] and Sauer et al. [46]. Briefly, one day post-transfection, medium was exchanged and cells were exposed or not to 100µM copper chloride hydrate ($CuCl_2$, Sigma) for 1 day. Then cells were washed with PBS 1x and fresh medium was added. Cells were then treated with 15µM 2', 7'dichloro-hydrofluorescein diacetate (H_2DCFDA, Molecular Probe) in the presence or in absence of 3mM hydrogen peroxide (H_2O_2, Merck) for 30min. The cells were washed with PBS and trypsinized. Then 100µl FACS buffer was added and FACScan analysis was performed using a

FACScan flow (Beckton Dickson Biosciences, Mountain view, CA) equipped with Cell Quest version 3.3 software. Data analysis was performed using FlowJo 6.0 program (TreeStar).

Mitochondrial membrane potential monitoring by FACS analysis

The use of tetramethylrhodamine ethyl ester perchlorate (TMRE) as a probe for mitochondrial membrane potential has been described by Nicholls et al. [47] and Scaduto et al.[48]. Briefly, one day post-transfection, medium was exchanged and cells were exposed or not to 100µM copper chloride hydrate ($CuCl_2$, Sigma) for 1 day. Then cells were washed with PBS 1x and fresh medium was added. Cells were treated with 4µM tetramethylrhodamine ethyl ester perchlorate (TMRE) for 15min. Cells were washed with PBS, trypsinized and resuspended in 100µl FACS buffer. Then a FACScan analysis was performed.

Statistics and normalization

Each individual experiment was done at least in duplicates and the average of those points yielded the respective experimental data point of the day, to be used for further statistical analysis of the experiments performed independently on different days.

Crude data of transfected N_2A were normalized as follows: The mean values from all untreated mock samples was set as100%. All other data were expressed as % compared to the mock value of the same day. A t-test was performed on FACS results. $p<0.05$ was considered significant. Analyse-it software was used (Analyse-it Software Ltd.).

RESULTS

In order to investigate the contribution of the TM1 domain of PrP^c to the physiological role(s) of this protein, N_2A cells were transfected with expression constructs for wt-PrP or Δ8TM1-PrP. The empty vector plasmid served as a control. In the transfected cultures, intracellular ROS levels in response to oxidative stress response, endogenous ROS levels and the mitochondrial membrane potential (ΔΨ) were assessed.

Endogenous ROS level after oxidant treatment of N_2A, N_2A subclones and HeLa cells

H_2DCFDA, which permits to monitor ROS level, was used as a probe, and its fluorescent intensity was measured by FACS. In order to set up the system, ROS levels were measured with or without prior addition of either H_2O_2, *tert*-butylhydroxid peroxide (tBOOH), or the GSH-depleting compound buthionine sulfoximine (BSO). In all three cases (Fig. 1B) a similar shift to the right (*i.e.*, increase of ROS) is observable, thus validating our readout system. All subsequent experiments were done with H_2O_2.

Further analyses on randomly picked subclones of N_2A [44] as well as on HeLa cells (human cervical carcinoma) revealed that the double peak observed Fig. 1B in the presence of H_2DCFDA and oxidants is due to some heterogeneity in the cell population. While HeLa cells showed a single peak (Fig. 2A), N_2A subclones (Fig. 2 B-F) showed varying patterns. For the subsequent experiments N_2A mass cultures were used.

Impact of overexpression of wt-PrP or Δ8TM1-PrP on ROS levels in N_2A cells exposed to exogenous hydrogen peroxide

As we performed transient transfections assays only, a GFP construct was used to assess transfection efficiency. Routinely, about 60% of cells were GFP-positive (data not show). Cells were transfected with the various PrP constructs and analyzed for ROS levels 24 h later. ROS levels were measured after exposure of the cells to H_2O_2 added directly to the medium in the presence of H_2DCFDA. In response to oxidative stress significantly lower ROS levels are present both in wt-PrP and in Δ8TM1-PrP overexpressing cells (Fig. 3A and B), indicative of an antioxidant effect of the two PrP versions.

One possible explanation for this effect could be a SOD-like activity of PrP, or else some change in upstream events controlling ROS levels. We therefore used a colorimetric test based on competition and xanthine/xanthine oxidase in N_2A cells overexpressing wt-PrP or Δ8TM1-PrP. No difference, however, between mock, wt-PrP and Δ8TM1-PrP transfected cells was observable in this system (data not shown), thus pointing to the relevance of (an)other mechanism(s).

Effect of copper on mock, wt-PrP, Δ8TM1-PrP and Δocta-PrP transfected N_2A after oxidative stress

Because PrP can bind copper it was interesting to investigate the possible influence of copper on the oxidative stress response in PrP^c-overexpressing N_2A cells. N_2A were seeded in 24 wells plates on day zero. On day 1 cells were transfected with empty vector, wt-PrP, Δ8TM1-PrP or Δocta-PrP, respectively. Medium was changed on day 2 and copper was added in fresh medium (100μM $CuCl_2$) to one of the parallel cultures. On day 3 cells were washed with PBS, fresh medium was added and fluorescent staining and FACS analyses were performed as described above. The

experiments were repeated independently and the results are expressed in percentage of DCF intensity for mock-transfected cells in the absence of copper treatment (Fig. 3C). Once again, after oxidative stress induced by H_2O_2 treatment the ROS level present in wt-PrP and Δ8TM1-PrP overexpressing cells is significantly reduced compared to mock transfected cells (p=0.003 and p=0.04, respectively), as shown above in Fig. 3A and B. By contrast, cells overexpressing Δocta-PrP did not show any change in ROS levels.

After copper treatment the ROS level in mock transfected cells showed a tendency to increase (p=0.058). Copper treatment induced a significant increase of ROS in wt-PrP and Δ8TM1-PrP overexpressing cells (p=0.046 for wt-PrP compared to mock; p=0.012 for the comparison between wt-PrP with and without copper treatment; p=0.021 for the comparison between Δ8TM1-PrP with and without copper treatment). Copper treatment had no effect on Δocta-PrP-overexpressing cells.

Effect of copper on mock, wt-PrP, Δ8TM1-PrP and transfected N_2A on endogenous ROS

In order to investigate the possible influence of copper on endogenous ROS in N_2A cells overexpressing the above PrP versions, the same experiments were repeated in the absence of an ROS inducer.

Here, no statistically significant differences could be observed (Fig. 4B), but nevertheless Δocta-PrP overexpressing cells displayed a tendency towards a different phenotype after copper treatment.

Effect of copper on mock, wt-PrP, Δ8TM1-PrP and Δocta-PrP transfected N_2A on mitochondrial membrane potential (ΔΨ)

We were also interested in investigating the influence of copper on ΔΨ in PrP overexpressing N_2A cells. N_2A were seeded in 24-wells plates on day zero. On day 1 cells were transfected with

empty vector, wt-PrP, Δ8TM1-PrP or Δocta-PrP, respectively. Medium was changed on day 2, and copper was added in fresh medium (100μM $CuCl_2$) to one of the parallel cultures. On day 3, cells were washed with PBS, fresh medium was added and fluorescent staining and FACS analysis were performed as described above.

Our data revealed that copper treatment induced a significant decrease of ΔΨ in the case of mock, wt-PrP, Δ8TM1-PrP and Δocta-PrP transfected cells (p=0.028 for mock, p= 0.041 for wt-PrP, p= 0.036 for Δ8TM1-PrP and p= 0.027 for Δocta-PrP compared to mock without copper treatment; Fig. 5B).

An explanation for this reduction of ΔΨ could be copper toxicity. However, microscopic inspection and viability tests did not reveal any difference between any of the transfected cultures in the presence or absence of copper (Fig.6).

Interestingly Δocta-PrP overexpressing cells showed a ΔΨ pattern different from that of mock transfected cells: Δocta-PrP overexpression without copper treatment significantly decreased ΔΨ compared to mock transfected cells (p = 0.029).

In order to exclude any non-specific effects due to overexpression of proteins that are GPI-anchored, N_2A cells were transfected with a Thy-1 expression construct. Thy-1 is a GPI-anchored protein commonly used as a control for GPI-anchorage effects. Experiments to assess ΔΨ, endogenous ROS and the reaction to oxidative stress experiments did not show any difference between mock and Thy-1-transfected cells (data not shown). Therefore the effects observed with wt-PrP, Δ8TM1-PrP and Δocta-PrP are apparently not the nonspecific consequence of overexpressing GPI-anchored proteins.

DISCUSSION

In the present work, we observed a significant decrease of ROS after oxidative stress in cells overexpressing either wt-PrP or Δ8TM1-PrP in N_2A mouse neuroblastoma cells (Fig. 3A and 3B). While an antioxidant role of wt-PrP^c has already been described, our results provide new information for the deletion mutant Δ8TM1-PrP, for which have already reported several biological phenotypes [11, 12].

A possible explanation for this protection against oxidative stress could be some SOD-like activity, as previously suggested by Brown et al ([23], [24], [29]). In our system, however, no enhanced SOD activity was detected in wt-PrP or Δ8TM1-PrP transfected N_2a (data not shown), in agreement with published data [25].

As the PrP^c molecule can bind several copper ions, the next question was if this copper binding was related with the protective effect of overexpressed PrP. After combined exposure to copper treatment and H_2O_2, ROS levels increased in mock, wt-PrP or Δ8TM1-PrP overexpressing cells (Fig. 3C). In the case of Δocta-PrP overexpressing cells no protective effect was observed, and addition of copper treatment had no significant impact either. Therefore the pathway involved in the protective effect of PrP involves the octarepeat region and not the TM1 region of PrP. This pathway is also sensitive to copper. Apparently aa His 99 and His 111 (representing an independent copper binding site outside the octarepeat region [28], [29]) are not implicated in the protective effect of PrP^c whereas the octarepeat region does play an important role.

Another explanation for the mitigated increase of ROS after oxidative stress in cells overexpressing PrP^c could simply be a low basal endogenous ROS level. As shown Fig. 4B this hypothesis can be dismissed because no difference between mock and all three PrP transfected cells are observable. Furthermore copper treatment had no impact on the basal endogenous ROS level in cultures expressing any of the three PrP versions.

Because of the close relationship between ROS formation and the mitochondrial respiratory chain [49], ΔΨ of mock and PrP-wt, Δ8TM1 and Δocta transfected was monitored (Fig. 5B). Neither wt-PrP nor Δ8TM1-PrP-overexpressing cells showed any alteration in ΔΨ compared to mock-transfected cells. Interestingly, though, Δocta-PrP transfected cells showed a statistically significant decrease of ΔΨ. In all cases, ΔΨ decreased after copper treatment.

Copper treatment coupled with oxidative stress led to an increase of ROS level in mock, wt-PrP or Δ8TM1-transfected N_2A cells but not in Δocta-PrP transfected N_2A cells. The Δocta-PrP protein can still bind copper on His99/His111 with high affinity. On the one hand this copper treatment has no impact on basal endogenous ROS but on the other hand the same copper treatment leads to a decrease of ΔΨ in mock, wt-PrP, Δ8TM1-PrP and Δocta-PrP overexpressing N_2A.

In summary, the protective effect of PrP^c against oxidative stress involves the octarepeat region but not the highly conserved TM1 domain, nor the high-affinity copper binding site at His99/His111. While it is attractive to hypothesize that the primordial physiological function of PrP^c is in antioxidant defense, this appears incompatible with our present data showing that the most highly conserved region of PrP^c is apparently not involved in this function. Therefore other known or suspected functions of PrP^c deserve increased scrutiny.

LIST OF ABBREVIATIONS

ΔΨ: mitochondrial membrane potential

BSO: buthionine sulfoximine

DMEM: Dulbecco's Modified Eagle's Medium

DNA: deoxyribonucleic acid

FACS: fluorescent activated cell sorting

FCS: Fetal calf serum

GPI: glycosyl-phosphatidyl-inositol

H_2DCFDA: 2', 7'dichloro-hydrofluorescein diacetate

H_2O_2: hydrogen peroxide

N_2A: mouse neuroblastoma cells

NaCl: Sodium chloride

PBS: phosphate buffered saline

PrP: Prion protein

ROS: reactive oxygen species

RT: room temperature

SOD: superoxide dismutase

tBOOH: *tert*-butylhydroxid peroxide

TM: transmembrane

TMRE: Tetramethylrhodamine ethyl ester perchlorate

TSE: Transmissible Spongiform Encephalopathies

REFERENCES

[1] Silveira, J. R.; Caughey, B.; Baron, G. S. Prion protein and the molecular features of transmissible spongiform encephalopathy agents. *Curr Top Microbiol Immunol* **284:**1-50; 2004.
[2] Budka, H. Neuropathology of prion diseases. *Br Med Bull* **66:**121-130; 2003.
[3] Basler, K.; Oesch, B.; Scott, M.; Westaway, D.; Walchli, M.; Groth, D. F.; McKinley, M. P.; Prusiner, S. B.; Weissmann, C. Scrapie and cellular PrP isoforms are encoded by the same chromosomal gene. *Cell* **46:**417-428.; 1986.
[4] Sparkes, R. S.; Simon, M.; Cohn, V. H.; Fournier, R. E.; Lem, J.; Klisak, I.; Heinzmann, C.; Blatt, C.; Lucero, M.; Mohandas, T.; et al. Assignment of the human and mouse prion protein genes to homologous chromosomes. *Proc Natl Acad Sci U S A* **83:**7358-7362; 1986.
[5] Simonic, T.; Duga, S.; Strumbo, B.; Asselta, R.; Ceciliani, F.; Ronchi, S. cDNA cloning of turtle prion protein. *FEBS Lett* **469:**33-38.; 2000.
[6] Wopfner, F.; Weidenhofer, G.; Schneider, R.; von Brunn, A.; Gilch, S.; Schwarz, T. F.; Werner, T.; Schatzl, H. M. Analysis of 27 mammalian and 9 avian PrPs reveals high conservation of flexible regions of the prion protein. *J Mol Biol* **289:**1163-1178.; 1999.
[7] Rivera-Milla, E.; Oidtmann, B.; Panagiotidis, C. H.; Baier, M.; Sklaviadis, T.; Hoffmann, R.; Zhou, Y.; Solis, G. P.; Stuermer, C. A.; Malaga-Trillo, E. Disparate evolution of prion protein domains and the distinct origin of Doppel- and prion-related loci revealed by fish-to-mammal comparisons. *Faseb J* **20:**317-319; 2006.
[8] Zahn, R.; Liu, A.; Luhrs, T.; Riek, R.; von Schroetter, C.; Lopez Garcia, F.; Billeter, M.; Calzolai, L.; Wider, G.; Wuthrich, K. NMR solution structure of the human prion protein. *Proc Natl Acad Sci U S A* **97:**145-150; 2000.
[9] Holscher, C.; Delius, H.; Burkle, A. Overexpression of nonconvertible PrPc delta114-121 in scrapie-infected mouse neuroblastoma cells leads to trans-dominant inhibition of wild-type PrP(Sc) accumulation. *J Virol* **72:**1153-1159; 1998.
[10] Baumann, F.; Tolnay, M.; Brabeck, C.; Pahnke, J.; Kloz, U.; Niemann, H. H.; Heikenwalder, M.; Rulicke, T.; Burkle, A.; Aguzzi, A. Lethal recessive myelin toxicity of prion protein lacking its central domain. *Embo J* **26:**538-547; 2007.
[11] Krebs, B.; Dorner-Ciossek, C.; Schmalzbauer, R.; Vassallo, N.; Herms, J.; Kretzschmar, H. A. Prion protein induced signaling cascades in monocytes. *Biochem Biophys Res Commun* **340:**13-22; 2006.
[12] de Almeida, C. J.; Chiarini, L. B.; da Silva, J. P.; PM, E. S.; Martins, M. A.; Linden, R. The cellular prion protein modulates phagocytosis and inflammatory response. *J Leukoc Biol* **77:**238-246; 2005.
[13] Mouillet-Richard, S.; Ermonval, M.; Chebassier, C.; Laplanche, J. L.; Lehmann, S.; Launay, J. M.; Kellermann, O. Signal transduction through prion protein. *Science* **289:**1925-1928.; 2000.
[14] Schneider, B.; Mutel, V.; Pietri, M.; Ermonval, M.; Mouillet-Richard, S.; Kellermann, O. NADPH oxidase and extracellular regulated kinases 1/2 are targets of prion protein signaling in neuronal and nonneuronal cells. *Proc Natl Acad Sci U S A* **100:**13326-13331; 2003.
[15] Brown, D. R.; Qin, K.; Herms, J. W.; Madlung, A.; Manson, J.; Strome, R.; Fraser, P. E.; Kruck, T.; von Bohlen, A.; Schulz-Schaeffer, W.; Giese, A.; Westaway, D.; Kretzschmar, H. The cellular prion protein binds copper in vivo. *Nature* **390:**684-687.; 1997.
[16] Burns, C. S.; Aronoff-Spencer, E.; Legname, G.; Prusiner, S. B.; Antholine, W. E.; Gerfen, G. J.; Peisach, J.; Millhauser, G. L. Copper coordination in the full-length, recombinant prion protein. *Biochemistry* **42:**6794-6803; 2003.
[17] Chattopadhyay, M.; Walter, E. D.; Newell, D. J.; Jackson, P. J.; Aronoff-Spencer, E.; Peisach, J.; Gerfen, G. J.; Bennett, B.; Antholine, W. E.; Millhauser, G. L. The Octarepeat Domain

of the Prion Protein Binds Cu(II) with Three Distinct Coordination Modes at pH 7.4. *J Am Chem Soc* **127:**12647-12656; 2005.
[18] Millhauser, G. L. Copper binding in the prion protein. *Acc Chem Res* **37:**79-85; 2004.
[19] Collinge, J.; Whittington, M. A.; Sidle, K. C.; Smith, C. J.; Palmer, M. S.; Clarke, A. R.; Jefferys, J. G. Prion protein is necessary for normal synaptic function. *Nature* **370:**295-297.; 1994.
[20] Gains, M. J.; Roth, K. A.; LeBlanc, A. C. Prion protein protects against ethanol-induced Bax-mediated cell death in vivo. *Neuroreport* **17:**903-906; 2006.
[21] Kristiansen, M.; Messenger, M. J.; Klohn, P. C.; Brandner, S.; Wadsworth, J. D.; Collinge, J.; Tabrizi, S. J. Disease-related prion protein forms aggresomes in neuronal cells leading to caspase activation and apoptosis. *J Biol Chem* **280:**38851-38861; 2005.
[22] Roucou, X.; Giannopoulos, P. N.; Zhang, Y.; Jodoin, J.; Goodyer, C. G.; LeBlanc, A. Cellular prion protein inhibits proapoptotic Bax conformational change in human neurons and in breast carcinoma MCF-7 cells. *Cell Death Differ* **12:**783-795; 2005.
[23] Brown, D. R.; Besinger, A. Prion protein expression and superoxide dismutase activity. *Biochem J* **334 (Pt 2):**423-429; 1998.
[24] Brown, D. R.; Wong, B. S.; Hafiz, F.; Clive, C.; Haswell, S. J.; Jones, I. M. Normal prion protein has an activity like that of superoxide dismutase. *Biochem J* **344 Pt 1:**1-5; 1999.
[25] Hutter, G.; Heppner, F. L.; Aguzzi, A. No superoxide dismutase activity of cellular prion protein in vivo. *Biol Chem* **384:**1279-1285; 2003.
[26] Guentchev, M.; Siedlak, S. L.; Jarius, C.; Tagliavini, F.; Castellani, R. J.; Perry, G.; Smith, M. A.; Budka, H. Oxidative damage to nucleic acids in human prion disease. *Neurobiol Dis* **9:**275-281; 2002.
[27] Petersen, R. B.; Siedlak, S. L.; Lee, H. G.; Kim, Y. S.; Nunomura, A.; Tagliavini, F.; Ghetti, B.; Cras, P.; Moreira, P. I.; Castellani, R. J.; Guentchev, M.; Budka, H.; Ironside, J. W.; Gambetti, P.; Smith, M. A.; Perry, G. Redox metals and oxidative abnormalities in human prion diseases. *Acta Neuropathol (Berl)* **110:**232-238; 2005.
[28] Jones, C. E.; Abdelraheim, S. R.; Brown, D. R.; Viles, J. H. Preferential Cu2+ coordination by His96 and His111 induces beta-sheet formation in the unstructured amyloidogenic region of the prion protein. *J Biol Chem* **279:**32018-32027; 2004.
[29] Thompsett, A. R.; Abdelraheim, S. R.; Daniels, M.; Brown, D. R. High affinity binding between copper and full-length prion protein identified by two different techniques. *J Biol Chem* **280:**42750-42758; 2005.
[30] White, A. R.; Collins, S. J.; Maher, F.; Jobling, M. F.; Stewart, L. R.; Thyer, J. M.; Beyreuther, K.; Masters, C. L.; Cappai, R. Prion protein-deficient neurons reveal lower glutathione reductase activity and increased susceptibility to hydrogen peroxide toxicity. *Am J Pathol* **155:**1723-1730; 1999.
[31] Sakudo, A.; Lee, D. C.; Li, S.; Nakamura, T.; Matsumoto, Y.; Saeki, K.; Itohara, S.; Ikuta, K.; Onodera, T. PrP cooperates with STI1 to regulate SOD activity in PrP-deficient neuronal cell line. *Biochem Biophys Res Commun* **328:**14-19; 2005.
[32] Milhavet, O.; Lehmann, S. Oxidative stress and the prion protein in transmissible spongiform encephalopathies. *Brain Res Brain Res Rev* **38:**328-339; 2002.
[33] Simonian, N. A.; Coyle, J. T. Oxidative stress in neurodegenerative diseases. *Annu Rev Pharmacol Toxicol* **36:**83-106; 1996.
[34] Sayre, L. M.; Perry, G.; Smith, M. A. Redox metals and neurodegenerative disease. *Curr Opin Chem Biol* **3:**220-225; 1999.
[35] Droge, W. Free radicals in the physiological control of cell function. *Physiol Rev* **82:**47-95; 2002.
[36] Boyd, C. S.; Cadenas, E. Nitric oxide and cell signaling pathways in mitochondrial-dependent apoptosis. *Biol Chem* **383:**411-423; 2002.
[37] Thannickal, V. J.; Fanburg, B. L. Reactive oxygen species in cell signaling. *Am J Physiol Lung Cell Mol Physiol* **279:**L1005-1028; 2000.

[38] Harman, D. Free radical theory of aging: an update: increasing the functional life span. *Ann N Y Acad Sci* **1067:**10-21; 2006.
[39] Widmer, R.; Ziaja, I.; Grune, T. Protein oxidation and degradation during aging: role in skin aging and neurodegeneration. *Free Radic Res* **40:**1259-1268; 2006.
[40] Peng, J.; Peng, L.; Stevenson, F. F.; Doctrow, S. R.; Andersen, J. K. Iron and paraquat as synergistic environmental risk factors in sporadic Parkinson's disease accelerate age-related neurodegeneration. *J Neurosci* **27:**6914-6922; 2007.
[41] Grune, T.; Merker, K.; Jung, T.; Sitte, N.; Davies, K. J. Protein oxidation and degradation during postmitotic senescence. *Free Radic Biol Med* **39:**1208-1215; 2005.
[42] Kupper, J. H.; de Murcia, G.; Burkle, A. Inhibition of poly(ADP-ribosyl)ation by overexpressing the poly(ADP-ribose) polymerase DNA-binding domain in mammalian cells. *J Biol Chem* **265:**18721-18724; 1990.
[43] Gilch, S.; Nunziante, M.; Ertmer, A.; Wopfner, F.; Laszlo, L.; Schatzl, H. M. Recognition of lumenal prion protein aggregates by post-ER quality control mechanisms is mediated by the preoctarepeat region of PrP. *Traffic* **5:**300-313; 2004.
[44] Zhang, Y.; Poirier, G. G.; Burkle, A. In-situ analysis of cellular poly(ADP-ribose) production in scrapie-infected mouse neuroblastoma cells. *Histochem J* **34:**357-363; 2002.
[45] Sohn, I. P.; Ahn, H. J.; Park, D. W.; Gye, M. C.; Jo do, H.; Kim, S. Y.; Min, C. K.; Kwon, H. C. Amelioration of mitochondrial dysfunction and apoptosis of two-cell mouse embryos after freezing and thawing by the high frequency liquid nitrogen infusion. *Mol Cells* **13:**272-280; 2002.
[46] Sauer, H.; Wefer, K.; Vetrugno, V.; Pocchiari, M.; Gissel, C.; Sachinidis, A.; Hescheler, J.; Wartenberg, M. Regulation of intrinsic prion protein by growth factors and TNF-alpha: the role of intracellular reactive oxygen species. *Free Radic Biol Med* **35:**586-594; 2003.
[47] Nicholls, D. G.; Ward, M. W. Mitochondrial membrane potential and neuronal glutamate excitotoxicity: mortality and millivolts. *Trends Neurosci* **23:**166-174; 2000.
[48] Scaduto, R. C., Jr.; Grotyohann, L. W. Measurement of mitochondrial membrane potential using fluorescent rhodamine derivatives. *Biophys J* **76:**469-477; 1999.
[49] Kowaltowski, A. J.; Vercesi, A. E. Mitochondrial damage induced by conditions of oxidative stress. *Free Radic Biol Med* **26:**463-471; 1999.

FIGURE LEGENDS

Figure 1A. **FACS Setting in order to measure ROS level in N_2a in response to oxidative stress.** In order to check endogenous reactive oxygen species H_2DCFDA was used (15µM 30min) and resulting fluorescent intensity were measured by FACS. **a)** Living cells gating; **b)** Cells none stained which determined the background; **c)** Cells stained with H_2DCFDA (FL-1) in presence of H_2O_2; **d)** Overlay b/ and c/.

Figure 1B. **Endogenous ROS and oxidative stress response due to different drugs in N_2a.** ROS levels were measured in presence of H_2O_2 (3mM 30min), tBOOH (tert buthylhydroxid peroxide, another ROS) and BSO (Buthionine sulfoximin, which is a GSH inhibitor) added directly in the medium in presence of H_2DCFDA (15µM 30min). Cells were seeded and stained a day after. All experiments were done in duplicate. In each case a representative FACS data is shown. **a)** in presence of H_2O_2; **b)** in presence of tBOOH; **c/** in presence of BSO. Note that the double peak is present in all cases.

Figure 2. **Background of cells and oxidative stress response to H_2O_2 in different cell types.** For each cells type a representative FACS data is shown. A) in HeLa; B) in N_2a subclone H12; C) in N_2a subclone D11; D) in N_2a subclone H6; E) in N_2a subclone F1; F) in N_2a subclone G9. Note that the different pattern in all cases: HeLa cells show one peak (Fig.2A) and the different subclones (Fig.2 B-F) show different pattern: normal peak (Fig.2 B and F), double peak (Fig.2 E) or large peak (Fig 2 C and D)

Figure 3. **Oxidative stress response of overexpressing N_2A.** ROS levels were also measured in presence of H_2O_2 (3mM 30min) added directly in the medium in presence of H_2DCFDA (15µM 30min). Cells were transfected and stained a day after.

Figure 3A **A representative FACS data** for mock, wt-PrP and Δ8TM1-PrP overexpressing cell.

Figure 3B **Analysis of 6 independent experiments of oxidative stress response in transfected N_2A**. All experiments were done in duplicate and the average of the two means values was given as a data point. 6 independent experiments were done. T-test were performed, ☆ $p<0.05$.

Figure 3C. **Effect of copper treatment on cellular ROS after oxidative stress in transfected N_2A.** Because PrP can bind copper which influence has copper on oxidative stress response in PrP overexpressing N_2A. N_2A were seeded in two 24 wells plates on day one. A day after (day two) cells were transfected with mock, wt-PrP, Δ8TM1-PrP or Δocta-PrP. Medium was changed on day three and copper was added in fresh medium (100µM $CuCl_2$) into one of the two plates. On day four cells were washed with PBS, fresh medium was added and cells were stained with H_2DCFDA As previously wt-PrP and Δ8TM1-PrP overexpressing cells show a significant decrease of ROS after H_2O_2 treatment whereas Δocta-PrP overexpressing cells show no difference compare to mock transfected cells. Copper treatment induces a significant increase of the ROS level in wt-PrP and Δ8TM1-PrP overexpressing cells whereas in Δocta-PrP overexpressing cells not. T-test were performed * comparison with mock, # comparison in absence or in presence of copper treatment in wt-PrP transfected cells, § comparison in absence or in presence of copper treatment in Δ8TM1-PrP transfected cells $p<0.05$. Results are expressed in percentage of DCF intensity for mock transfected cells in absence of copper treatment. The number of independent experiments is noted in bracket.

Figure 4A. **FACS Setting in order to measure endogenous ROS level in N_2a. a/** Living cells gating; **b/** Cells none stained which determined the background; **c/** Cells stained with H_2DCFDA (FL-1); **d/** Overlay b/ and c/.

Figure 4B. **Effect of copper treatment on cellular ROS in transfected N_2A.** N_2A were seeded in two 24 wells plates on day one. A day after (day two) cells were transfected with mock, wt-PrP, Δ8TM1-PrP or Δocta-PrP. Medium was changed on day three and copper was added in fresh medium (100µM $CuCl_2$) into one of the two plates. On day four cells were washed with PBS, fresh medium was added and

cells were stained with H_2DCFDA in absence of ROS enhancer No significant difference is observable. T-tests were performed. The number of experiments is noted in bracket.

Figure 5A. **FACS Setting in order to measure ΔΨ in N_2a. a)** Living cells gating; **b)** Cells none stained which determined the background; **c)** Cells stained with TMRE (FL-2); **d)** Overlay b/ and c/.

Figure 5B. **Effect of copper treatment on mitochondrial potential in transfected N_2A.** N_2A were seeded in two 24 wells plates on day one. A day after (day two) cells were transfected with mock, wt-PrP, Δ8TM1-PrP or Δocta-PrP. Medium was changed on day three and copper was added in fresh medium (100μM $CuCl_2$) into one of the two plates. On day four cells were washed with PBS, fresh medium was added and cells were stained with TMRE. Δocta-PrP overexpressing cells show a significant decrease of ΔΨ. After copper treatment in all cases ΔΨsignificantly decreases. T-test were performed * comparison with mock $p<0.05$. The number of experiments is noted in bracket.

Figure 6. **Viability after copper treatment in overexpressing N_2A.** The percentage of viability after copper treatment in transfected N_2A was determined by Casy cell counter. The procedure was identical to which used for FACS analysis till the staining. In stead of staining and FACS only Casy cell counter was used. 4 independent experiments were performed. T-test were performed and no significant difference was observable.

Figure 1

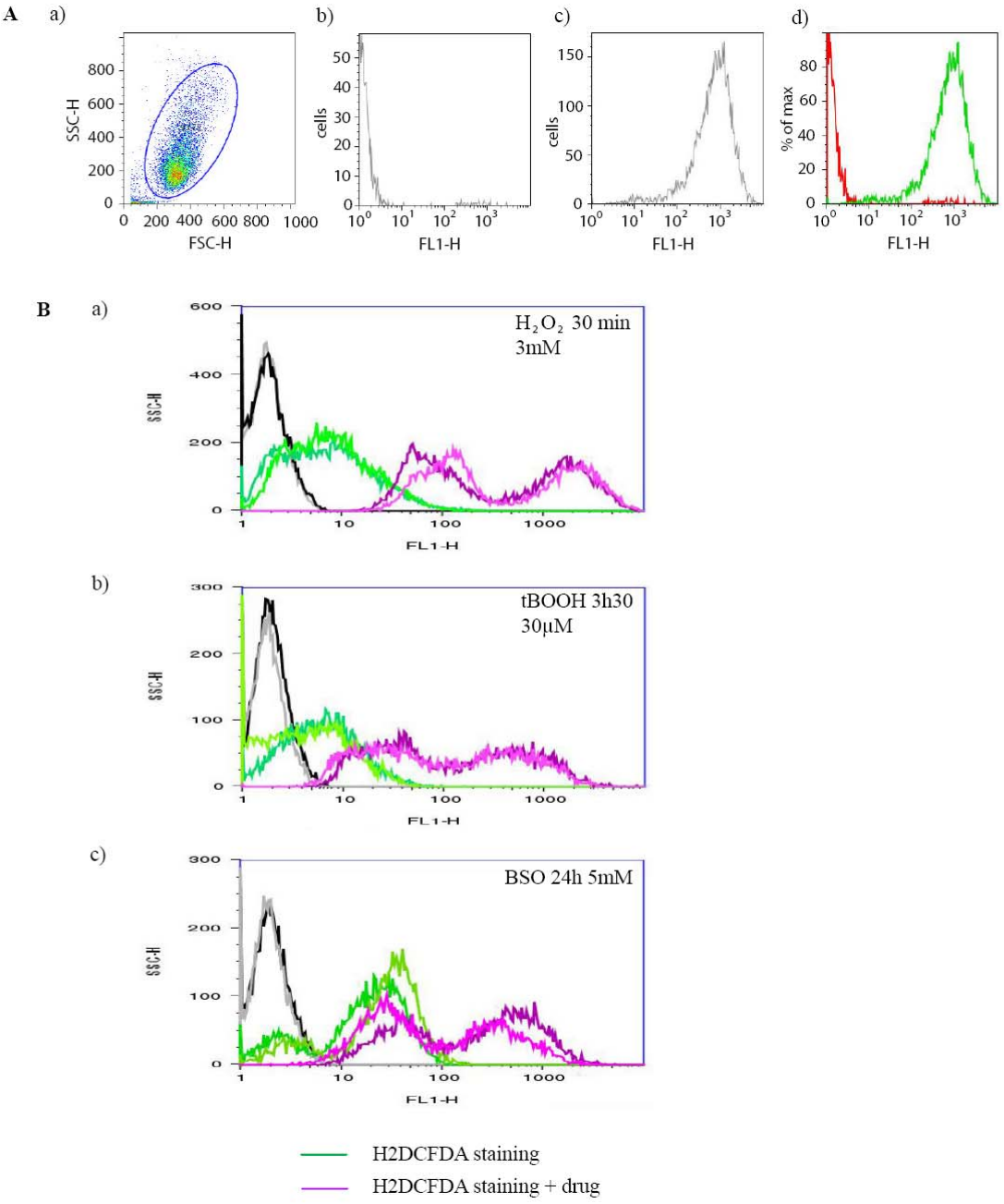
A
a)
b)
c)
d)
SSC-H
FSC-H
cells
FL1-H
% of max
B
a)
H_2O_2 30 min
3mM
b)
tBOOH 3h30
30µM
c)
BSO 24h 5mM
H2DCFDA staining
H2DCFDA staining + drug

Figure 2

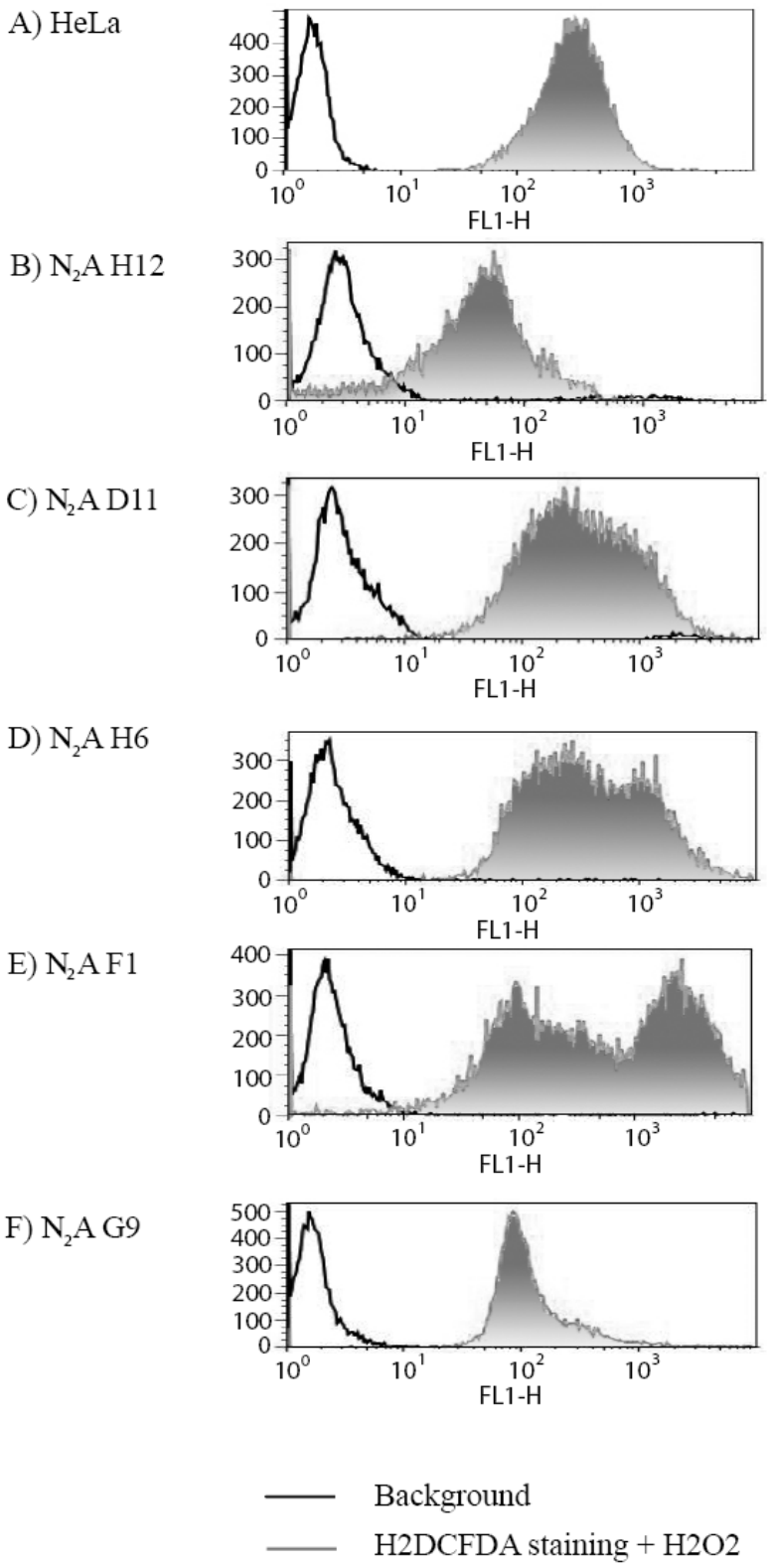
A) HeLa
B) N2A H12
C) N2A D11
D) N2A H6
E) N2A F1
F) N2A G9
FL1-H
Background
H2DCFDA staining + H2O2

Figure 3

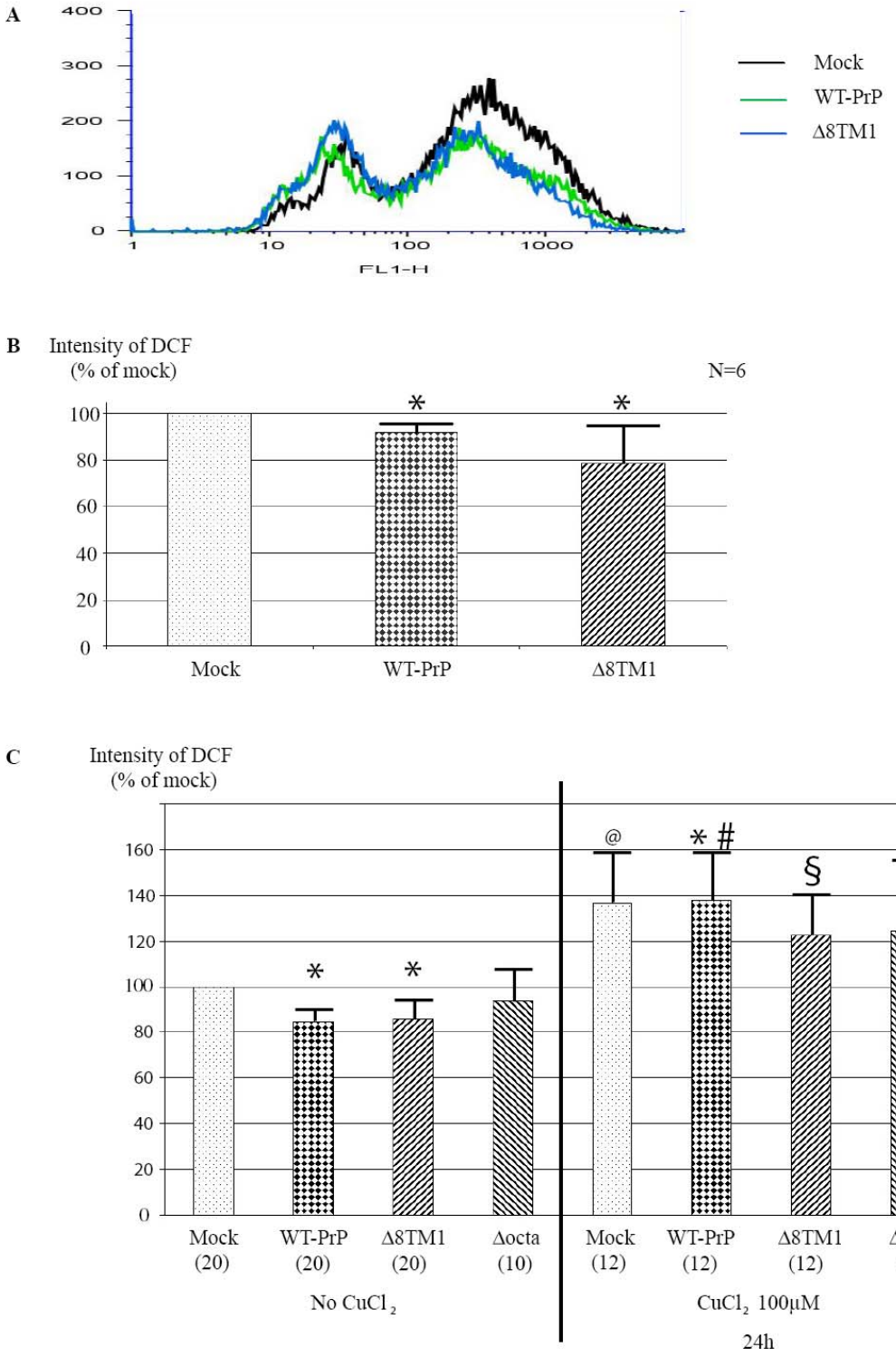
A
400
300
200
100
0
1
10
100
1000
FL1-H
Mock
WT-PrP
Δ8TM1
B
Intensity of DCF
(% of mock)
N=6
100
80
60
40
20
0
*
*
Mock
WT-PrP
Δ8TM1
C
Intensity of DCF
(% of mock)
160
140
120
100
80
60
40
20
0
*
*
@
* #
§
Mock (20)
WT-PrP (20)
Δ8TM1 (20)
Δocta (10)
Mock (12)
WT-PrP (12)
Δ8TM1 (12)
Δocta (6)
No CuCl2
CuCl2 100µM
24h

Figure 4

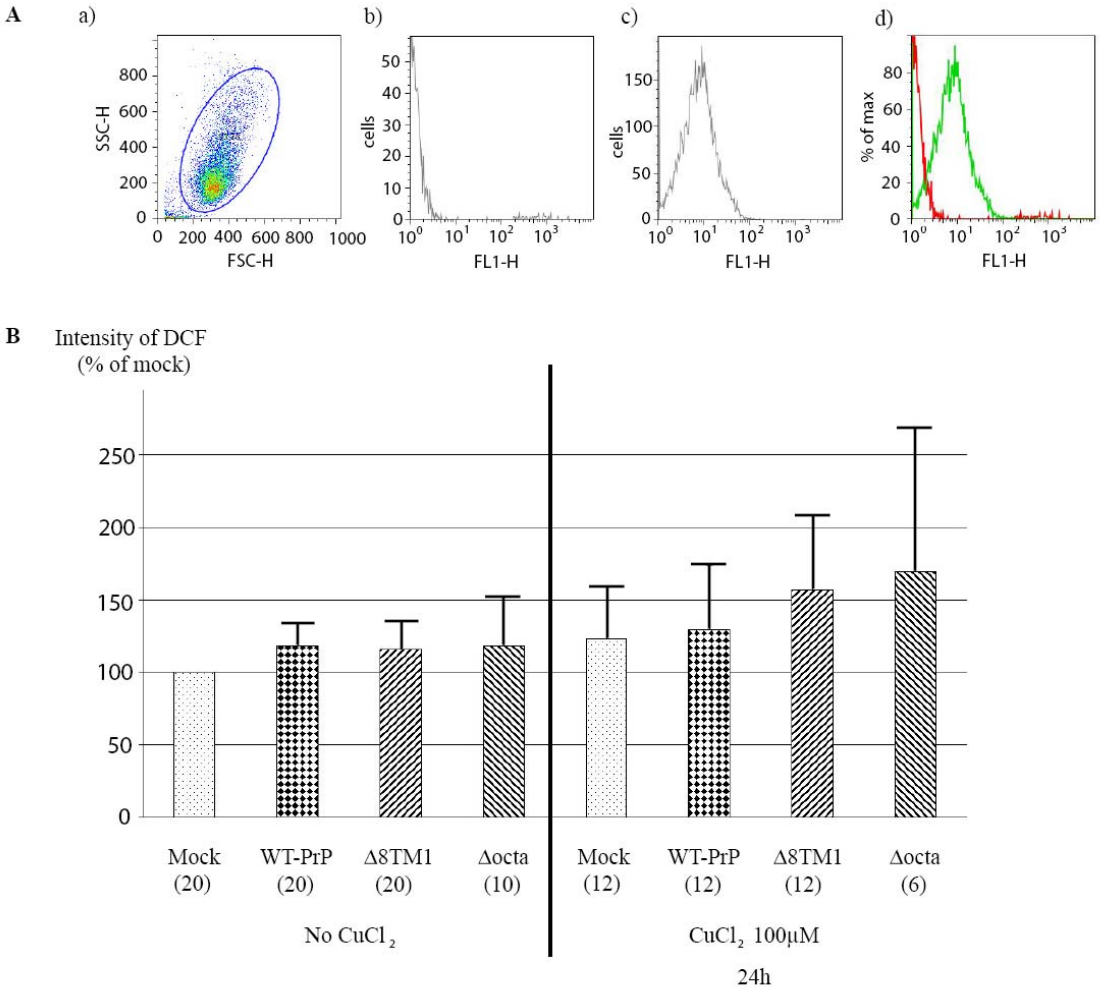
A
a)
b)
c)
d)
SSC-H
FSC-H
cells
FL1-H
% of max
B
Intensity of DCF
(% of mock)
Mock (20)
WT-PrP (20)
Δ8TM1 (20)
Δocta (10)
Mock (12)
WT-PrP (12)
Δ8TM1 (12)
Δocta (6)
No CuCl2
CuCl2 100µM
24h

Figure 5

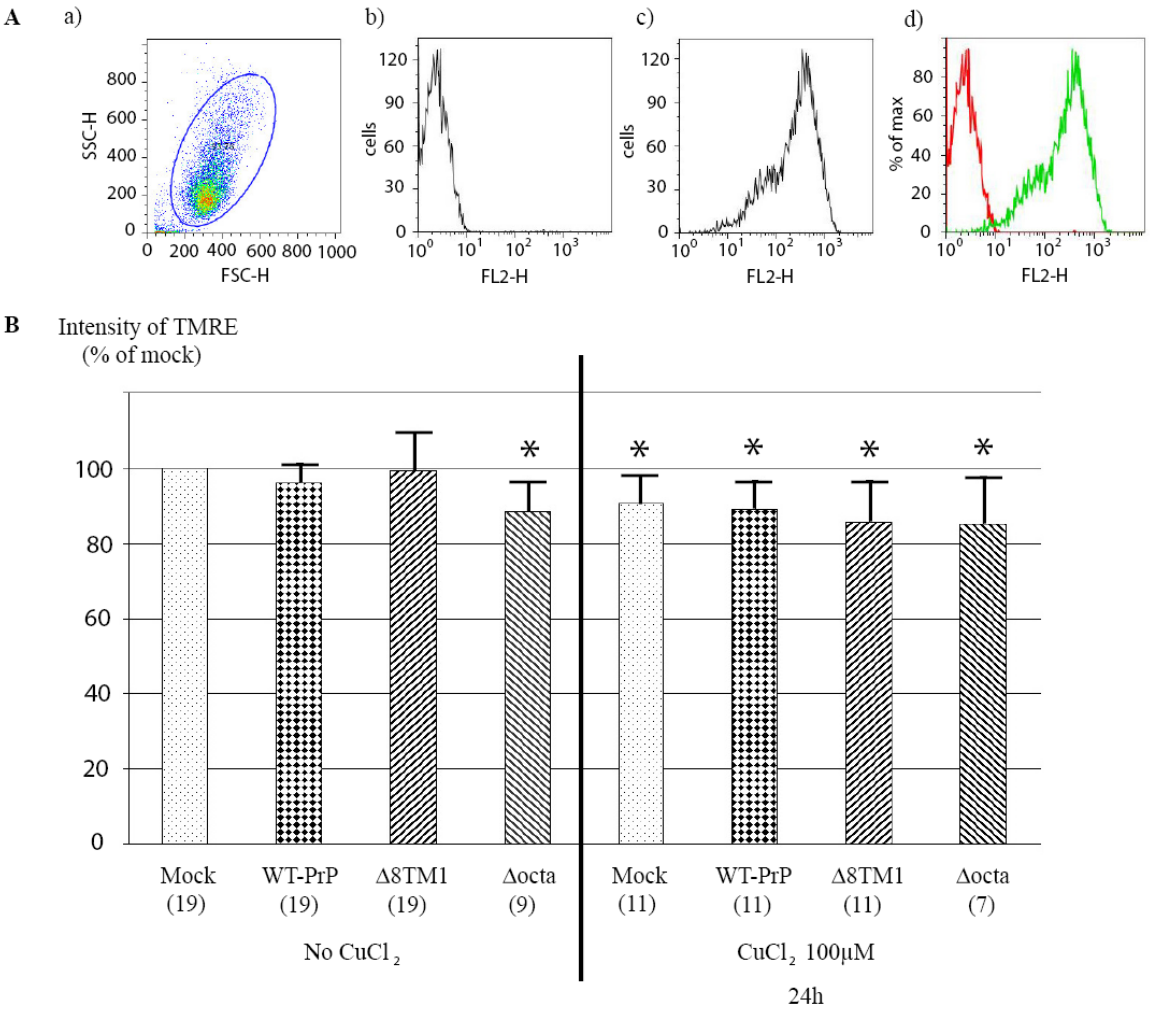
A
a)
b)
c)
d)
SSC-H
FSC-H
cells
FL2-H
% of max
B
Intensity of TMRE
(% of mock)
Mock (19)
WT-PrP (19)
Δ8TM1 (19)
Δocta (9)
Mock (11)
WT-PrP (11)
Δ8TM1 (11)
Δocta (7)
No CuCl2
CuCl2 100µM
24h

Figure 6

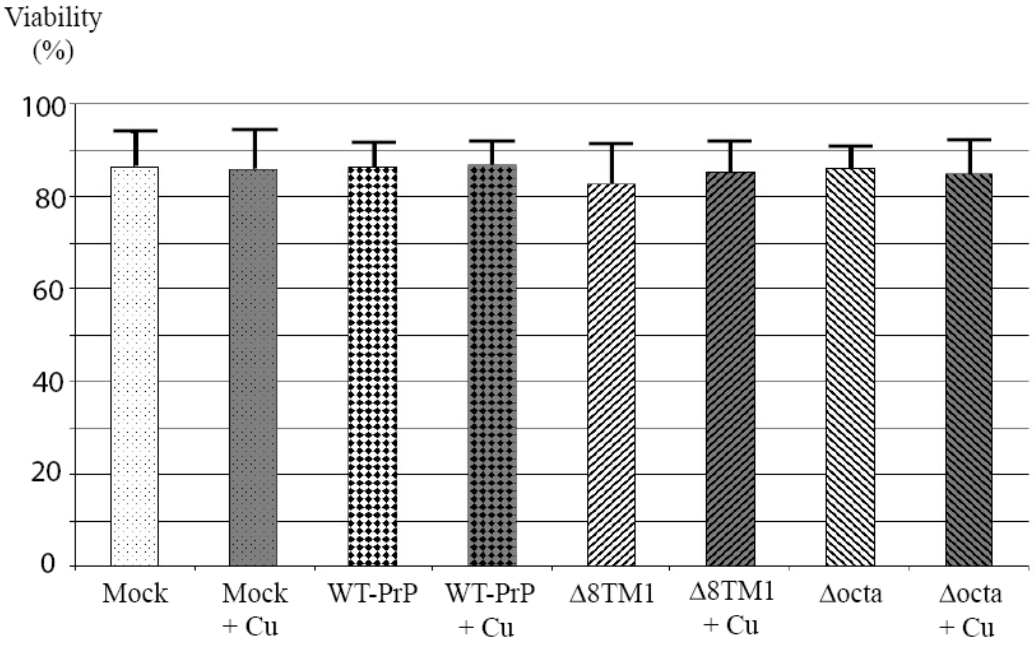
Viability
(%)
100
80
60
40
20
0
Mock
Mock
+ Cu
WT-PrP
WT-PrP
+ Cu
Δ8TM1
Δ8TM1
+ Cu
Δocta
Δocta
+ Cu

10 Erklärung

1. Ich versichere hiermit, dass ich die anliegende Arbeit mit dem Thema: *„Functional analysis of TM1 Mutants of Prion Protein“* selbstständig verfasst und keine anderen Hilfmittel als die angegebenen benutzt habe. Die Stellen, die anderen Werken dem Wortlaut oder dem Sinne nach entnommen sind, habe ich in jedem einzelnen Falle durch Angaben der Quelle, auch der benutzten Sekundärliteratur, als Entlehnung kenntlich gemacht.

2. Diese Arbeit wird nach Abschluss des Prüfungsverfahrens der Universitätsbibliothek Konstanz übergeben und ist durch Einsicht und Ausleihe somit der Öffentlichkeit zugänglich.

Als Urheber der anliegenden Arbeit stimme ich diesem Verfahren zu.

Konstanz, den .....
.

(Muriel MALAISÉ)

Eingetragene Warenzeichen und geschützte Warennamen sind *nicht* besonders kenntlich gemacht; es darf also aus dem Fehlen eines derartigen Hinweises nicht geschlossen werden, dass es sich um einen freien Warennamen handelt.